RTCA, Inc.
1150 18th Street, NW, Suite 910
Washington, DC 20036
Phone: (202) 833-9339
Fax: (202) 833-9434
www.rtca.org

THE GOLD STANDARD FOR AVIATION SINCE 1935

June 16, 2011

BEFORE THE
FEDERAL COMMUNICATIONS COMMISSION
WASHINGTON, D.C. 20554

SUBMISSION FOR THE RECORD

Marlene H. Dortch, Secretary
Federal Communications Commission
Office of the Secretary
445 12th Street SW
Room TW-A325
Washington, DC 20554

Re: Ex Parte Presentation re LightSquared Subsidiary, LLC, File No. SAT-MOD-20101118-00239

Dear Ms. Dortch,

In a March 3, 2011 letter (Attachment 1), the FAA asked RTCA, Inc. to conduct a study (Attachment 2) to address the issue of compatibility between the operation of a terrestrial wireless broadband network by LightSquared, pursuant to its FCC Order and Authorization (DA 11-133), January 26, 2011, and GPS receivers onboard aircraft utilizing the GPS L1 signal for navigation and positioning within the National Airspace System.

A private, not-for-profit corporation utilized as a Federal advisory committee, RTCA develops consensus-based recommendations for the government on issues ranging from technical performance standards to policies and priorities for air transportation. Our deliberations are open to the public.

On June 3, 2011, the attached report was delivered to the FAA by RTCA and is provided for Federal Communications Commission consideration.

Sincerely,

Margaret Jenny
President
RTCA, Inc.

cc: Mr. Michael P. Huerta
Deputy Administrator
Federal Aviation Administration (FAA)

Attachments: FAA Letter Requesting Report

"Assessment of the Light Squared Ancillary Terrestrial Component Radio Frequency Interference Impact on GNSS L1 Band Airborne Receiver Operations" (RTCA DO-327)

This Page Intentionally Left Blank

U.S. Department
of Transportation
**Federal Aviation
Administration**

RTCA Paper No. 047-11/PMC-881

MAR 3 2011

Ms. Margaret Jenny
President
RTCA Inc.
1828 L Street, NW., Suite 605
Washington, DC 20036

Dear Ms. Jenny:

The 1525-1559 MHz and 1626.5-1660.5 MHz bands have been allocated for many years for mobile satellite service (MSS) communications (e.g., Inmarsat).

A few years ago a United States satellite company "LightSquared" (previously called Mobile Satellite Ventures (MSV), then SkyTerra) started a process with the Federal Communications Commission (FCC) to also allow terrestrial communications in the 1525-1559 MHz band. These "ancillary terrestrial components", or *ATC*[1], were terminals that were an integral part of the MSS network. The stated intent was to act as "gap fillers" to allow the company to service users in areas where the satellite signals had difficulty reaching (e.g., cities and "urban canyons" where buildings caused blockages of the satellite signals). After considerable study that approach was approved, and in fact was recently updated based on agreements between LightSquared and Inmarsat.

In November 18, 2010, LightSquared requested to the FCC to amend their license to allow them to service terminals that are not combined MSS/terrestrial, rather are simply just purely terrestrial terminals. In the longer term that capability could be leased-out by LightSquared making it impossible for the *ATC* portion to be an "integral part of the satellite network", rather it would simply become another cellular-type service. This raised the concern that the number of such terminals will increase. In fact, the current projection is that the number of these terminals will explode to an order of magnitude more than previously proposed. This presents a potential interference threat to the aviation community which is increasingly relying on Global Positioning System (GPS) L1 for navigation for not only approach and landing, but for enroute (automatic dependent surveillance broadcast) and surface navigation on airport tarmac.

The Federal Aviation Administration (FAA) believes that studies using the new assumptions need to be undertaken to ensure protection of the GPS. These studies should include

[1] For this document *ATC* in italics refers to ancillary terrestrial component and not air traffic control. Due to confusion on the topic some have started writing the acronym as ATCt and the international term for *ATC* is complementary ground component (CPG).

receiver vulnerability, as well as scenario studies including aggregate effects of LightSquared transmissions on GPS receivers used in aircraft.

After reviewing the current terms of reference, we have determined that the evaluation of this potential interference is already within the scope of Special Committee 159. Therefore, I would like to add this issue to those already being addressed by SC 159. In order to provide timely input to the FAA, this evaluation will need to be completed quickly. LightSquared is required by the FCC to help organize and fully participate in a working group that includes the GPS community and federal agencies to study the potential for overload to GPS devices and to identify any measures necessary to prevent harmful interference to GPS. LightSquared will submit a final report by June 15 to the FCC. The RTCA evaluation should proceed in parallel, with a deliverable to the FAA by June 3.

Please let me know as soon as possible your response to this request at (202) 267-9722 or by e-mail at robert.frazier@faa.gov.

Sincerely,

Robert A. Frazier
Acting Group Manager, Spectrum
Engineering Services

RTCA, Inc.
1828 L Street, NW, Suite 805
Washington, DC 20036-5133 USA

Assessment of the LightSquared Ancillary Terrestrial Component Radio Frequency Interference Impact on GNSS L1 Band Airborne Receiver Operations

RTCA/DO-327
June 3, 2011

Prepared by: SC-159
© 2011, RTCA, Inc.

Copies of this document may be obtained from

RTCA, Inc.

Telephone: 202-833-9339
Facsimile: 202-833-9434
Internet: www.rtca.org

Please visit the RTCA Online Store for document pricing and ordering information.

FOREWORD

This report was prepared by Special Committee 159 (RTCA SC-159) and approved by the RTCA Program Management Committee (PMC) on June 3, 2011.

RTCA, Inc. is a not-for-profit corporation formed to advance the art and science of aviation and aviation electronic systems for the benefit of the public. The organization functions as a Federal Advisory Committee and develops consensus based recommendations on contemporary aviation issues. RTCA's objectives include but are not limited to:

- coalescing aviation system user and provider technical requirements in a manner that helps government and industry meet their mutual objectives and responsibilities;
- analyzing and recommending solutions to the system technical issues that aviation faces as it continues to pursue increased safety, system capacity and efficiency;
- developing consensus on the application of pertinent technology to fulfill user and provider requirements, including development of minimum operational performance standards for electronic systems and equipment that support aviation; and
- assisting in developing the appropriate technical material upon which positions for the International Civil Aviation Organization and the International Telecommunication Union and other appropriate international organizations can be based.

The organization's recommendations are often used as the basis for government and private sector decisions as well as the foundation for many Federal Aviation Administration Technical Standard Orders.

Since RTCA is not an official agency of the United States Government, its recommendations may not be regarded as statements of official government policy unless so enunciated by the U. S. government organization or agency having statutory jurisdiction over any matters to which the recommendations relate.

This page intentionally left blank.

TABLE OF CONTENTS

EXECUTIVE SUMMARY .....

1 INTRODUCTION 1

1.1 Background 1
1.1.1 Brief History 1
1.1.2 Further Developments Since 2009 1
1.1.3 January 2011 FCC Order and Authorization 2
1.1.4 FAA Request to RTCA 2

1.2 Terms of Reference 2

1.3 Assessment Study Objectives 3

1.4 Report Organization 3

1.5 References 3

2 AERONAUTICAL RFI EFFECTS ANALYSIS METHOD 5

2.1 Introduction and Basic Methodology 5

2.2 GPS Receiver Performance and RFI Susceptibility Model 5
2.2.1 General RFI Effects on Aeronautical GPS Receivers 5
2.2.2 GPS L1 Receiver RFI Effects Model 6
2.2.2.1 GPS L1 Antenna and Receiver RF Front-end Performance Model 6
2.2.2.2 GPS L1 Narrow- and Wide-bandwidth Near-band RFI Effect Models 7
2.2.2.3 GPS L1 Wide- and Narrow- Bandwidth In-band RFI Effect Model 8

2.3 RFI Propagation Path Models 8
2.3.1 Background 8
2.3.2 Short-Range Path Segment (Two-Ray) Model 9
2.3.3 Medium-Range Path Segment Model 10
2.3.4 Long-Range Path Model 11
2.3.5 Free-Space Path Model 12

2.4 LightSquared ATCt Base and Mobile Station Emission Models 12
2.4.1 ATCt Base and Mobile Station Emission Parameters 13
2.4.1.1 ATCt Base Station Emission Parameters 13
2.4.1.2 ATCt Mobile Station (User Equipment) Emission Parameters 13
2.4.2 ATCt Base Station Antenna Pattern and Siting Parameters 14
2.4.2.1 ATCt Base Station Antenna Pattern Parameters 14
2.4.2.2 ATCt Base Station Location Parameters 16
2.4.3 Mobile Station Antenna Pattern and Siting Parameters 17
2.4.3.1 ATCt Mobile Station Antenna Pattern Parameters 17
2.4.3.2 ATCt Mobile Station Location and Concentration Parameters 17

2.5 References 17

3 AERONAUTICAL RFI ENCOUNTER SCENARIO DESCRIPTIONS 19

3.1 Scenario Selection , General Features, and Other Related Aviation GPS Uses 19
3.1.1 RFI Encounter Scenario General Definition 19
3.1.1.1 RFI Encounter Scenario - General Aircraft Location and Receiver Function 19
3.1.1.2 RFI Encounter Scenario ATCt RFI Sources 19
3.1.1.3 RFI Encounter Scenario Key Geometry Features 20
3.1.1.4 RFI Encounter Scenario Baseline Non-ATCt RFI 20
3.1.2 Other Related Aviation GPS Uses 20

3.2 High Altitude Enroute RFI Encounter Scenario 21
3.2.1 Basic High Altitude Scenario RFI Encounter Geometry 21
3.2.2 ATCt Base Station Source Concentration and Source-Free Zones 21
3.2.3 Specific Case: South-Central Pennsylvania Details 21

3.3 Generic Low Altitude / Terminal Area (FAF WP) RFI Encounter Scenario 22
3.3.1 Basic Terminal Area Scenario RFI Encounter Geometry 22
3.3.2 Base and Mobile Station Source Concentration and Source-Free Zones 22

3.4 Generic Category I Precision Approach RFI Encounter Scenario 23
3.4.1 Basic Category I DH Scenario Encounter Geometry 23
3.4.2 Base and Mobile Station Source Concentration and Source-Free Zones 24

3.5 Generic Category II/III Precision Approach RFI Encounter Scenario 24
3.5.1 Basic Category II Decision Height Scenario Encounter Geometry 24
3.5.2 Base Station Source Concentration and Source-Free Zones 25

3.6 Generic Surface Movement (Taxiway) Guidance RFI Encounter Scenario 25
3.6.1 Basic Surface (Taxiway) Scenario RFI Encounter Geometry 26
3.6.2 Base and Mobile Station Source Concentration and Source-Free Zones 26

3.7 Aeronautical RFI Encounter Scenario Parameter Summary 26

3.8 References 27

4 AGGREGATE LIGHTSQUARED ATCT RFI EFFECT ANALYSES 29

4.1 Introduction 29

4.2 Low Altitude Enroute / Terminal Area (FAF WP) Scenario Aggregate RFI Analysis 29
4.2.1 Generic Aggregate ATCt Base Station Fundamental RFI Effect Analysis (FAF WP) 29
4.2.1.1 Random Method Base Station Fundamental RFI Effect Analysis (FAF WP) 30
4.2.1.2 Discrete Method Base Station Fundamental RFI Effect Analysis (FAF WP) 30
4.2.2 Aggregate ATCt Mobile Station Unwanted RFI Effect Analysis (FAF WP) 30

4.3 Generic Category I Precision Approach Scenario Aggregate RFI Analysis 31
4.3.1 Aggregate ATCt Base Station Fundamental RFI Effect Analysis (Category I DH) 31
4.3.1.1 Random Method Base Station Fundamental RFI Effect Analysis (Category I DH) 31
4.3.1.2 Discrete Method Base Station Fundamental RFI Effect Analysis (Category I DH) 32
4.3.2 Aggregate ATCt Mobile Station Unwanted RFI Effect Analysis (Category I DH) 32

4.4 Category II Precision Approach Scenario Aggregate RFI Analysis 32
4.4.1 Aggregate ATCt Base Station Fundamental RFI Effect Analysis (Category II DH) 33
4.4.1.1 Random Method Base Station Fundamental RFI Effect Analysis (Category II DH) 33
4.4.1.2 Discrete Method Base Station Fundamental RFI Effect Analysis (Category II DH) 33
4.4.2 Aggregate ATCt Mobile Station Unwanted RFI Effect Analysis (Category II DH) 34

4.5 Surface Movement (Taxiway) Scenario Aggregate RFI Analysis 34
4.5.1 Random Aggregate ATCt Base Station Fundamental RFI Effect Analysis (Taxiway) 34
4.5.2 Discrete Aggregate ATCt Base Station Fundamental RFI Effect Analysis (Taxiway) 35

4.6 High Altitude Enroute Scenario Analysis 35
4.6.1 Random Aggregate ATCt Base Station Fundamental RFI Effect Analysis (Enroute) 35
4.6.1.1 Rural Concentration Zone Random Aggregate RFI Analysis 36
4.6.1.2 Metro Concentration Zone and Combined ATCt Base Station Aggregate Analyses 36
4.6.2 Discrete Aggregate ATCt Base Station Fundamental RFI Effect Analysis (Enroute) 37

4.7 Summary Results 38

4.8 References 39

5 POSSIBLE RFI MITIGATION TECHNIQUES 41
5.1 Interference Mitigation at the Source 41
5.1.1 ATCt Frequency Shift 41
5.1.2 ATCt Power Reduction 41
5.2 GPS Receiver Susceptibility Reduction 42
5.2.1 Improved Preselection 42
5.2.2 Adaptive Spatial (Antenna) Processing 43
5.2.3 Improved Receiver Tracking Processes 43
5.3 References 44
6 SUMMARY AND CONCLUSIONS 45
6.1 Summary Overview 45
6.2 Assessment Element Summaries 45
6.2.1 Aeronautical RFI Effect Analysis Methodology and Element Models 45
6.2.1.1 ATCt Source Model Summary 45
6.2.1.2 Isotropic Propagation Path Model Summary 46
6.2.1.3 GNSS Airborne Receiver Model Summary 46
6.2.2 Aeronautical RFI Encounter Scenario Development 47
6.2.3 Aggregate ATCt Base and Mobile Station RFI Analysis Summary 48
6.2.3.1 ATCt Location Methods Summary 48
6.2.3.2 Aggregate ATCt Base Station RFI Analysis Summary 49
6.2.3.3 Aggregate ATCt Mobile Station RFI Analysis Summary 50
6.2.4 Possible Mitigation Techniques 50
6.3 Conclusions and Recommendations 51
6.4 References 52
MEMBERSHIP 53
A MOPS-BASED GNSS RECEIVER BROAD BAND RFI TEST PROCEDURES A-1
A.1 MOPS-based GPS Receiver Overload RFI Effect Test Procedures A-1
A.1.1 Carrier-to-Noise Ratio (CNR) Degradation Baseline Test A-1
A.1.1.1 CNR Degradation Baseline Test Satellite Simulator and Interference Conditions A-1
A.1.1.2 CNR Degradation Baseline Test Procedure A-3
A.1.2 Measurement Accuracy Test A-4
A.1.2.1 Measurement Accuracy Test Satellite Simulator and Interference Conditions A-4
A.1.2.2 Measurement Accuracy Test Procedure A-5
A.1.3 SBAS Message Loss Tests A-7
A.2 References A-8
B AGGREGATE RF INTERFERENCE COMPUTATION METHOD B-1
B.1 Introduction B-1
B.2 Derivation of Analytic Statistical Aggregate Received RFI Model B-1
B.2.1 Derivation of RFI Emitter Source Probability Factors B-1
B.2.1.1 RFI Source Number and Location Factors B-1
B.2.1.2 Median Single-Source Received Power Probability Factors B-2
B.2.2 Mean Aggregate Received RFI Derivation B-3
B.3 RFI Propagation Isotropic Path Loss Models B-4
B.3.1 General Isotropic Path Loss Model Methodology B-4
B.3.1.1 Isotropic Path Loss Model for Aircraft Antenna Height Below 550 Meters B-4

B.3.1.1.1 Two-Ray Isotropic Path Loss Model B-5
B.3.1.1.2 Hata-Okumura Isotropic Median Path Loss Model B-6
B.3.1.1.3 Erceg/Greenstein Isotropic Median Path Loss Model (ATCt Mobile) B-6
B.3.1.2 Isotropic Path Loss Model for Aircraft Antenna Height Above 550 Meters B-7
B.3.2 RFI Scenario-Specific Isotropic Path Loss Models B-7
B.3.2.1 Generic Terminal Area (FAF WP) Scenario Isotropic Path Loss B-8
B.3.2.2 Generic Category I Decision Height Waypoint Path Loss B-9
B.3.2.3 Generic Category II Decision Height Waypoint Path Loss B-10
B.3.2.4 Generic Surface (Taxiway) Path Loss B-11

B.4 Scenario-Specific Aggregate Received RFI Detailed Computations B-12
B.4.1 ATCt RFI Source Location Methods and Location Constraints B-12
B.4.1.1 Random and Fixed Discrete Location Methods – General Description B-12
B.4.1.2 ATCt RFI Source Location Constraints B-12
B.4.2 Random ATCt Base Station Location Method Computations B-15
B.4.2.1 Terminal Area (FAF WP) Aggregate ATCt Base Station RFI (Random Method) B-16
B.4.2.2 Category I Decision Height Aggregate ATCt Base Station RFI (Random Method) B-17
B.4.2.3 Category II Decision Height Aggregate ATCt Base Station RFI (Random Method) B-17
B.4.2.4 Generic Surface (Taxiway) Scenario Aggregate ATCt Base Station RFI B-18
B.4.2.5 US East Coast High Altitude Scenario Aggregate ATCt Base Station RFI B-18
B.4.2.5.1 Low Tower Concentration Zone Aggregate RFI Analysis B-19
B.4.2.5.2 Metro Concentration Zone and Combined Aggregate RFI Analysis B-20
B.4.3 Fixed Discrete ATCt Base Station Location Method Computations B-21
B.4.3.1 Generic Terminal Area (FAF WP) Scenario Aggregate ATCt Base Station RFI B-23
B.4.3.2 Generic Category I Decision Height Scenario Aggregate ATCt Base Station RFI B-24
B.4.3.3 Generic Category II Decision Height Scenario Aggregate ATCt Base Station RFI B-24
B.4.3.4 Generic Surface (Taxiway) Scenario Aggregate ATCt Base Station RFI B-24
B.4.3.5 US East Coast High Altitude Scenario Aggregate ATCt Base Station RFI B-24
B.4.4 Random ATCt Mobile Station Location Method Computations B-26
B.4.4.1 Generic Terminal Area (FAF WP) Scenario Aggregate ATCt Mobile Station RFI B-26
B.4.4.2 Generic Category I Decision Height Scenario Aggregate ATCt Mobile Station RFI B-27
B.4.4.3 Generic Category II Decision Height Scenario Aggregate ATCt Mobile Station RFI B-28

B.5 Aggregate RFI Results Comparison and Discussion B-29

B.6 References B-30

C ANALYTICAL DERIVATION OF MAXIMUM TOLERABLE INTERFERENCE LEVELS C-1

C.1 Wide Bandwidth Near-band Aggregate RFI Limit C-1

C.2 Third-Order Intermodulation RFI Effect Limit C-2
C.2.1 Active Antenna LNA Model C-2
C.2.2 Response of Active Antenna LNA to LightSquared Emissions C-4
C.2.3 Preselector Filter Model C-4
C.2.4 Simulation Results C-5

C.3 Earlier Generation GPS Aviation Receiver Susceptibility C-8

C.4 References C-9

D EXPERIMENTAL TEST RESULTS FOR AVIONICS GPS RECEIVERS D-1

D.1 MOPS-based GNSS Receiver Broad Band Tests D-1
D.1.1 Test Configuration D-1
D.1.2 Aviation LNA D-3
D.1.3 LightSquared Signal Generation D-4
D.1.4 Narrow- and Wide-bandwidth 1 dB CNR Degradation and Loss of Tracking Results D-6

D.1.5 SBAS Message Loss Test Results D-7
D.2 References D-8
E ACRONYMS, ABBREVIATIONS AND DEFINITIONS E-1
E.1 Acronyms and Abbreviations E-1
E.2 Definitions E-7

TABLE OF FIGURES

Figure 2-1 GPS L1 Receive System Block Diagram 6
Figure 2-2 GPS Receive Antenna Lower Hemisphere Max. Gain Model 6
Figure 2-3 GPS Receive Antenna Upper Hemisphere Max. Gain Model 7
Figure 2-4 Example Two-Ray Median Path Loss 10
Figure 2-5 Example Erceg/Greenstein Median Path Loss 11
Figure 2-6 Example Hata-Okumura Median Path Loss 12
Figure 2-7 ATCt Base Station Lower Hemisphere Vertical Gain Pattern Model 15
Figure 2-8 ATCt Base Station Upper Hemisphere Vertical Gain Pattern Model 15
Figure 2-9 ATCt Base Station Single-City Tower Concentration Pattern 16
Figure 2-10 ATCt Base Station Multi-City Tower Concentration Pattern 16
Figure 3-1 General Runway Approach Geometry (Side View) 23
Figure 3-2 Airport Runway Protection Zones - Top View 25
Figure 3-3 Surface RFI Encounter Geometry - Front View 26
Figure 5-1 Estimated Max. ATCt Base Station EIRP versus Channel Center Freq. 42

TABLE OF TABLES

Table 2-1 LightSquared AMT Band Unwanted Emission Limits 13
Table 3-1 Current Aircraft Uses of GPS 21
Table 3-2 Metropolitan Areas Visible in High Altitude Enroute Specific Case 22
Table 3-3 Aeronautical Scenario Antenna Height and Radio Horizon Parameters 27
Table 3-4 Aeronautical Scenario ATCt Source Exclusion Zone Parameters 27
Table 4-1 Random Method Aggregate Calculation Summary (FAF WP) 30
Table 4-2 Mobile Unit Terminal Area (FAF WP) Scenario Results 31
Table 4-3 Random Method Aggregate Calculation Summary (Category I DH) 32
Table 4-4 Mobile Unit Category I DH Scenario Aggregate RFI Results 32
Table 4-5 Random Method Aggregate Calculation Summary (Category II DH) 33
Table 4-6 Mobile Unit Category II DH Scenario Aggregate RFI Results 34
Table 4-7 Random Method Aggregate Calculation Summary (Taxiway) 35
Table 4-8 Composite Integration Zone Model –Rural Results 36
Table 4-9 Composite Integration Zone Model – Metro Results 37
Table 4-10 Enroute Scenario Discrete Method Results 38
Table 4-11 ATCt Base Station Fundamental RFI Effect Aggregate Results Summary 38
Table 4-12 ATCt Mobile Station Unwanted RFI Effect Aggregate Results Summary 39
Table 6-1 Aeronautical Scenario Antenna Height and Radio Horizon Parameters 47
Table 6-2 Metropolitan Areas Visible in High Altitude Enroute Specific Case 48
Table 6-3 Aeronautical Scenario ATCt Source Exclusion Zone Parameters 48
Table 6-4 ATCt Base Station Fundamental RFI Effect Aggregate Results Summary 49
Table 6-5 ATCt Mobile Station Unwanted RFI Effect Aggregate Results Summary 50

Table of Figures - Appendices

Figure A-1 Example Test Set-up and Compensation of Signals, Noise and Interference A-3
Figure B-1 Generic Runway Approach Geometry-Top View B-1
Figure B-2 Two-Ray Path Loss Model Geometry (Profile View) B-5
Figure B-3 Terminal Area Isotropic Median Path Loss (Base Station Case) B-8
Figure B-4 Terminal Area Isotropic Median Path Loss (Mobile Station Case) B-9
Figure B-5 Vertical Polarization Wave Reflection Coefficient (1552.7 MHz) B-10
Figure B-6 Category I DH Isotropic Median Path Loss (Base Station Case) B-10
Figure B-7 Category II DH Isotropic Median Path Loss (Base Station Case) B-11
Figure B-8 Surface (Taxiway) Isotropic Median Path Loss (Base Station Case) B-12
Figure B-9 Approach Obstacle Surface (Top and Side Views) B-13
Figure B-10 Random Method Exclusion Zone Example Diagram (Top View) B-14
Figure B-11 Fixed Hexagonal Cellular Grid Structure (Top View) B-22
Figure B-12 Enroute Discrete Method Interference Scenario Geometry B-25
Figure B-13 Median Path Loss For Mobile Terminal Area (FAF WP) Scenario B-27
Figure B-14 Median Path Loss For Mobile Unit Category I Scenario B-27
Figure B-15 Median Path Loss for Mobile Unit Category II Scenario B-28
Figure C-1 Antenna Port CW Interference Limit C-1
Figure C-2 Low Noise Amplifier System Model C-2
Figure C-3 Input-Output Voltage Characteristic for Modeled Airborne Active Antenna LNA C-3
Figure C-4 Modeled LNA Input-Output Power Characteristics C-4
Figure C-5 Modeled Active Antenna Preselector Attenuation C-5
Figure C-6 Input (top) and Output (bottom) Power Spectrum of Modeled LNA; LightSquared Signal Power at Antenna Output Port is -45 dBm (LNA in Linear Region) C-6
Figure C-7 Input (top) and Output (bottom) Power Spectrum of Modeled LNA; LightSquared Signal Power at Antenna Output Port is -35 dBm (LNA Entering into Compression) C-6
Figure C-8 Input (top) and Output (bottom) Power Spectrum of Modeled LNA; LightSquared Signal Power at Antenna Output Port is -25 dBm (LNA Entering Deeper into Compression) C-7
Figure C-9 Degradation to Receiver Effective Noise Floor due to the Third Order Intermodulation Product Created by Active Antenna LNA C-8
Figure D-1 Functional Test Block Diagram D-1
Figure D-2 RFI Generator Detail D-3
Figure D-3 LNA Representative of Aviation LNA D-3
Figure D-4 Antenna Frequency Response Specified in RTCA DO-301 ..... D-4
Figure D-5 Representative Unfiltered Phase 1 Signal D-5
Figure D-6 Representative Filtered Phase 1 Signal with DO-301 Slope D-6

Table of Tables - Appendices

Table A-1 Steady State Accuracy Test CWIValues* A-2
Table A-2 Satellite Equivalent Power Spectral Density A-3
Table A-3 Pass Threshold Table A-7
Table B-1 Aircraft and RFI Source Antenna Heights B-8
Table B-2 Radio Horizon from Aircraft to ATCt Base and Mobile Stations B-13
Table B-3 Aeronautical Scenario ATCt Source Exclusion Zone Parameters B-15
Table B-4 Terminal Area (FAF) Aggregate RFI Results (Random Method) B-16
Table B-5 Cat. I Decision Height Aggregate RFI Results (Random Method) B-17
Table B-6 Cat. II Decision Height Aggregate RFI Results (Random Method) B-18
Table B-7 Airport Surface (Taxiway) Aggregate RFI Results (Random Method) B-18
Table B-8 High Altitude East Coast Hotspot Parameters B-19
Table B-9 Composite Integration Zone Model Dimensions B-20

Table B-10 Composite Integration Zone Model –Rural Results B-20
Table B-11 Composite Integration Zone Model –Metro Results..... B-21
Table B-12 Generic Terminal Area (FAF) Discrete Model Interference..... B-23
Table B-13 Generic Category I Discrete Model Interference..... B-24
Table B-14 Generic Category II Discrete Model Interference..... B-24
Table B-15 Generic Surface (Taxiway) Discrete Model Interference..... B-24
Table B-16 Enroute Scenario Discrete Method Results B-26
Table B-17 Mobile Unit Terminal Area (FAF WP) Scenario Results..... B-27
Table B-18 Mobile Unit Category I DH Scenario Results B-28
Table B-19 Mobile Unit Category II DH Scenario Results B-29
Table B-20 ATCt Base Station Fundamental RFI Aggregate Results Summary B-29
Table B-21 ATCt Mobile Station Unwanted RFI Effect Aggregate Results Summary B-29
Table D-1 Aviation LNA Characteristics D-4
Table D-2 Power Corrections using RTCA DO-301 Filtered Signals..... D-5
Table D-3 Signal Power (dBm/channel) for 1 dB C/No Degradation Caused by LightSquared..... D-6
Table D-4 Signal Power (dBm/channel) for Loss of Satellite Tracking Caused by LightSquared..... D-6
Table D-5 Power Ratio for 1 dB C/No Degradation from LightSquared vs. CW RFI D-7

This page intentionally left blank.

Executive Summary

This report documents a study conducted by RTCA Special Committee 159 in response to a request from the Federal Aviation Administration to address the issue of compatibility between the operation of a terrestrial wireless broadband network in the bands 1525-1559/1626.5-1660.5 MHz by LightSquared, pursuant to its FCC license, and GPS receivers onboard aircraft. The report addresses the issues analytically based on existing domestic and international standards and includes results of tests of four certified aircraft GPS receivers.

The study concludes that the current LightSquared terrestrial authorization would be incompatible with the current aviation use of GPS, however modifications could be made to allow the LightSquared system to co-exist with aviation use of GPS. The study's conclusions and recommendations are strictly based on an assumed set of operational parameters for the LightSquared system and identified source mitigations. These operational parameters would produce less Radio Frequency Interference (RFI) than if LightSquared were to operate at its fully-authorized limits.

In addition, the analysis is based upon the assumption that all equipment is minimally compliant with the interference rejection requirements in harmonized domestic and international standards. Additionally since GPS is an aviation safety service, the analysis includes a 6 dB safety margin as is standard practice. Results from the four receivers tested show that these receiver models are significantly more resilient to interference from the LightSquared terrestrial base stations than limits derived from the standards.

The impact of a LightSquared upper channel spectrum deployment is expected to be complete loss of GPS receiver function. Because of the size of the single-city station deployment, GPS-based operations below about 2000 feet will be unavailable over a large radius from the metro deployment center (assuming no other metro deployments are nearby). Given the situation in the high altitude U.S. East Coast scenario, GPS-based operations will likely be unavailable over a whole region at any normal aircraft altitude.

The results of this study indicate that terrestrial base station operation at the lower 5 MHz wide channel (1526.3 – 1531.3 MHz) is compatible with aviation GPS operations for all the representative scenarios (including both signal tracking and initial acquisition). The study indicates that for terrestrial base stations using only the lower 10 MHz channel at 1526-1536 MHz, there is a small positive margin for GPS tracking (but not necessarily initial acquisition) in the presence of mean aggregate terrestrial network interference. As noted above, these conclusions are based upon specific assumptions about LightSquared operation.

The main recommendations from this aviation GPS receiver operational assessment are:

1. From an aviation perspective, LightSquared upper channel operation should not be allowed.
2. Further study is recommended to more carefully determine a refined terrestrial base station power versus frequency limit considering:
    a. determination of the lowest path loss for the low altitude enroute scenario,
    b. confirmation of acceptable receiver susceptibility for GPS initial acquisition and signal tracking in the presence of the 10 MHz bandwidth terrestrial network interference,
    c. computation of the cumulative probability distribution function for the aggregate path loss.

©2011 RTCA, Inc.

This page intentionally left blank.

1 INTRODUCTION

1.1 Background

1.1.1 Brief History

LightSquared, whose planned signals are the subject of analyses in this report, is a privately held company. Its predecessor companies were SkyTerra Communications, Inc. (SkyTerra), Mobile Satellite Ventures (MSV), Motient Services Inc. and American Mobile Satellite Company (AMSC). The initial L-Band Mobile-Satellite Service (MSS) license, currently held by LightSquared, was issued by the Federal Communications Commission (FCC) to AMSC in 1989. In 2001, LightSquared (then MSV) filed the first application to deploy an integrated satellite-terrestrial system to provide broadband wireless communications, using L-band frequencies already authorized for LightSquared's MSS use in the band 1525-1559 MHz (space-to-Earth).

To address concerns regarding potential interference to GPS L1 signals, in 2002 LightSquared voluntarily agreed to meet certain restrictive emission limits in the band 1559-1610 MHz. In 2003, the FCC established, and then revised in 2005, rules for Ancillary Terrestrial Component (ATCt)[1] service in various MSS bands, including the L-band. The FCC defined "ancillary" based on a number of criteria, including the provision of "integrated service," for which it created a safe harbor if all customers used dual-mode handsets capable of communicating via both MSS and ATC. In 2004, the FCC granted LightSquared's application for ATCt authority. In its 2005 Second Order on Reconsideration, the FCC, among other things, granted an 8 dB increase in power over the power limits authorized in 2003 (See, 47 CFR 25.253 (d)(1)-(6)).

RTCA Special Committee-159 (SC-159) took note of some of the ATCt regulatory developments and unwanted out-of-band emissions (OOBE) limits but did not study fundamental emission overload effects in RTCA/DO-235B [1-1].

No ATCt deployment was made between 2003 and 2010.

1.1.2 Further Developments Since 2009

In March 2010, the FCC authorized the transfer of control of LightSquared to Harbinger Capital Partner Funds and imposed a condition that LightSquared expeditiously deploy a nationwide network, which would consist of approximately 36,000 base stations, covering hundreds of millions of people.

In an order issued on the same day, the FCC separately approved LightSquared's 2009 ATCt modification application seeking additional flexibility for the technical operation of the ATCt network (including allowance for a base station to transmit at power levels up to 42 dBW effective isotropic radiated power (EIRP) per sector; see section 2.4 for specific technical details).

On November 18, 2010, LightSquared applied to the FCC for a license modification that would permit the use of terrestrial-only devices on its ATCt network. The application proposed no technical or operational changes to the ATCt network. In response, the GPS community first raised concerns to the FCC that high-powered LightSquared terrestrial transmitters adjacent to the 1559 MHz band edge would overload GPS signal reception.

[1] This report uses ATCt as the abbreviation for Ancillary Terrestrial Component rather than the FCC designation, ATC, to avoid confusion with the standard aviation abbreviation (ATC) for air traffic control.

©2011 RTCA, Inc.

1.1.3 January 2011 FCC Order and Authorization

On January 26, 2011, the FCC conditionally granted[1] a waiver of its rules, permitting LightSquared to use terrestrial-only devices on its ATCt network. Because of the concerns raised by the GPS community, the FCC conditioned the grant on LightSquared organizing and participating in a technical working group (TWG). The FCC tasked the TWG with analyzing a variety of types of GPS devices for their susceptibility to overload interference from LightSquared's terrestrial network of base stations, identifying near-term technical and operational measures that can be implemented to reduce the risk of overload interference to GPS devices, and providing recommendations on steps that can be taken going forward to permit broadband wireless services to be provided in the L-band MSS frequencies and coexist with GPS devices. The TWG consists of representatives from LightSquared, GPS manufacturers, and GPS users (federal and non-federal). LightSquared is required to provide periodic status reports on the progress made by the TWG and submit a final report by June 15, 2011, which addresses the tasks identified by the FCC.

1.1.4 FAA Request to RTCA

Since the extent and impact of the interference to aviation GPS receivers and to GPS-based aviation operations was unknown, the Federal Aviation Administration (FAA) asked RTCA to undertake studies of this source of potential radio frequency interference[2]. These studies "should include receiver vulnerability, as well as [operational] scenario studies including aggregate effects of LightSquared transmissions on GPS receivers used in aircraft." In order to provide timely input to the FAA, RTCA was requested to work in parallel with the FCC-mandated TWG and deliver a final report of its independent evaluation to the FAA by June 3, 2011. The RTCA Program Management Committee accepted this request March 17, 2011, as consistent with the existing Terms of Reference of RTCA SC-159 (Global Positioning System).

1.2 Terms of Reference

RTCA SC-159 develops minimum standards that form the basis of FAA approval of equipment using GPS as a primary means of civil aircraft navigation. One of its terms of reference (#6) is to address GPS receiver susceptibility to radio frequency interference (RFI). SC-159 Working Group 6 (WG-6), organized to perform and document detailed GPS RFI studies, has two specific terms that apply to the particular FAA request:

Develop quantitative assessments of the current and projected RF interference (RFI) environment;

Recommend measures to reduce RFI at the source where it is technically feasible and cost-effective to do so.

[1] LightSquared Subsidiary LLC, Request for Modification of its Authority for an Ancillary Terrestrial Component, Order and Authorization, DA 11-133 (Chief, International Bureau, 26 Jan., 2011)

[2] Letter to RTCA President, Margaret Jenny, from R. A. Frazier, Acting Group Manager, FAA Spectrum Engineering Services, RTCA Paper No. 047-11/PMC-881, 3 Mar. 2011

©2011 RTCA, Inc.

1.3 Assessment Study Objectives

To address the FAA request, the assessment study objectives are to determine:

1. impact on GPS airborne receiver performance from fundamental emissions of a single LightSquared ATCt base station

and, through operational scenario analyses,

2. aggregate emissions impact from a distribution of LightSquared ATCt base and mobile stations on GPS airborne receivers and GPS receiver-based aviation operations.

The primary focus of the RFI effects analyses in this report is the LightSquared Phase 0 deployment (details in Section 2.4) and certain RFI effects of later planned and potential deployment phases are also considered.

1.4 Report Organization

Besides this introduction section, the report main body is organized into five more major sections with supporting material contained in five appendices. Section 2 describes the basic analysis framework and key model parameters of the RFI sources, GPS receiver, and the radio propagation path. Section 3 details five operational scenarios that each pull in various aspects of the RFI source, receiver, and propagation path to set up the analysis cases. Section 4 describes computations for each of the five operational scenarios and compares aggregate received RFI results against receiver susceptibility limits. Section 5, Possible RFI Mitigation Techniques, briefly describes some possible RFI source and GPS receiver measures to mitigate the estimated RFI effects. Section 6 contains the summary, conclusions, and recommendations.

Appendix A contains a GPS MOPS-based aviation receiver test procedure for wide bandwidth near-band RFI effects. Appendix B contains a detailed description of the aggregate RFI analysis method and the scenario analysis details. Appendix C contains detail of the GPS aviation receiver susceptibility to in- and near-band RFI (including an estimate of the RF front-end third-order intermodulation effect). Appendix D contains a summary of laboratory RFI measurement results on production GPS receivers. Appendix E contains a list of report acronyms, abbreviations, and definitions.

1.5 References

[1-1] SC-159, “Assessment of Radio Frequency Interference Relevant to the GNSS L1 Frequency Band,” RTCA Document No. RTCA/DO-235B, 13 Mar. 2008.

©2011 RTCA, Inc.

This page intentionally left blank.

©2011 RTCA, Inc.

2 AERONAUTICAL RFI EFFECTS ANALYSIS METHOD

After a brief introduction on the basic analysis method, the remaining subsections give RFI analysis method element descriptions for the GPS receiver, propagation path models, and LightSquared ATCt base and mobile sources. These elements are brought together in the RFI scenarios described in Section 3 to form the complete analysis model set. That set is used in Section 4 to determine aggregate RFI effects on GNSS L1 band aviation operations.

2.1 Introduction and Basic Methodology

The basic framework for the RFI effects analysis in this report is the classic source-path-receiver method used in previous RTCA SC-159 analyses [2-1]. For RFI sources the method prescribes collection of key parameters such as EIRP (both fundamental and unwanted) and carrier frequency, antenna gain pattern, and modulation type and spectral shape. For the aggregate RFI analysis in this report, information on number of RFI sources and source-to-source spacing is also needed. Key characteristics collected for the "path" element include distances and directions from the receiver to the RFI sources, propagation type (free-space or other type), and propagation statistics. The path parameters are determined largely by the particular RFI encounter scenario to be analyzed (details in Section 3). Key characteristics for the receiver generally include signal sensitivity, selectivity, RFI susceptibility, receive antenna gain patterns, and minimum performance requirements. The receiver RFI susceptibility and performance requirements form the basis for comparison in Section 4 of RFI effects analyses of the ATCt base and mobile stations.

2.2 GPS Receiver Performance and RFI Susceptibility Model

2.2.1 General RFI Effects on Aeronautical GPS Receivers

An aeronautical GPS receiver typically acquires and tracks satellite signals using both code and carrier phase-tracking loops. The carrier phase provides two important functions for an aviation receiver: a reference to demodulate the satellite signal phase modulated data, and a means to smooth out the large fluctuations in the code delay measurements from the code tracking loop. As the RFI level increases, phase error increases until the carrier-tracking loop has cycle slips and eventually no longer tracks the satellite signal. Aircraft dynamics limit the amount of averaging that can be applied.

In addition to directly affecting the range measurement accuracy and data demodulation performance, RFI can also impact receiver integrity monitor performance. The required receiver monitoring function estimates the navigation error using a number of inputs that include local real-time signal quality, SBAS (WAAS) and GBAS (LAAS) data on the satellite constellation health, and ABAS (RAIM) autonomous satellite fault detection[1]. RFI can increase the pseudorange measurement variance. Excessive RFI could therefore cause the navigation error estimate at some point to exceed prescribed limits. RFI can also increase GNSS satellite data parity errors and SBAS message error rates and ultimately deprive the receiver of timely constellation health status and other necessary data.

[1] SBAS, GBAS and ABAS are ICAO terms referring, respectively, to Satellite-Based, Ground-Based, and Aircraft-Based Augmentation Systems. The parenthetical terms WAAS and LAAS are FAA augmentation system names. Refer to Appendix E.

©2011 RTCA, Inc.

2.2.2 GPS L1 Receiver RFI Effects Model

The L1 GPS receiver system model in this assessment is a "minimum operational performance" model [2-1], i.e.; the least complex configuration needed to meet GPS L1 MOPS performance requirements. The RFI model used here assumes GPS equipment (Figure 2-1) comprising an active antenna unit (requirements per RTCA/DO-301) and the latest GPS/WAAS, /LAAS or /ABAS MOPS receiver (RTCA/DO-229D, DO-253C, DO-316, respectively). Desired satellite signal, system noise, and RFI levels are referenced to Point A, the output terminal of the passive antenna radiating element. Discussion of earlier generation GPS receivers is contained in Appendix C.3.

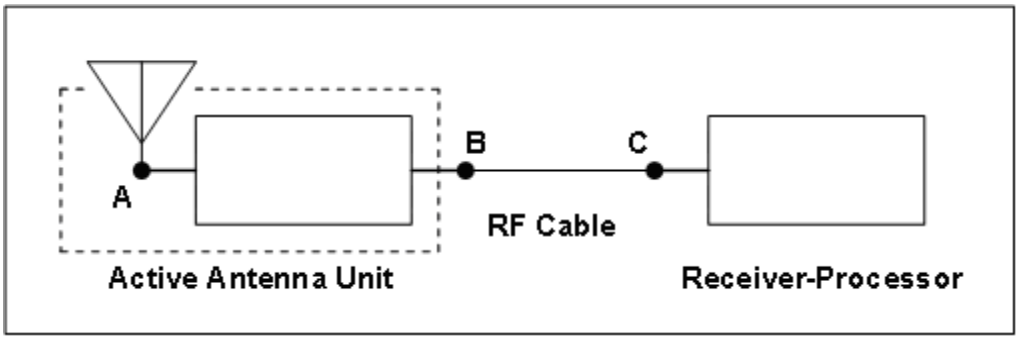

Figure 2-1 GPS L1 Receive System Block Diagram

2.2.2.1 GPS L1 Antenna and Receiver RF Front-end Performance Model

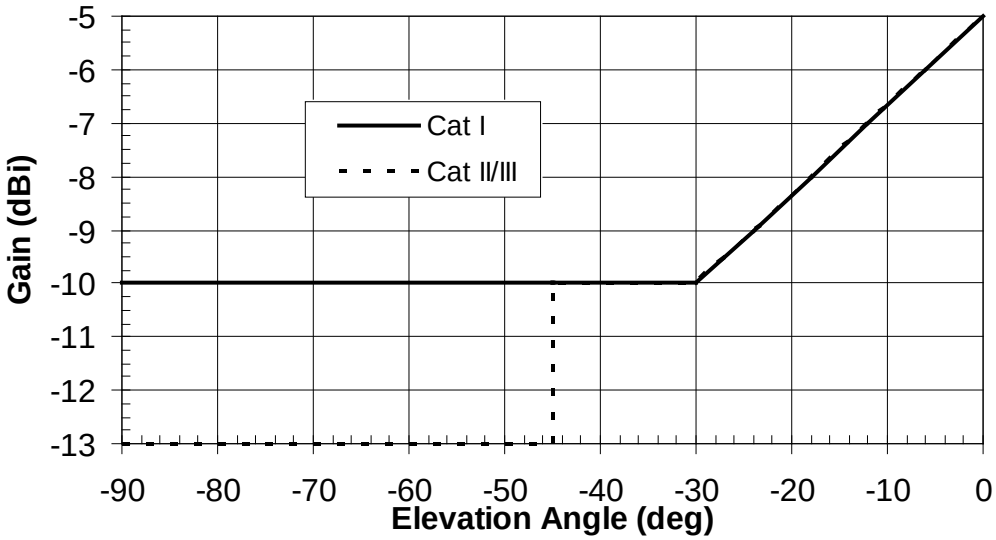

Figure 2-2 GPS Receive Antenna Lower Hemisphere Max. Gain Model
(G_{RCV-1} = -10 dBi for -90° ≤ el <-30°; = -10+(5+elev/6) for -30°≤ el ≤ 0°)
(G_{RCV-2} = -13 dBi, el <-45°, = -10 dBi,-45° < el < -30°; =-10+(5+el/6), -30°≤ el ≤ 0°)

Receive antenna maximum gain limit models, for the lower and upper hemisphere, have been developed for previous RFI analyses. They represent the aircraft-installed GPS antenna pattern limits (referenced to Point A, Figure 2-1) for linear vertical polarization, the assumed polarization from the ATCt sources. The lower hemisphere pattern model (Figure 2-2) is taken directly from RTCA/DO-235B [2-1]. The upper hemisphere vertical polarization model (Figure 2-3) is derived from the RTCA/DO-235B model maximum circular polarization gain by subtracting 3 dB from each point. Gain model equations are listed under each figure. The receiver system model (Figure 2-1) has 513 K

©2011 RTCA, Inc.

input thermal noise temperature (maximum), which includes an estimated 100 K sky noise (black-body radiation).

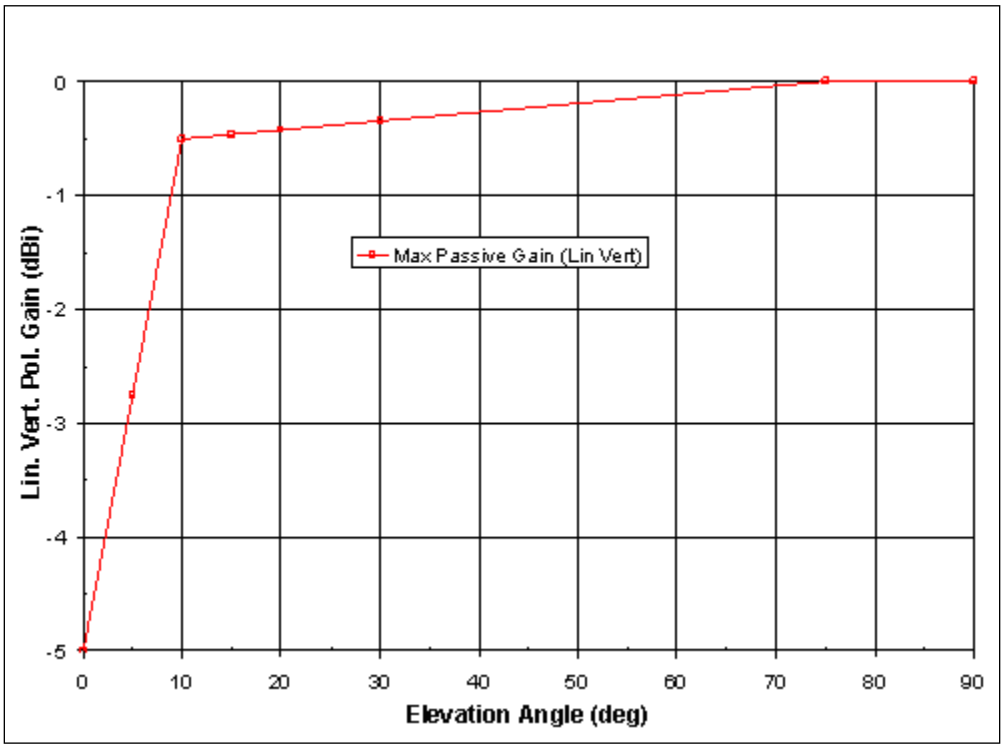

Figure 2-3 GPS Receive Antenna Upper Hemisphere Max. Gain Model
(G_{RCV} = 0 dBi, 75°≤ el; = -0.5+0.0077·(el-10), 10°≤ el ≤ 75°; = -5+4.5·el, 0 ≤ el < 10°)

2.2.2.2 GPS L1 Narrow- and Wide-bandwidth Near-band RFI Effect Models

Appendix C has a detailed plot of the required maximum narrow bandwidth (CW) interference test condition under which the GPS aviation receiver must be able to meet basic performance requirements (e.g,, measurement accuracy, data demodulation). That CW power limit curve is given as a function of interference center frequency (in dBm, Point A, Figure 2-1) by: $P_{TEST}(f)$ = -120.5 + 2.6843·(1565.42-f), for f ≤ 1565.42 MHz. Particular points on the limit curve are specified test conditions for certain GPS receiver MOPS performance tests (e.g., in RTCA/DO-229D [2-2]). The spectrum management strategy for this interference is to keep the mean RFI environment at least 6 dB below this receiver test limit as a safety margin[1] [2-1, Section 2.6.3]. The total power limit for narrowband emissions below 1565.42 MHz (in dBm) is then:

$$P_{ENV}(f) = -126.5+2.6843\cdot(1565.42-f). \qquad \text{Equation 2-1}$$

For initial acquisition, for the purposes of this study, the test limit curve is 6 dB lower than for tracking. Although the MOPS only specifies this adjustment for in- and near-band interference, a 6 dB adjustment for out-of-band interference is provided for in ICAO SARPs and is consistent with the need for higher C/N_0 for initial acquisition versus tracking as derived in [2-1]. With safety margin incorporated, the initial acquisition environmental total RFI power limit (dBm) is, by similarity

$$Pacq_{ENV}(f) = -132.5+2.6843\cdot(1565.42-f).$$

[1] The safety margin is to account for adverse deviations from the mean and other factors not quantifiable in the model. See also recommendation ITU-R M.1477.

©2011 RTCA, Inc.

The principal effect mechanism of a single strong near-band RFI signal, such as from an ATCt base station, is overload of the receiver selectivity that results in receiver RF/IF gain compression for the desired signal. Other degradation mechanisms are possible; overload was chosen for simplicity. This effect mechanism is modeled initially for this report as a function of total received RFI power essentially independent of RFI signal bandwidth. The P_{ENV} equation (in dBW/MHz for a 5 MHz bandwidth signal) becomes:

$$PSD5_{ENV}(f) = -163.5 + 2.6843 \cdot (1565.42 - f). \qquad \text{Equation 2-2}$$

Thus at 1552.7 MHz, the ATCt base station planned uppermost channel center (see 2.4.4.1), $PSD5_{ENV}$ = -129.36 dBW/MHz.

The other principal near-band ATCt base station RFI mechanism, third-order intermodulation distortion, which generates a modulated RFI signal in the GPS receiver passband, is discussed further in Appendix C.

2.2.2.3 GPS L1 Wide- and Narrow- Bandwidth In-band RFI Effect Model

For in-band RFI, GPS receivers have a wideband RFI test limit representing aeronautical RFI sources, of -141.9 dBW/MHz (Point A, Figure 2-1). It also has a simultaneous wideband RFI power spectral density test limit representing non-aeronautical sources, of -140.5 dBW/MHz, at 1575.42 ± 10 MHz. After applying the 6 dB safety margin for the non-aeronautical source component, that environment limit becomes -146.5 dBW/MHz. Receiver performance with these source components present has been determined previously [2-1]. Therefore this report will use the environment limit -146.5 dBW/MHz as the basis for comparison with ATCt unwanted RFI analysis results. Although not explicitly used in this report, the narrow bandwidth RFI test limit is -150.5 dBW (0-1 kHz bandwidth).

2.3 RFI Propagation Path Models

2.3.1 Background

All the RFI propagation path loss models used in this report are based on the flat-earth approximation. In other words, the ground under the aircraft is assumed to be essentially smooth and flat out to a radio horizon radius from the point on the ground directly under the aircraft. In line-of-sight propagation conditions at radio frequencies near the GPS L1 carrier, this radio horizon value depends, in general, on the aircraft GNSS and RFI source antenna heights and the amount of atmospheric refraction along the path. This report uses the 4/3 Earth radius approximation for the refractive effect on the radio horizon.

Two general propagation model categories are used in this report to evaluate the impact of LightSquared ATCt base and mobile unit RFI to airborne GPS receivers. Those scenarios where blockage is a factor are typically evaluated using probabilistic models while clear line of sight scenarios are analyzed using free space path loss.

Four of the five scenarios described in Section 3 of this report involve environments in which emissions from LightSquared equipment undergo scattering, reflections, and absorption prior to arriving at an aircraft's GPS antenna. The analysis of these scenarios must incorporate propagation models that adequately address such random propagation phenomena. These propagation environments were the subject of much research during the development of cellular radio systems. As a result, the cellular radio community has over the years developed propagation models which for the most part are applicable to the present RFI evaluation scenarios.

In this report the point above which a free space path loss is used is an aircraft antenna height of 550 meters. Above 550 meters, various parameter limits associated with the

©2011 RTCA, Inc.

probabilistic models are exceeded thereby making their use problematic. Also at these aircraft heights, line of sight conditions generally prevail which means that free space path loss is the more appropriate model.

Below the 550 meter aircraft antenna height the probabilistic models developed by the cellular radio community become applicable. Each of these models has one feature in common; the probabilistic nature of the path loss is very well approximated by a log-normal probability distribution. A log-normal distribution is completely determined by two parameters, μ and σ. The range-dependent median path loss between the GPS antenna and interference source determines the parameter μ while σ is generally invariant with range (See Appendix B.2.1.2).

The median isotropic path loss model for aircraft antenna height values below 550 meters consists in general of 3 segments appropriately blended together. They form a continuous function of the lateral separation radius, *r* (in meters) between the aircraft and RFI source antennas. For radii less than a few hundred meters, conventional 2-Ray propagation is chosen. That model assumes a direct path ray between the 2 antennas interacts with one other ray reflected from the ground between antennas. For radii greater than about 1 km, the Hata-Okumura suburban propagation model [2-3] is chosen. At radii beyond 20 km, a long-distance extension is made to the standard Hata-Okumura formulation. If necessary to achieve path loss continuity, the 2-Ray and Hata-Okumura model segments are connected together by one of two means. One means is by a constant-slope logarithmic fit function that covers radius values in between the segment ranges. The other means used in ATCt mobile station scenarios with aircraft heights below 80 m is a modified Erceg/Greenstein path loss segment. Since the median isotropic path loss is generally a function of the aircraft and RFI source antenna heights, the path loss model is adapted to each specific RFI scenario. The path loss examples in the following subsections are all computed at 1552.7 MHz.

2.3.2 Short-Range Path Segment (Two-Ray) Model

Measurements indicate that at short ranges, where few obstructions are present, the GPS antenna receives interference from an RFI source by both a direct and a reflected path. On the reflected path, the electromagnetic wave is reflected from the earth's surface with a range-dependent complex reflection coefficient $\rho_V(r)$. In addition to the relative phase delay between the direct and reflected rays, the complex reflection coefficient both attenuates and adds phase shift to the reflected ray. When the two rays additively combine at the receive antenna, the resulting received power fluctuates with range r. Hence the path loss, defined as (received power)/(transmitted power), fluctuates as shown in Figure 2-4.

©2011 RTCA, Inc.

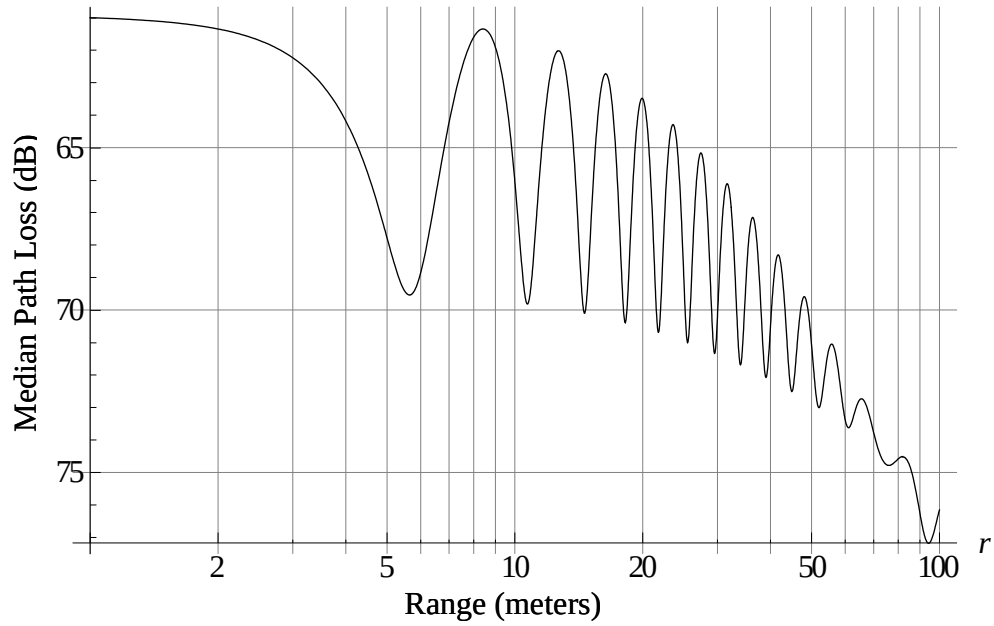

Figure 2-4 Example Two-Ray Median Path Loss

Since the path loss (Figure 2-4) at a range r is the median value, there is a 50% chance that the actual path loss will be greater than what the graph line shows and 50% chance that it will be less. The probability that the path loss will take on any particular value is given by the log-normal distribution.

This two-ray median path loss model is applicable to ranges of a few hundred meters and is used in the analysis of several of the interference scenarios as discussed in this report. The mathematical details of the two ray path loss model can be found in Appendix B (see B.3.1.1.1).

2.3.3 Medium-Range Path Segment Model

Median path loss models were initially developed for cellular mobile phones at lateral separation ranges beyond 1 km and out to 20 km. This left a need for some type of model to cover ranges from 100 meters out to 1 km. In the mid 1990's this need was met by researchers from ATT Laboratories who developed a mid-range model that came to be known as the Erceg/Greenstein model [2-4]. Their model pertains to ranges from 100 meters out to 8 km with base station antenna heights between 10 and 80 meters and a mobile unit antenna height of 2 meters. The model was developed for suburban environments using three different terrain categories to make it more flexible. An operating frequency of 1.9 GHz was used in developing the model although extrapolations to other frequencies are possible. In the Erceg/Greenstein model the median path loss is proportional to $(r / r_o)^{\gamma}$ where r_o is usually taken to be 100 meters. The loss exponent γ changes with terrain type but is greater than 2 meaning that the path loss is more severe than that associated with a free space model. A modification of the Erceg/Greenstein model is used at medium ranges in analyzing several of the LightSquared interference scenarios. The modification involves the standard deviation about the median path loss that is allowed by the model. The classic Erceg/ Greenstein model has the actual path loss variation about the median increasing slightly as the range gets larger. The modified model holds this variance constant over all ranges. Figure 2-5 shows a sample median path loss produced by the modified Erceg/Greenstein model.

©2011 RTCA, Inc.

Since the path loss (Figure 2-5) at a range *r* is a median value, there is a 50% chance that the path loss will be above the graph line and 50% chance it will fall below the line.

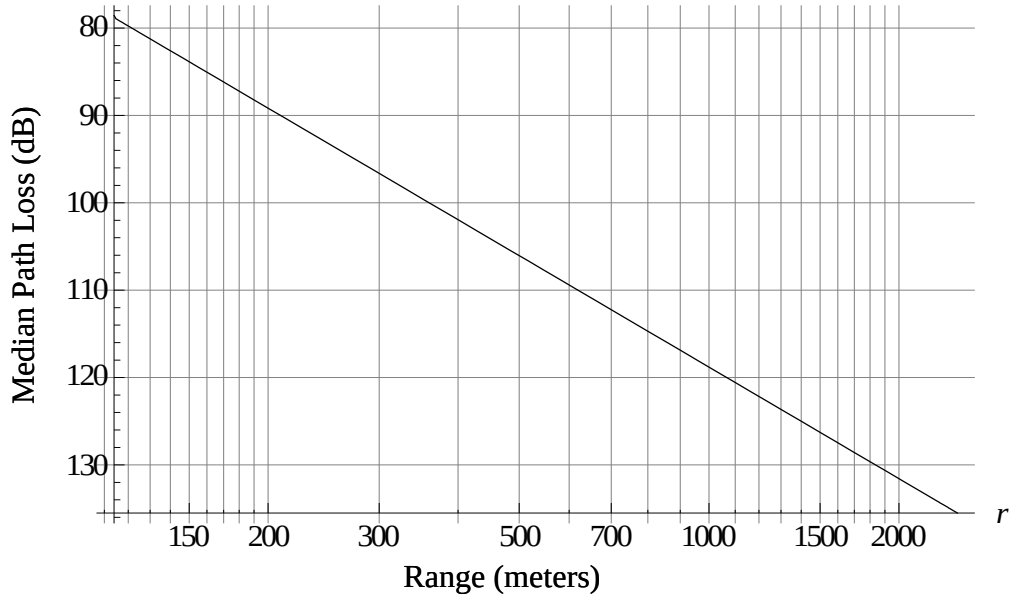

Figure 2-5 Example Erceg/Greenstein Median Path Loss

Because the Erceg/Greenstein model limits the lower of the two antenna heights involved to 2 m, the model is only used in this report to evaluate the ATCt mobile unit RFI. The ATCt base station RFI evaluations use a constant-slope logarithmic fit function that covers radius values between the short and long range model segments.

2.3.4 Long-Range Path Model

For propagation from RFI sources at distances beyond about 1 km from the aircraft antenna, the well-known Hata-Okumura median path loss model is used. It was originally developed for predicting UHF cellular mobile telephone propagation at distances beyond 1 km from the base station for three terrain types: urban areas, suburban areas and open areas. In this report the suburban terrain parameters are used to represent the environment around a large metropolitan airport. As with the Erceg/Greenstein model, the Hata-Okumura path loss is proportional to $(r / r_o)^{\gamma}$ but in this case r_o is set to 1000 meters. The exponent γ varies with antenna height, and with range as well as operating frequency for those ranges beyond 20 km. With the ITU-R extension to the original model, it is useable to ranges of 100 km. Figure 2-6 shows the median path loss generated by the Hata-Okumura model.

©2011 RTCA, Inc.

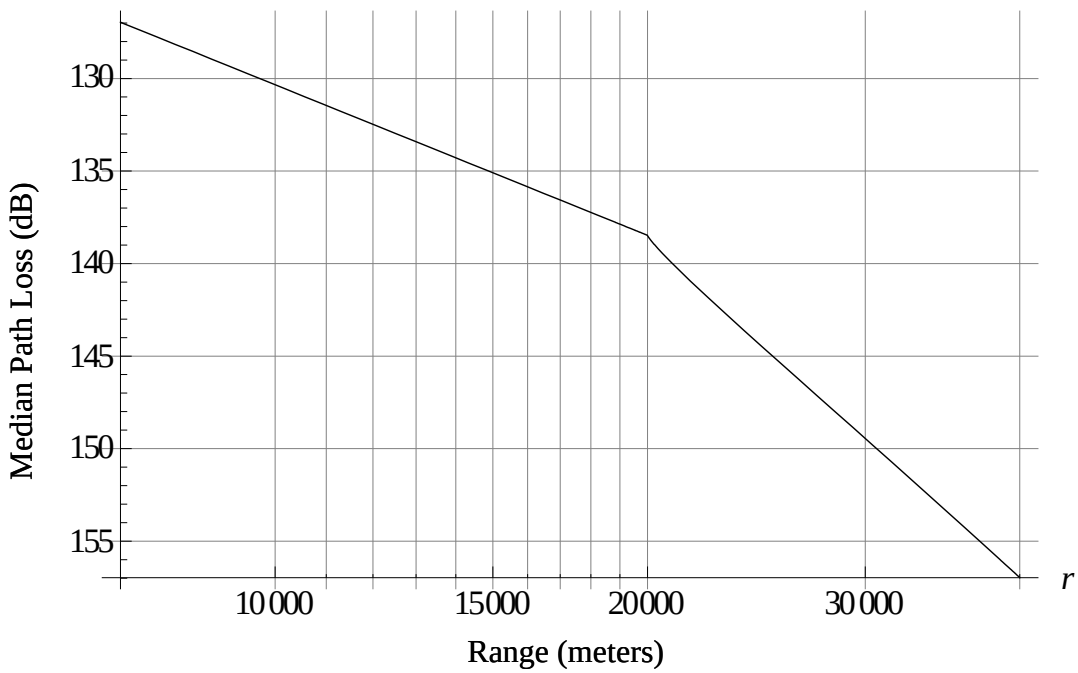

Figure 2-6 Example Hata-Okumura Median Path Loss

As in the other models, since the path loss (Figure 2-6) at a range *r* is a median value, there is a 50% chance that the path loss will be above the graph line and 50% chance it will fall below the line. Mathematical details regarding the Hata-Okumura model can be found in Appendix B (B.3.1.1.2).

2.3.5 Free-Space Path Model

In the high altitude enroute scenario there is predominately clear line of sight to all the interfering cell towers. In such cases a free space path loss model is most appropriate. It is the most basic model in which the path loss is proportional to the square of the separation range. This is a deterministic model with no associated probability distribution. Hence the path loss can be exactly determined once the range between GPS antenna and interfering source is known. It is also the model (among those applicable to this report), that in equivalent range scenarios, produces the least path loss. Although it yields the lowest path loss, the long range values in the high altitude enroute scenario already reduce interference levels. More discussion on free space path loss can be found in Appendix B (B.3.1.2).

2.4 LightSquared ATCt Base and Mobile Station Emission Models

This section describes LightSquared ATCt base station and mobile station/User Equipment (UE) technical characteristics as related to RFI analysis. This includes in-band and out-of-band emission power levels, transmit antenna gain and radiation patterns, and other pertinent information to predict RFI levels. ATCt base and mobile station operational parameters in the following subsections are from the LightSquared development plans briefed to SC-159, except where indicated in the text. As a result, transmission signal characteristics do not necessarily represent the worst case (from a GPS interference standpoint) scenario permitted by FCC authorization.

©2011 RTCA, Inc.

2.4.1 ATCt Base and Mobile Station Emission Parameters

2.4.1.1 ATCt Base Station Emission Parameters

LightSquared's present deployment plans call for a maximum of 62 dBm[1] (32 dBW) EIRP per channel. As LightSquared plans to deploy up to two channels per sector, EIRP per sector will be up to 65 dBm (35 dBW) per sector.

The out-of-channel emission (OOCE)[2] power spectral density (PSD) limits at the transmit antenna output (including the antenna gain) are as follows:

- At 1 MHz offset from edge of ATCt channel: - 32.4 dBW/MHz
- At 2 MHz offset from edge of ATCt channel: - 39.4 dBW/MHz

The out-of-band emission (OOBE) PSD limits are as follows:

- In the RNSS band (1559 – 1610 MHz) band: -100 dBW/MHz (1 MHz bandwidth)
  -110 dBW discrete in 1 kHz bandwidth
- In the AMT band (1435 – 1525 MHz) the limits are per 47 CFR 25.202(f):

Table 2-1 LightSquared AMT Band Unwanted Emission Limits

Frequency offset (f_offset) from the FCC authorized bandwidth (B)	Attenuation (dB) below the mean output power in watts (P) of the transmitter	Measurement bandwidth
B/2 ≤ f_offset < B	25	4 kHz
B ≤ f_offset < 5B/2	35	4 kHz
5B/2 ≤ f_offset	43 + 10log(P)	4 kHz

LightSquared has three planned spectrum deployment phases:

- Phase 0: One 5 MHz channel: 1550.2 MHz - 1555.2 MHz, 62 dBm EIRP per 5 MHz channel.
- Phase 1: Two 5 MHz channels: 1526.3 MHz -1531.3 MHz & 1550.2 MHz - 1555.2 MHz, 62 dBm EIRP per 5 MHz channel.
- Phase 2: Two 10 MHz channels: 1526 MHz -1536 MHz & 1545.2 MHz - 1555.2 MHz, 62 dBm EIRP per 10 MHz channel.

The channel modulation is 3GPP LTE (OFDM).

Network loading effect: 2.2 dB reduction from maximum aggregate transmit EIRP

*Note: In a 4G LTE network not all the sites will be transmitting on all subcarriers at the same time and networks are typically designed with 60% load during busy hour. When a large number of base stations are considered for an aggregate interference calculations, the average Tx EIRP per base station would be 2.2 dB (10 * LOG_{10} (0.6)) lower than the maximum EIRP of 32 dBW. In non-busy hour the network loading will be even smaller.*

2.4.1.2 ATCt Mobile Station (User Equipment) Emission Parameters

LightSquared's deployment plans call for a maximum EIRP of +23 dBm (-7 dBW) from its UE device. When communicating with LightSquared towers, LightSquared User Equipment (UE) will transmit in the MSS uplink L-band (1626.5 MHz -1660.5 MHz).

[1] FCC authorization allows a maximum EIRP of 42 dBW

[2] The term "OOCE" is used to refer to adjacent channel emissions that are contained within the MSS L-band. When these emission fall outside the MSS L-band, they are referred to as OOBE.

©2011 RTCA, Inc.

LightSquared has three spectrum deployment phases:

- Phase 0: One 5 MHz channel: 1651.7 MHz - 1656.7 MHz with smallest bandwidth a user can transmit is 180 kHz
- Phase 1: Two 5 MHz channels: 1627.8 MHz - 1632.8 MHz & 1651.7 MHz - 1656.7 MHz with smallest bandwidth a user can transmit is 180 kHz
- Phase 2: Two 10 MHz channels: 1627.5 MHz - 1637.5 MHz & 1646.7 MHz - 1656.7 MHz with smallest bandwidth a user can transmit is 180 kHz

The out-of-channel emission (OOCE) limit is -58dBW/4kHz at 1 MHz offset beyond the edges of assigned spectrum bands.

The out-of-band emission (OOBE) limit in the adjacent RNSS band (1559 – 1610 MHz) is -90 dBW/MHz wideband (1 MHz bandwidth) initially, improving to -95 dBW/MHz after 5 years of start of service. Narrowband OOBE limits are -100 and -105 dBW, respectively, in a 1 kHz bandwidth.

Average UE transmit power backoff: 10 dB

Note: LTE systems, employ (UE) uplink power control. This power control is used for interference management and to make the most efficient use of UE power, while the link quality is maintained. The power control is driven by the uplink data rate assigned to the UE by the base station Scheduler. It is very unlikely that all UEs will be transmitting at their maximum data rates simultaneously. When a large number of UEs are considered for an aggregate interference calculation, the average Tx EIRP per UE is expected to be at least 10 dB lower than the maximum EIRP of 23 dBm. However, since the RFI effect on the GPS receiver is from UE unwanted emissions more that 52 MHz below the UE carrier, the assumed unwanted EIRP value for analysis in this report is the OOBE limit independent of power control.

2.4.2 ATCt Base Station Antenna Pattern and Siting Parameters

2.4.2.1 ATCt Base Station Antenna Pattern Parameters

The typical base station sector antenna characteristics are listed below. The lower and upper hemisphere vertical radiation patterns models are shown in Figure 2-7 and Figure 2-8. The base station antenna height assumed in this report is 30 meters.

- Horizontal plane beam width (-3 dB): 66.32 degrees
- Vertical plane beam width (-3 dB): 7.95 degrees
- Gain: 16.5 dBi
- Front to back ratio: 35.03 dB
- Electrical down tilt: 2 degrees (elevation)
- Polarization: +45 and – 45 degrees, linear, cross polarized

The lower and upper hemisphere vertical plane relative gain pattern models for the analysis were derived, within SC-159, from principal plane measured data on a representative ATCt base station sector antenna. The sidelobe relative gain levels were set to represent actual vertical plane sidelobe values without the minor lobe details. In both hemispheres this simplification helps to reduces model complexity. It also covers for the lack of data over the azimuth sector from vertical plane pattern cuts at other azimuth angles. The main beam relative gain (in dB versus elevation) is modeled by a simple parabolic fit equation:

$G_{REL}(elev) = -0.181818 \cdot (2+elev°)^2$ for elevation angles $-11° \leq elev \leq +9°$

©2011 RTCA, Inc.

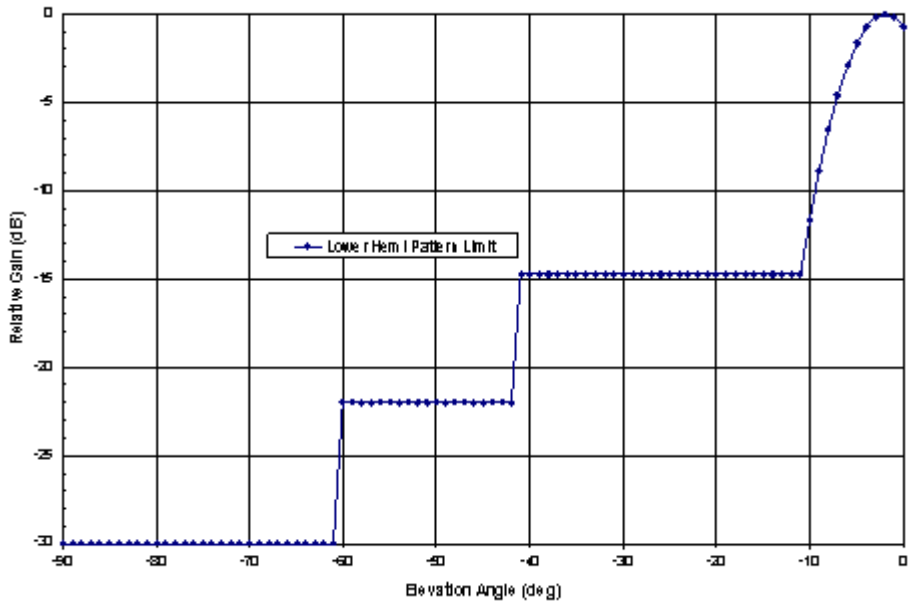

Figure 2-7 ATCt Base Station Lower Hemisphere Vertical Gain Pattern Model

In the RFI analysis the lower hemisphere vertical pattern model (Figure 2-7) is used at all azimuth angles without correction for azimuth plane scalloping effect due to the sector azimuth beamwidth. This represents a reasonable upper bound for the actual lower hemisphere pattern where scattering from the ground and structures tends to make coverage away from beam center in azimuth angle more uniform over a sector.

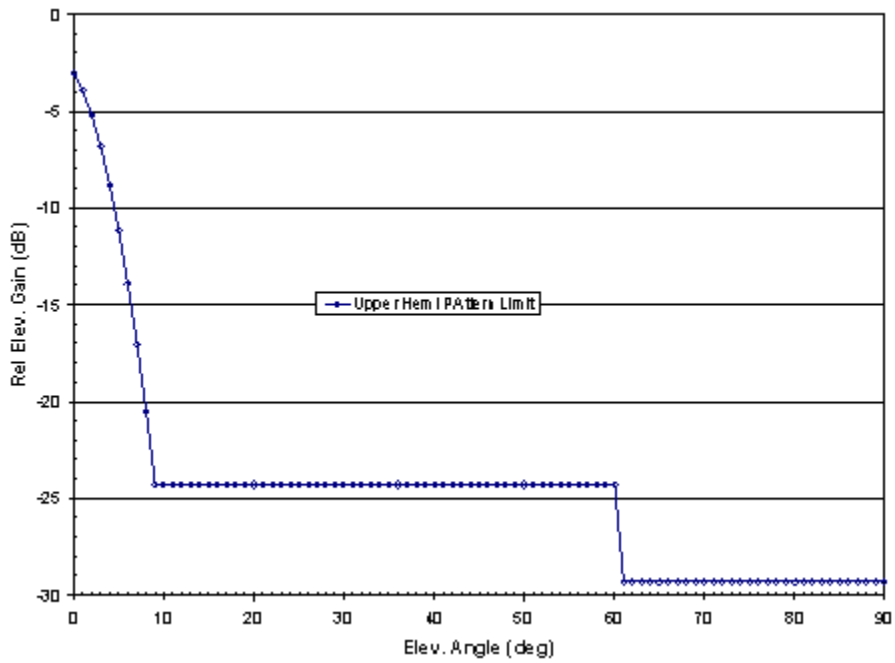

Figure 2-8 ATCt Base Station Upper Hemisphere Vertical Gain Pattern Model

For the upper hemisphere vertical pattern model (Figure 2-8), every vertical pattern point in the main beam and sidelobe regions is reduced by 2.3 dB to represent an average of the azimuth sector beam pattern scalloping effect over each sector.

©2011 RTCA, Inc.

2.4.2.2 ATCt Base Station Location Parameters

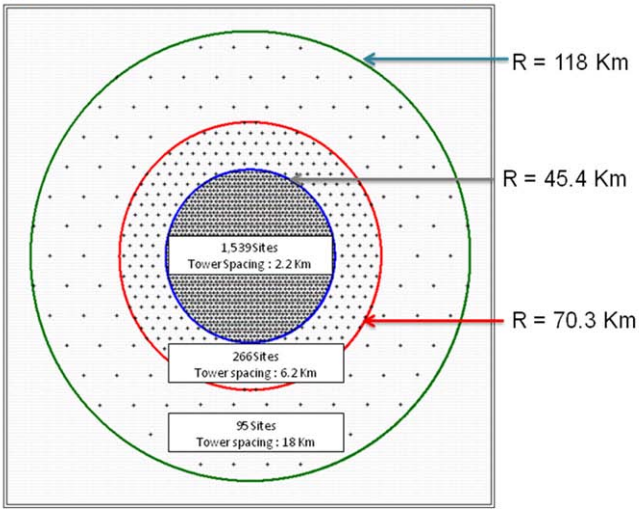

Figure 2-9 ATCt Base Station Single-City Tower Concentration Pattern

In typical 4G network installations, average inter cell (base station) tower distance varies, and depends on user density and morphology. For the purpose of calculating aggregate path loss to the aircraft, the coverage area of a single city is modeled as shown in Figure 2-9 with three concentric circles. The inner circle with a radius of ~ 45 km is most densely populated with an average cell tower spacing of 2.2 km and represents dense-urban/urban environment. Next to the inner circle, a middle ring area between radii of 45 km and 70 km represents suburban environment with cell tower average spacing of 6.2 km. Finally, an outer ring area between radii of 70 km and 118 km represents a rural environment with cell tower average spacing of 18 km[1].

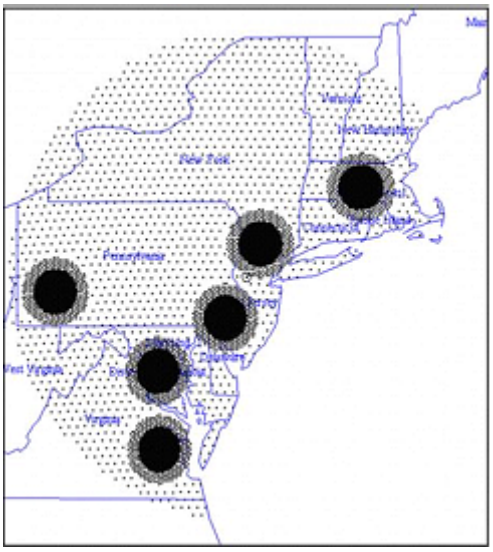

Figure 2-10 ATCt Base Station Multi-City Tower Concentration Pattern

At a higher aircraft altitude the radio horizon distance becomes larger and covers multiple cities as shown in Figure 2-10. The multicity scenario is modeled by assuming rural area base station density beyond the single city coverage radius of 70 km. The multi-city scenario has a total of 9,223 sites in the 6 dense areas (dark spots, ~90 km diam.), 1,583

[1] The cell tower densities in the suburban and rural areas should be taken as signifying average values, not necessarily that the cell radius is half the average inter-site distance.

©2011 RTCA, Inc.

sites in the sparser areas (lighter gray, ~ 25 km thick rings), and 1,429 sites in the rural area for a total of 12,235 sites in the entire depicted region.

2.4.3 Mobile Station Antenna Pattern and Siting Parameters

2.4.3.1 ATCt Mobile Station Antenna Pattern Parameters

The typical UE antenna characteristics are listed below.

- Azimuth from 0 to 360 degrees
- Max gain = - 2.41 dBi at azimuth = 105 degrees
- Elevation from 0 to 360 degrees where zenith is 0 degrees
- Max gain = - 4.01 dBi at Theta = 57 degrees (i.e. 43 degrees from horizon)

As mentioned previously (Section 2.4.1.2), the principal RFI effect on GNSS airborne receivers by the UE is from unwanted or unintentional RFI falling in the 1559-1610 MHz band. The OOBE EIRP limit (-90 dBW/MHz) is the value chosen for this report. The UE antenna model chosen for this report to represent the emission is an isotropic pattern (0 dBi). The mobile station antenna height assumed in this report is 1.8 meters.

2.4.3.2 ATCt Mobile Station Location and Concentration Parameters

The location of any particular mobile terminal within a cell is modeled as random but governed by a uniform probability distribution. Although base station control software controls the number of mobiles transmitting simultaneously, all units serviced in the cell that are transmitting or idling are assumed to be emitting either unwanted or unintentional emission at the OOBE limit (Sec. 2.4.1.2). Because of some uncertainty of the number of units in a cell, the analysis will cover a range of values for the count within a nominal 2.2 km cell radius: 100, 300, and 1000 units. The 300 unit count is believed to be a nominal value.

2.5 References

[2-1] SC-159, “Assessment of Radio Frequency Interference Relevant to the GNSS L1 Frequency Band,” RTCA Document No. RTCA/DO-235B, 13 Mar. 2008

[2-2] SC-159, “Minimum Operational Performance Standards for Global Position System/Wide Area Augmentation System Airborne Equipment,” RTCA Document No. RTCA/DO-229D, 13 Dec. 2006

[2-3] D. Parsons, *The Mobile Radio Propagation Channel*. Chichester, England: John Wiley & Sons, 1996

[2-4] V. Erceg, L.J. Greenstein, *et al*, “An Empirically Based Path Loss Model for Wireless Channels in Suburban Environments,” *IEEE Journal on Selected Areas in Communications*, vol. 17, no. 7, July 1999.

©2011 RTCA, Inc.

This page intentionally left blank.

©2011 RTCA, Inc.

3 AERONAUTICAL RFI ENCOUNTER SCENARIO DESCRIPTIONS

The RFI encounter scenario provides a description of the interaction between the sources of interference and a victim radio receiver. Elements of the scenario description for the receiver include the receiver location, motion, and function(s) being performed with associated requirements. Scenario elements for the RFI sources include location (relative to the receiver), motion, and, for aggregate RFI calculations, source-to-source spacing. The path element contains characteristics of the radio propagation path between the RFI source and the receiver, e.g. path geometry (distance, transmit and receive angles) propagation type (free-space or other), propagation statistics. In general, the scenario description also leverages basic operational characteristics of the receiver and RFI sources (see Section 2 for details). For an aeronautical GNSS RFI assessment, the encounter scenario defines the parameters of a representative limiting case RF link between the RFI source and the aircraft receiver, from which the electromagnetic compatibility between source and receiver can be determined.

3.1 Scenario Selection , General Features, and Other Related Aviation GPS Uses

Based on normal aircraft operations, five operational scenarios from past SC-159 reports were selected for the analyses in this report. Each operational scenario uses GNSS receivers[1] operating in the 1559-1610 MHz band and providing navigation for the aircraft. The selected scenarios are high altitude enroute operation, low altitude enroute and terminal area operation, Category I precision approach, Category II/III precision approach, and surface movement. The operational scenario names were retained here since they convey information regarding the aircraft evaluation point associated with each of the navigation scenarios.

3.1.1 RFI Encounter Scenario General Definition

Basic RFI encounter scenarios for each of the operations, developed within SC-159 for previous RFI assessments, were adapted to address the ATCt sources. As the actual basis for the RFI analyses, they will be described in detail in Section 3.2 and following subsections.

3.1.1.1 RFI Encounter Scenario - General Aircraft Location and Receiver Function

Each RFI encounter scenario places the aircraft at a certain representative location and height above ground for a given aircraft operation. In each scenario, the GNSS receiver is assumed to be tracking the desired navigation satellite and augmentation signals. In the surface movement, low altitude, and high altitude enroute scenarios, the receiver may also be acquiring new satellite signals.

Satellite acquisition may either be routine due to initial receiver power-up or normal satellite rising and setting or it can be as a result of some significant interruption of normal receiver operation. Causes of a significant interruption include a receiver power interruption, long duration RFI, or abrupt aircraft maneuver. The receiver RFI test condition for initial acquisition is 6 dB lower than for signal tracking (Section 2.2.2).

3.1.1.2 RFI Encounter Scenario ATCt RFI Sources

The scenarios in this report address two different sets of RFI sources. The primary RFI sources are a collection of ATCt base stations, each of which is a fixed source located on

[1] GPS receiver outputs are already in use or are being developed for use in each of these operations.

©2011 RTCA, Inc.

the ground with a particular spacing to adjacent base stations. The second set of RFI sources are the ground-based ATCt mobile terminals associated with each base station. By definition this source type is mobile, but for the purposes of these scenarios the mobile terminals will be considered to be essentially fixed emitters, randomly located within a cell, with a specified surface concentration within a cell.

3.1.1.3 RFI Encounter Scenario Key Geometry Features

One key geometric factor for each scenario for aggregate RFI is the lateral separation radius between each RFI source antenna and the GNSS receive antenna. The lower altitude scenarios each have constraints on base station antenna placement based on airport and approach layout guidelines [3-1][1]. Another key factor for each scenario is the relative angle-of-arrival of the RFI, which determines both the GNSS receive antenna gain toward the RFI source and the RFI source transmit antenna gain.

3.1.1.4 RFI Encounter Scenario Baseline Non-ATCt RFI

Each of the scenarios assume the presence of a certain amount (scenario-dependent) of baseline continuous RFI within the GNSS receiver passband from sources other than ATCt elements [3-2]. The group of aeronautically-related sources generally includes GNSS satellite self-interference (CDMA-like), unintentional RFI from non-transmitting installed avionics equipment, and unwanted RFI from installed avionics transmitters. The non-aeronautical source group generally includes certain on-board PEDs (enroute only) and a widely diverse set of off-board sources, both non-transmitting and licensed and unlicensed transmitting sources (e.g., conventional cellular and cordless phones, wireless LANs and PANs, 47 CFR 15 Class A and Class B digital devices, etc.).

3.1.2 Other Related Aviation GPS Uses

Although the study was based upon these five navigation scenarios, GPS aviation use is not limited to navigation applications and operations. This study is representative of, but does not directly address, all aviation use of GPS. For the purposes of this study, compatibility with all encounter scenarios would tend to imply compatibility with current and planned expanded use of GPS. Table 3-1 identifies current applications and operations using GPS. The majority of entries in Table 3-1 “map” to both the study’s low altitude terminal area and/or high altitude enroute encounter scenarios. For surface movement operations, there is currently limited approved operational credit for GPS use, although there are significant operational benefits (e.g. own ship situational awareness) today and surface movement applications for operational credit are in work. Surface movement scenarios must ensure that GPS signals are acquired by the navigation/positioning equipment during maintenance and pilots’ pre-flight system checks for any planned or required use of GPS.

[1] The FAA’s Airport Design Guidelines define obstacle clearance surfaces, object free areas, and controlled activity areas surrounding the airport and the extended runway centerline. These regions are used to identify exclusion zones where ATCt base stations and/or mobile terminals will not be present. See Appendix B for more details.

©2011 RTCA, Inc.

Table 3-1 Current Aircraft Uses of GPS

Enroute and terminal area RNAV	Automatic Dependent Surveillance Broadcast
SIDS, STARS, RNP	Terrain Awareness & Warning System
RNP SAAAR/AR	Traffic Alert & Collision Avoidance System
WAAS LPV	Cockpit Position Display (moving map)
GLS approach	Low-cost Attitude-Heading Reference System
Automatic landing and rollout	Weather Radar Optimization
Missed approach	Emergency Locator Transmitter
Guided take-off / departure	Synthetic Vision System

Before dispatch, GPS availability must be determined for the planned route of flight using preflight prediction tools. If GPS is determined to be unavailable, then the flight must be re-planned without use of GPS, or used only when and where GPS is predicted to be available. Any predictable interference would impact preflight planning and operational use of GPS. Additionally, non-aviation qualified GPS is extensively used for situational awareness in VFR flight operations that is not addressed by this study.

3.2 High Altitude Enroute RFI Encounter Scenario

This scenario represents an aircraft operating in the enroute portion of a flight. The aircraft is in high speed level flight at a representative limiting altitude of 18,000 feet. Two basic receiver modes are considered in this scenario: tracking and data demodulation of both GPS and SBAS satellite signals; and initial (warm-start) acquisition (see [3-3] for detailed requirements).

The baseline continuous RFI emissions present in this scenario include GNSS intra- and inter-system (CDMA) noise and on-board installed avionics emissions. Continuous passenger cabin aggregate PED emissions are assumed to be present along with the aggregate continuous emissions from a set of general ground-based RFI sources [3-2].

3.2.1 Basic High Altitude Scenario RFI Encounter Geometry

For the high altitude enroute scenario, the aircraft antenna is at a height of 5.49 km (18,000 feet). The base station antenna height is assumed to be 30 meters (see Section 2.4). The radio horizon radius for the GNSS receiver at this altitude is 328.2 km (based on a 4/3 Earth radius estimate). Depending on the location, the resulting visible area may include multiple metropolitan areas.

3.2.2 ATCt Base Station Source Concentration and Source-Free Zones

The 328.2 km radio horizon is such that the resulting area visible to the receiver is much larger than any single metropolitan area. Therefore it is necessary to use a multi-city, regional model for deployed base station concentration, Figure 2-10. The base station tower average spacing is assumed to be 2.2 km within a particular urban region. To simplify the analysis outside urban regions, a rural tower average spacing of 40 km is assumed. Areas of ocean within the radio horizon (e.g., beyond 298.99 km in the specific case below) are the only places considered to be completely free of base stations. See Appendix B for more details

3.2.3 Specific Case: South-Central Pennsylvania Details

A specific case location over South-central Pennsylvania is used to evaluate the aggregate RFI that may be encountered in a high altitude scenario. This case is believed to be representative of enroute operations near densely populated coastal regions of the United

©2011 RTCA, Inc.

States. An aircraft flying at altitude over this region will be within radio line of sight of seven different metropolitan areas, as indicated in Table 3-2.

Because of the large distances involved and the relatively low unwanted emission from ATCt mobile terminals compared to fundamental base station emission, only the base station fundamental RFI effect will be addressed in this scenario analysis.

Table 3-2 Metropolitan Areas Visible in High Altitude Enroute Specific Case

Location	Lat. (°N)	Long. (°W)	Distance to aircraft (km)	City Radius (km)
Aircraft	39.819	77.573	N/A	N/A
Baltimore, MD	39.291	76.610	122.26	45.4
Washington, DC	38.899	77.036	118.58	45.4
Harrisburg, PA	40.260	76.882	91.25	30.0
Philadelphia, PA	39.952	75.162	268.80	45.4
Pittsburgh, PA	40.438	79.997	278.49	45.4
Allentown, PA	40.603	75.470	249.84	30.0
Richmond, VA	37.541	77.434	254.06	30.0

3.3 Generic Low Altitude / Terminal Area (FAF WP) RFI Encounter Scenario

For the terminal area scenario the aircraft is assumed to be in level flight with its GNSS antenna at an intermediate value between the enroute and Category I precision approach scenarios. It is based on the representative case of the final approach fix waypoint (FAF WP) on the Category I approach LAX Runway 25L (Los Angeles, CA) where the nominal waypoint height above the touchdown surface is 1799 feet (= 1900-101). After further adjustments for altitude error (-50 feet) and antenna displacement (+7 feet), the final antenna height value becomes 1756 feet (535.2 meters). Tracking and data demodulation of both GPS and SBAS satellite signals are considered.

Receiver tracking for GPS C/A satellite signals and data demodulation for SBAS (WAAS) signals are considered as the limiting case performance conditions. Baseline GPS, SBAS (WAAS), and Galileo GNSS continuous self interference is assumed along with aeronautical on-board equipment aggregate case emissions. Baseline aggregate continuous RFI from a general set of ground-based sources is also assumed to be present [3-2]. Continuous fundamental RFI emissions from ATCt base stations and unwanted RFI emissions from ATCt mobile terminals are the subjects of analyses in the scenario.

3.3.1 Basic Terminal Area Scenario RFI Encounter Geometry

For the terminal area scenario, the aircraft is assumed to be about to start on a nominal 3° glideslope at a distance of 10.46 km from the touchdown point. The GNSS receive antenna is at an altitude of 535.2 meters. Multiple ATCt base stations and mobile terminals are considered with antenna heights of 30 meters and 1.8 meters, respectively (see Section 2.4). Using a 4/3 Earth-radius estimate, the radio horizon radius to ATCt base stations is 118 km. The radio horizon radius to ATCt mobile terminals is 101 km.

3.3.2 Base and Mobile Station Source Concentration and Source-Free Zones

The base station source concentration for a single metropolitan area is modeled as shown in Figure 2-9. In this scenario the aircraft is considered to be at the center of the region. The inner 45.5 km radius represents the base station concentration in the urban center, with an average tower spacing of 2.2 km. Beyond this inner core the base station concentration decreases with a tower spacing of 6.2 km out to a radius of 70.3 km and finally to a tower spacing of 18 km out to the radio horizon of 118 km.

©2011 RTCA, Inc.

Three different source concentrations for ATCt mobile terminals will be evaluated: 100, 300, and 1000 Mobile Terminals in a single 3.8 km^2 cell. Because of the relatively long distance to the airport runway, no ATCt base or mobile station exclusion zones are assumed in this scenario.

3.4 Generic Category I Precision Approach RFI Encounter Scenario

For the Category I Precision Approach scenario the aircraft is assumed to be in a stabilized descent on a 3° glideslope at the Category I decision height (DH) for the approach. Tracking and data demodulation of both GPS and SBAS satellite signals are considered.

Receive performance for GPS C/A and SBAS satellite signals is considered as the limiting case condition. Baseline GPS, SBAS (WAAS), and Galileo GNSS continuous self interference is assumed along with aeronautical on-board equipment aggregate case emissions. Baseline aggregate continuous RFI from a general set of ground-based sources is also assumed to be present [3-2]. Continuous fundamental RFI emissions from ATCt base stations and unwanted RFI emissions from ATCt mobile terminals are the subjects of analyses in the scenario.

3.4.1 Basic Category I DH Scenario Encounter Geometry

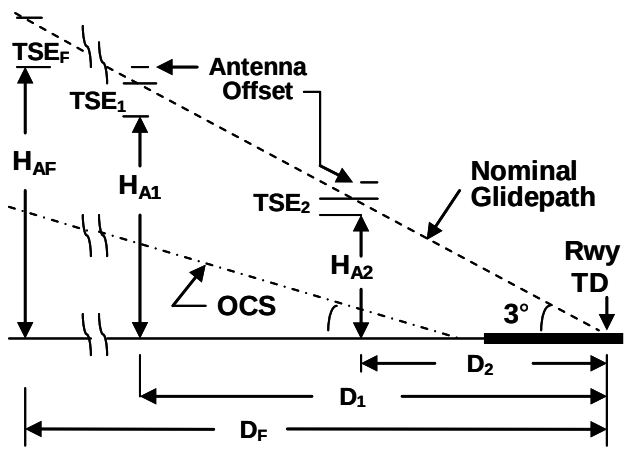

<u>Figure 3-1</u> General Runway Approach Geometry (Side View)

The GNSS Category I precision approach scenario geometry (<u>Figure 3-1</u>) has a minimum DH of 200 feet and the glideslope angle of 3 degrees. The corresponding distance along the ground to the touchdown point (D_1) is 1163 meters. The GNSS aircraft antenna location, i.e. the GNSS navigation reference point, is typically above the aircraft control point location (basis for DH value) when in landing configuration. A minimum estimate for this distance is 7 feet. On any given Category I approach, the actual aircraft height (H_{A1}) may be above or below the decision height by a nominal random error, the Total System Error (TSE_1 = NSE+FTE). For Category I approach, the TSE is assumed to be≤ 32 feet ([3-2], paragraph 3.2). Combining these adjustments gives a GNSS antenna height for this scenario of 175 feet (= 200 + 7 - 32) or 53.34 m.

Multiple ATCt base stations and mobile terminals are considered with antenna heights of 30 meters and 1.8 meters, respectively (see Section 2.4). Using a 4/3 earth radius estimate, the radio horizon radius to ATCt base stations is 52.7 km. The radio horizon radius to ATCt mobile terminals is 35.7 km.

©2011 RTCA, Inc.

3.4.2 Base and Mobile Station Source Concentration and Source-Free Zones

The ATCt base station concentration in the Category I approach scenario follows the same single city model used for the Terminal Area scenario. The aircraft is considered to be at the center of the city region. Three different source concentrations for ATCt mobile terminals will be evaluated: 100, 300, and 1000 terminals in a single 3.8 km^2 cell.

The inclined surface labeled "OCS" in Figure 3-1 is the obstacle clearance surface which is one of the constraints on the 30 m high ATCt base antenna location near airports. The OCS height above the ground directly underneath the aircraft Category I DH waypoint is 23.87 m (78.3 feet) and does not exceed 30 meters for another 208.6 meters (684 feet) out along the extended runway centerline. The OCS lateral constraint also forces the 30 m ATCt antenna away from on each side of the extended runway centerline.

For this report analysis the Category I model ATC base station source exclusion zone[1] consists of a complete source-free zone of 350 m radius centered under the aircraft. Outside that radius is an annular sector (570 m outer radius, 40° half-angle) centered on the runway extended centerline and oriented toward the runway threshold. Beyond that is a narrow wedge centered on the runway with 5.5 km outer radius and 12° half-angle

3.5 Generic Category II/III Precision Approach RFI Encounter Scenario

For the Category II/III Precision Approach scenario the aircraft is assumed to be in a stabilized descent on a 3° glideslope at the 100 foot decision height for the Category II approach. Tracking and data demodulation of both GPS and SBAS satellite signals are considered.

Receive performance for GPS C/A satellite signals is considered as the limiting case condition. GPS, SBAS (WAAS), and Galileo GNSS continuous self interference is assumed along with aeronautical on-board equipment aggregate case emissions. Baseline aggregate continuous RFI from a general set of ground-based sources is also assumed to be present [3-2]. Continuous fundamental RFI emissions from ATCt base stations and unwanted RFI from ATCt mobile terminals are the subjects of analyses in this scenario.

3.5.1 Basic Category II Decision Height Scenario Encounter Geometry

The GNSS precision approach scenario geometry is depicted in Figure 3-1. For Category II operations, the minimum decision height (DH) is 100 feet and the glideslope angle (EL) is 3 degrees. The corresponding distance along the ground to the touchdown point (D_2) is 582 meters. The GNSS aircraft antenna location, i.e. the GNSS navigation reference point, is typically above the aircraft control point location (basis for DH value) when in landing configuration. A minimum estimate for this distance is 7 feet. On any given Category II approach, the actual aircraft height may be above or below the decision height by a nominal random error, the Total System Error (TSE = NSE+FTE). For Category II approach, the TSE is assumed to be ≤ 21.9 feet ([3-2], paragraph 3.4.2). Combining these adjustments gives a GNSS antenna height for this scenario of 85.1 feet (= 100 + 7 – 21.9) or 25.94 m.

The Category III vertical encounter geometry is the same as Category II up to the Category II decision point. Beyond that point on the approach, the airport runway object-free area protection from potential ground-based RFI sources begins to apply (Figure 3-2). The effect of the Object-Free Area is to exclude RFI sources from directly under the approach path between the runway and the Category II decision height point.

[1] The parameters listed here are determined for the "Random Location" method. See Appendix B for "Discrete Location" method details.

©2011 RTCA, Inc.

Thus the Category II DH scenario also represents a Category III approach as well. The Surface (taxiway) scenario conditions (Section 3.4.2) are believed to be representative of the Category III landing and roll-out phases.

Multiple ATCt base stations and mobile terminals are considered with antenna heights of 30 meters and 1.8 meters, respectively (Section 2.4). Using a 4/3 earth radius estimate, the radio horizon radii to ATCt base stations and mobile terminals are 43.6 km and 26.5 km, respectively.

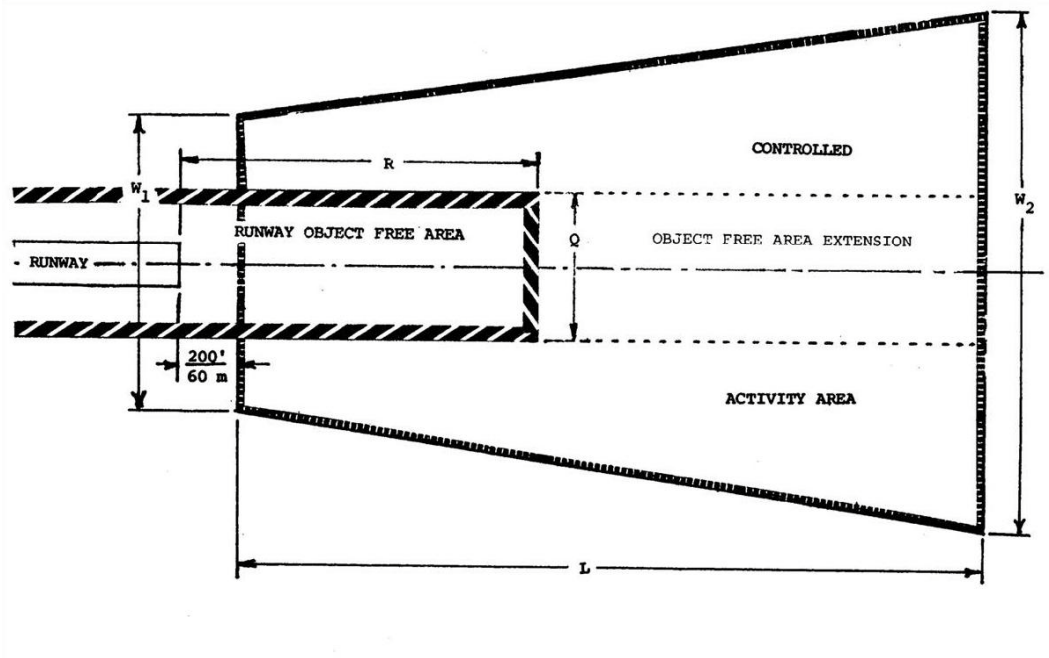

Figure 3-2 Airport Runway Protection Zones - Top View

3.5.2 Base Station Source Concentration and Source-Free Zones

The ATCt base station concentration in the Category II/III approach scenario follows the same single city model used for the Category I approach scenario. The aircraft is considered to be at the center of the city region. Three different mobile terminal source concentrations are evaluated: 100, 300, and 1000 terminals in a single 3.8 km^2 cell.

The Category II DH exclusion zone for ATCt base stations has similar shape to the Category I case but is adjusted to account for shorter aircraft distance to the runway threshold. The complete exclusion zone radius is 420 m. The next annular sector has an 840 m outer radius and 60° half-angle. The outer runway oriented annular wedge extends to 4.47 km at 10° half-angle. See Appendix B for further details.

3.6 Generic Surface Movement (Taxiway) Guidance RFI Encounter Scenario

This scenario represents an aircraft located on a taxiway. The aircraft is either stationary or in a slow taxi. Two receiver modes are considered in this scenario: tracking and data demodulation of both GPS and SBAS satellite signals; and initial acquisition.

The baseline continuous RFI emissions present in this scenario include GNSS intra- and inter-system (CDMA) noise and on-board installed avionics emissions. Baseline aggregate continuous RFI from a general set of ground-based sources is also assumed to be present [3-2]. Fundamental RFI emissions from ATCt base stations are the subject of analysis for this scenario, but unwanted RFI emissions from ATCt mobile terminals (either on- or off- board) are not considered.

©2011 RTCA, Inc.

3.6.1 Basic Surface (Taxiway) Scenario RFI Encounter Geometry

The surface RFI encounter (Figure 3-3) has the minimum GNSS antenna-to-RFI source separation, D_0, a function of the Obstacle Free Zones defined [3-1] for the airport and its taxiways. Other ATCt base station location constraints exist due to limitations from the runway approaches, but stations are assumed to be located beyond the airport exclusion zone constraints to the radio horizon. The GNSS antenna height is assumed to be 4 meters (typical for a regional or business jet) and the ATCt base station antenna height is 30 meters (Section 2.4). Using a 4/3 earth radius estimate, the radio horizon radius to ATCt base stations is 30.8 km. Similar to the Category II DH case, the ATCt base is illuminating with its high gain pattern region, the aircraft antenna high gain pattern region.

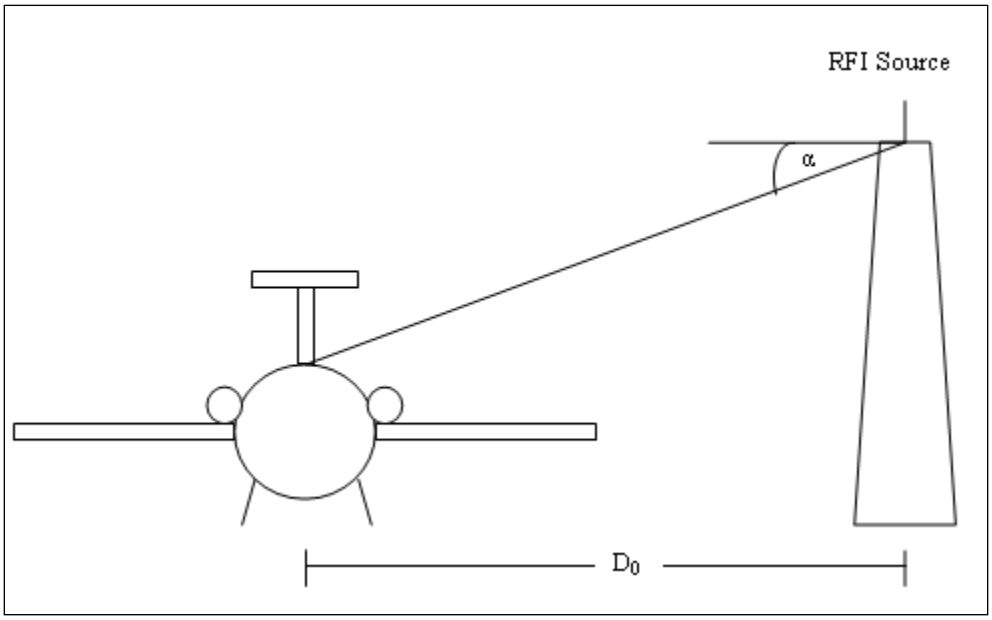

Figure 3-3 Surface RFI Encounter Geometry - Front View

3.6.2 Base and Mobile Station Source Concentration and Source-Free Zones

The ATCt base station concentration in the surface scenario is based on a 2.2 km tower spacing. This spacing corresponds to the highest base station concentration expected to be found in an urban center. The ATCt base station exclusion zone is adjusted from the cases above to account for the aircraft taxiway position. The complete exclusion radius is 550 m and the runway-oriented annular wedge extends to 4.2 km outer radius at 22.5° half-angle (see Appendix B for further details). Unwanted RFI from ATCt mobile terminals is not considered in this case because the combination of lower transmitter power, increased propagation loss at low elevation, and large exclusion zones relative to the radio horizon limits their potential contribution.

3.7 Aeronautical RFI Encounter Scenario Parameter Summary

The high altitude enroute scenario South-central Pennsylvania location and city distances are listed in Table 3-2 above and are not repeated here. Table 3-3 summarizes the key antenna height and radio horizon parameters assumed and calculated in this section for the five RFI encounter scenarios.

Table 3-4 summarizes the scenario RFI source exclusion zone parameters.

©2011 RTCA, Inc.

Table 3-3 Aeronautical Scenario Antenna Height and Radio Horizon Parameters

Scenario Case	Aircraft Ant. Ht. (m)	ATCt Base Ant. Ht (m)	ATCt Mobile Ant. Ht. (m)	Radio Horiz. to Base (km)	Radio Horiz. to Mobile (km)
Surface	4.0	30	N/A	30.84	N/A
Cat. II DH	25.94	30	1.8	43.59	26.54
Cat. I DH	53.34	30	1.8	52.71	35.65
FAF WP	535.2	30	1.8	118.00	100.94
High Altitude	5490	30	N/A	328.16	N/A

Table 3-4 Aeronautical Scenario ATCt Source Exclusion Zone Parameters

Scenario Case	Base Inner Rad. (m)	Base Outer Rad. (m)	Annular Half-Ang. (deg)	Mobile Inner Rad. (m)	Mobile Outer Rad. (m)	Annular Half-Ang. (deg)
Surface (Taxiway)	0 550	550 4200	180 22.5	N/A	N/A	N/A
Cat. II DH	0 420 840	420 840 4470	180 60 10	449.3	2842	25
Cat. II DH	0 350 570	350 570 5500	180 40 12	488	5830	17
Term. Area (FAF WP)	N/A	N/A	N/A	N/A	N/A	N/A
High Alt. Enroute	298985*	328160*	45*	N/A	N/A	N/A

* This high altitude exclusion zone annular segment represents the Atlantic Ocean off New Jersey and the Delmarva Peninsula (45° full angular extent).

3.8 References

[3-1] FAA AAS-100, “Airport Design Advisory Circular”, AC 150/5300-13 (Changes 1-15), Dec. 31. 2009

[3-2] SC-159, “Assessment of Radio Frequency Interference Relevant to the GNSS L1 Frequency Band,” RTCA Document No. RTCA/DO-235B, 13 Mar. 2008

[3-3] SC-159, “Minimum Operational Performance Standards for Global Position System/Wide Area Augmentation System Airborne Equipment,” RTCA Document No. RTCA/DO-229D, 13 Dec. 2006

©2011 RTCA, Inc.

This page intentionally left blank.

©2011 RTCA, Inc.

4 AGGREGATE LIGHTSQUARED ATCt RFI EFFECT ANALYSES

The following subsections describe the aggregate analyses and present results for fundamental ATCt base station and unwanted and unintentional ATCt mobile station RFI effects on GPS airborne receivers. The analyses make use of the source, propagation path, and receiver models described in Section 2 and the operational scenarios developed in Section 3 of this report. As mentioned in Section 1.3, the focus of this report is on the Phase 0 spectrum deployment of the LightSquared network. This section provides results for total received power spectral density at point A in Figure 2-1, assuming one 5 MHz base station channel centered at 1552.7 MHz with 32 dBW (25 dBW/MHz (Phase 0)) EIRP. The results may be readily extended to the other spectrum deployment phases.

4.1 Introduction

The aggregate LightSquared ATCt RFI effect on airborne GPS receivers has been analyzed for the scenarios described in Section 3 of this report using the path loss and emission models described in Section 2 with the methodology described in Appendix B. This methodology uses both probabilistic and deterministic path loss formulations as appropriate to the particular scenario. Base station RFI effects have been analyzed assuming both random and fixed grid locations while mobile units are assumed to be randomly located. Both location methods share common features of median path loss to a given radial location and the radio horizon for a given RFI scenario. They also share a measure of the relative ATCt base station tower spacing but use it somewhat differently. The random location method uses the tower spacing within a given deployment zone to determine an average value of source concentration (probabilistic parameter). The fixed discrete method, however, uses the spacing to set the fixed hexagonal grid size.

RFI effects have been evaluated for interference sources that are within the radio horizon. The radio horizon for a given aircraft antenna height is a constraint on the location of ATCt sources that can affect the aggregate received RFI. The estimated radio horizon, R_0 (in meters), between the aircraft antenna and the RFI emitter antenna is based on the 4/3 Earth radius approximation. The radio horizon values to ATCt base station and mobile antennas for each aircraft operational scenario are taken from Table 3-2.

Runway exclusion zones summarized in Table 3-3 have been incorporated in the analysis for several of the operational scenarios as discussed in Section 3.6. The exclusion zones for the random emitter location method are implemented as described in Section B.4.1 while for the discrete location method an exclusion zone is implemented by simply removing one or more of the grid points (see Section B.4.3).

4.2 Low Altitude Enroute / Terminal Area (FAF WP) Scenario Aggregate RFI Analysis

Although this operational scenario is formulated at a specific aircraft height above terrain (535.2 meters, 1756 feet), it is intended to represent effects over a range of aircraft heights from about 1500 to 2000 feet for general low-altitude aircraft operations above a large metropolitan area.

4.2.1 Generic Aggregate ATCt Base Station Fundamental RFI Effect Analysis (FAF WP)

As described in Section 3.3, the RFI scenario for a generic low altitude / terminal area GNSS receiver operation is represented by an aircraft nominally at the FAF waypoint (aircraft antenna height = 535.2 m). The aircraft antenna is 505.2 m above the ATCt base station antenna so the lower hemisphere aircraft and upper hemisphere ATCt base antenna patterns are used. The nadir point on its ground track is roughly centered within a metropolitan ATCt base station deployment (average tower spacing = 2.2 km out to

©2011 RTCA, Inc.

45.4 km radius, then 6.2 km out to 70.3 km, and 18 km out to 118 km radius radius). No source exclusion zone around the airport is used since its effect is insignificant (large distance to the runway threshold). The isotropic median path loss is described in Section B.3.2.1, while the base station emitted power spectral density is 25 dBW/MHz (Phase 0).

4.2.1.1 Random Method Base Station Fundamental RFI Effect Analysis (FAF WP)

Details of the contributions from the ATCt base station deployment regions to overall aggregate results are listed in Table 4-1. Annular regions #1 and #2 together comprise the central metro base station deployment zone (average station concentration = 0.26307 km^{-2} or $10^{-6.580}$ m^{-2}). The outer regions #3 and #4 represent the suburban and rural deployment zones, respectively, with concentrations relative to the metro center as listed. The exclusion angle column entries indicate no source exclusion zone within the region.

Table 4-1 Random Method Aggregate Calculation Summary (FAF WP)

Annular Region #	Rel Conc.	Excl. Angle (deg)	Inner Rad. (m)	Outer Rad. (m)	F_{AGG}	Rel. Inv. PL_{AGG}
1	1	0	0	20000	4.137E-04	4.137E-04
2	1	0	20000	45400	1.170E-04	1.170E-04
3	0.1259	0	45400	70300	4.254E-06	5.356E-07
4	0.0149	0	70300	117996	6.580E-07	9.829E-09
Total					5.356E-04	5.312E-04

The last two columns of Table 4-1 list the regional mean aggregate received RFI factors (F_{AGG}) and relative mean aggregate inverse path loss factors (Rel. Inv. PL_{AGG}) computed with Equations B-24 and B-23, respectively. By extension of Appendix B Equations B-23 and B-25, the overall mean aggregate path loss, PL_{AGG}(dB), and mean aggregate received RFI power density, P_{SDR}(dB), are given as:

$$PL_{AGG}(dB) = -10 \log(\rho_E \, IPL_{AGG}), \text{ and } P_{SDR}(dB) = P_{SDE}(dB) - PL_{AGG}(dB);$$

where IPL_{AGG} is the total relative inverse path loss factor for the scenario, ρ_E is the central metro base station concentration and P_{SDE} is the ATCt base station EIRP spectral density (25 dBW/MHz (Phase 0) for these scenarios). Using these equations and the Table 4-1 total relative path loss factor, this scenario results are 98.55 dB mean aggregate path loss and -73.55 dBW/MHz mean aggregate received RFI power density.

4.2.1.2 Discrete Method Base Station Fundamental RFI Effect Analysis (FAF WP)

For the discrete method, the mean aggregate received RFI, computed as per Equation B-26 in Section B.4.3, is determined to be -73.60 dBW/MHz at the output port of the passive antenna (Point A in Figure 2-1) while the corresponding aggregate path loss is 98.61 dB. ATCt base stations are assumed present in all the fixed cells within view with cell sizes appropriate to the single city zone model (Figure 2-9).

4.2.2 Aggregate ATCt Mobile Station Unwanted RFI Effect Analysis (FAF WP)

For the Final Approach Fix (FAF) scenario the GPS antenna height is 535.2 meters, the mobile height at 1.8 meters, and a radio horizon of 100.94 km. The mobile unit emission density P_{SDE} was set at -90 dBW/MHz in the GPS L1 band. The median path loss model used is a blending of the two-ray and Hata-Okumura (Hata) models as discussed in Section B.3.1.1.2.

©2011 RTCA, Inc.

The analysis was done for a mobile unit surface density ρ_E of 100, 300, and 1000 units per cell. The term "cell" represents 3.80 square kilometers (area of circular region with 2.2 km average diameter). Analysis results are summarized in the Table 4-2 below.

Table 4-2 Mobile Unit Terminal Area (FAF WP) Scenario Results

Case	A/C Ant Height (m)	Excl. Zone Param's	100 UE/cell Rcv PSD (dBW/MHz)	300 UE/cell Rcv PSD (dBW/MHz)	1000 UE/cell Rcv PSD (dBW/MHz)	Agg PSD w/o ATCt
FAF WP	535.2	None	-166.16	-161.39	-156.16	-151.04

The right hand column in the table shows results from a prior analysis of mobile unit interference to airborne GPS receivers in which a variety of mobile and portable unit types were assumed present including cell phones, laptop computers, PDAs, WiFi equipment, etc., but without LightSquared mobiles. These units were assumed to radiate power at -81.1 dBW/MHz, approximately 10 dB below the 47 CFR 15 limit, and were distributed with a surface concentration ρ_E of 1 per 10,000 m^2 (equivalent to 380 units in a 2.2 km diameter average ATCt cell). The ATCt unit columns are for RFI from only the ATCt mobiles.

4.3 Generic Category I Precision Approach Scenario Aggregate RFI Analysis

As in previous SC-159 RFI analyses [4-1], the generic Category I precision approach scenario is represented by its lowest expected antenna height case, the Cat. I DH. The other limiting case for precision approach operations is the FAF WP case (Section 4.2 above)

4.3.1 Aggregate ATCt Base Station Fundamental RFI Effect Analysis (Category I DH)

As described in Section 3.3, the RFI scenario for a generic Category I GNSS receiver precision approach operation is represented by an aircraft nominally at the Category I DH waypoint (aircraft antenna height = 53.34 m). The aircraft antenna is 23.34 m above the ATCt base antenna so the lower hemisphere aircraft and upper hemisphere ATCt base antenna patterns are used. The nadir point on its ground track is again roughly centered within a metropolitan ATCt base station deployment (average tower spacing = 2.2 km out to 45.4 km radius). The radio horizon to a 30 m high ATCt antenna is 52.71 km. A source exclusion zone around the airport runway is used as described in Section B.4.2.2. Only two deployment zones of the single city model (Figure 2-9) fall within the aircraft radio horizon. As in the FAF WP scenario above the central metro ATCt base concentration factor ρ_E value is 0.26307 km^{-2} ($10^{-6.580}$ m^{-2}) for an average 2.2 km diameter cell. The isotropic median path loss is described in Section B.3.2.2 and the base station fundamental EIRP spectral density is 25 dBW/MHz (Phase 0).

4.3.1.1 Random Method Base Station Fundamental RFI Effect Analysis (Category I DH)

Details of the contributions from the ATCt base station exclusion zones and deployment regions to overall aggregate results are listed in Table 4-3. Annular regions #1 - #3 together encompass the airport exclusion zone. The exclusion angle column values represent the annular half-angle (half the overall annulus angular portion) for zero sources. The innermost annular region, with 180° half-angle, is completely free of ATCt base stations. Regions #4 and #5 together represent the remaining area within the metro zone. Region #6 represents the suburban deployment zone portion within the radio horizon with the base station concentration relative to the metro central concentration as listed (column 2).

©2011 RTCA, Inc.

Table 4-3 Random Method Aggregate Calculation Summary (Category I DH)

Annular Region #	Rel Conc.	Excl. Angle (deg)	Inner Rad. (m)	Outer Rad. (m)	F_{AGG}	Rel. Inv. PL_{AGG}
1	1	180	0	350	0.000	0.000
2	1	40	350	570	7.053E-05	7.053E-05
3	1	12	570	5500	2.220E-04	2.220E-04
4	1	0	5500	20000	1.406E-05	1.406E-05
5	1	0	20000	45400	8.071E-07	8.071E-07
6	0.125911	0	45000	52708	9.500E-09	1.196E-09
Total					3.074E-04	3.074E-04

The last two columns of Table 4-3 list the regional mean aggregate received RFI factors and relative mean aggregate inverse path loss factors computed with Equations B-24 and B-23, respectively. Using the technique from 4.2.1.1 and the Table 4-3 total relative inverse path loss factor, the scenario results are 100.92 dB mean aggregate path loss and -75.92 dBW/MHz mean aggregate received RFI power density.

4.3.1.2 Discrete Method Base Station Fundamental RFI Effect Analysis (Category I DH)

The discrete method mean aggregate received RFI, is computed as per Equation B-26 in Section B.4.3. The median path loss model used is the Hata model as all ranges are beyond 1 km. A single grid point at a radius of 2.91 km was used for the exclusion zone (u=-1 and v=2 in Section B.4.3). The mean aggregate power spectral density is determined to be -77.63 dBW/MHz while the corresponding aggregate path loss is 102.64 dB.

4.3.2 Aggregate ATCt Mobile Station Unwanted RFI Effect Analysis (Category I DH)

For the Category I Decision Height scenario the GPS antenna height is 53.34 meters, the mobile height at 1.8 meters, and a radio horizon of 35.65 km. The emission density P_{SDE} was set at -90 dBW/MHz. The median path loss model used is a blending of two-ray, Erceg/Greenstein, and Hata models. A wedge shaped exclusion zone was used consistent with airport and approach constraints on the shorter mobile unit antenna height (see Section B.4.2.2).

Again the analysis was done for a mobile unit surface density ρ_E of 100, 300, and 1000 units per cell where a "cell" represents 3.80 square kilometers (see Table 4-4 below).

Table 4-4 Mobile Unit Category I DH Scenario Aggregate RFI Results

Case	A/C Ant Height (m)	Excl. Zone Param's	100 UE/ cell Rcv PSD (dBW/MHz)	300 UE/cell Rcv PSD (dBW/MHz)	1000 UE/cell Rcv PSD (dBW/MHz)	Agg PSD w/o ATCt
Cat I DH	53.34	R_1=488m R_2=5830m θ_o=17°	-166.23	-161.46	-156.23	151.11

4.4 Category II Precision Approach Scenario Aggregate RFI Analysis

The Category II DH case represents the lowest antenna height case in the Category II precision approach operational scenario. As with the Category I precision approach operational secenario, the FAF WP case is the other limiting case. The Category II DH

©2011 RTCA, Inc.

case also represents the limiting case for the Category III precision approach (Section 3.4)

4.4.1 Aggregate ATCt Base Station Fundamental RFI Effect Analysis (Category II DH)

The RFI scenario for a generic Category II GNSS receiver precision approach operation, as described in Section 3.5, is represented by an aircraft nominally at the Category II DH waypoint (aircraft antenna height = 25.94 m). This scenario also represents the limiting case for Category III approach operations. The nadir point on its ground track is again roughly centered within a metropolitan ATCt base station deployment (average tower spacing = 2.2 km out to 45.4 km radius). The radio horizon to a 30 m high ATCt antenna is 43.59 km. The aircraft antenna height is slightly (4.06 m) below the ATCt tower height so the aircraft primary antenna pattern region is being illuminated by the primary base station antenna pattern. The central metro base station deployment and a source exclusion zone around the airport runway similar to the Category I case are used in the Category II DH analyses. The isotropic median path loss is described in Section B.3.2.3 and the base station fundamental EIRP spectral density is 25 dBW/MHz (Phase 0).

4.4.1.1 Random Method Base Station Fundamental RFI Effect Analysis (Category II DH)

Details of the contributions from the ATCt base station exclusion zones and deployment regions to overall aggregate results are listed in Table 4-5. Annular regions #1 - #3 together encompass the airport exclusion zone. The exclusion angle column values represent the annular half-angle (half the overall annulus angular portion) for zero emission. Regions #4 and #5 together represent the remaining area of the metro deployment zone within the radio horizon.

Table 4-5 Random Method Aggregate Calculation Summary (Category II DH)

Annular Region #	Rel Conc.	Excl. Angle (deg)	Inner Rad. (m)	Outer Rad. (m)	F_{AGG}	Rel. Inv. PL_{AGG}
1	1	180	0	420	0.000	0.000
2	1	60	420	840	1.751E-04	1.751E-04
3	1	10	840	4470	1.149E-04	1.149E-04
4	1	0	4470	20000	8.957E-06	8.957E-06
5	1	0	20000	43593	7.031E-07	7.031E-07
Total					2.997E-04	2.997E-04

The last two columns of Table 4-5 list the regional mean aggregate received RFI factors and relative mean aggregate inverse path loss factors computed with Equations B-24 and B-23, respectively. Using the technique from 4.2.1.1 and the Table 4-5 total relative inverse path loss factor, the scenario results are 101.03 dB mean aggregate path loss and -76.03 dBW/MHz mean aggregate received RFI power density.

4.4.1.2 Discrete Method Base Station Fundamental RFI Effect Analysis (Category II DH)

The discrete method mean aggregate received RFI, is computed as per Equation B-26 in Section B.4.3. The median path loss model used is the Hata model as all ranges are beyond 1 km. A single grid point at a radius of 2.91 km was used for the exclusion zone (u=-1 and v=2 in Section B.4.3). The mean aggregate RFI power spectral density is -79.09 dBW/MHz while the corresponding aggregate path loss is 104.10 dB.

©2011 RTCA, Inc.

4.4.2 Aggregate ATCt Mobile Station Unwanted RFI Effect Analysis (Category II DH)

For the Category II Decision Height scenario the GPS antenna height is 25.94 meters, the mobile height at 1.8 meters, and a radio horizon of 26.54 km. The emission density P_{SDE} was set at -90 dBW/MHz. The median path loss model used is a blending of two-ray, Erceg/Greenstein, and Hata models. A wedge shaped exclusion zone was used consistent with airport and approach constraints on the mobile unit antenna height (see Section B.4.1.2).

The analysis was done for a mobile unit surface density ρ_E of 100, 300, and 1000 units per cell where a "cell" represents 3.80 square kilometers. Analysis results are shown in the Table 4-6 below. Idling mobiles may emit less in the receive mode than in the transmit mode. These results assume all units emit the same value (-90 dBW/MHz, OOBE regulatory limit) regardless of mode.

Table 4-6 Mobile Unit Category II DH Scenario Aggregate RFI Results

Case	A/C Ant Height (m)	Excl. Zone Param's	100 UE/cell Rcv PSD (dBW/MHz)	300 UE/cell Rcv PSD (dBW/MHz)	1000 UE/cell Rcv PSD (dBW/MHz)	Agg PSD w/o ATCt
Cat II DH	25.94	R_1=449.3m R_2=2842m θ_o=25°	-164.98	-160.21	-154.98	-149.86

4.5 Surface Movement (Taxiway) Scenario Aggregate RFI Analysis

As described in Section 3.4, the RFI scenario for a generic airport surface GNSS receiver operation is represented by an aircraft nominally at the end of the taxiway (aircraft antenna height = 4 m). This also represents the limiting case for Category III landing operations. The nadir point is again roughly centered within a metropolitan ATCt base station deployment (average tower spacing = 2.2 km out to 45.4 km radius). The radio horizon to a 30 m high ATCt antenna is 30.84 km. The aircraft antenna height is again below the ATCt tower height (by 26 m) so its primary antenna pattern region is being illuminated by the primary base station antenna pattern. An exclusion zone is used around the airport runway similar to the Category II zone but adjusted for the different aircraft location. The median isotropic path loss is described in Section B.3.2.4. The ATCt base deployment zone concentration factor ρ_E value is 0.26307 km^{-2} ($10^{-6.580}$ m^{-2}). As in the previous scenarios, the base station fundamental EIRP spectral density is 25 dBW/MHz (Phase 0).

4.5.1 Random Aggregate ATCt Base Station Fundamental RFI Effect Analysis (Taxiway)

Details of the contributions from the ATCt base station exclusion zones and deployment regions to overall aggregate results are listed in Table 4-7. Annular regions #1 and #2 together encompass the airport exclusion zone. The exclusion angle column values represent the annular half-angle (half the overall annulus angular portion) for zero emission. Regions #3 and #4 together represent the remaining area of the metro deployment zone within the radio horizon.

©2011 RTCA, Inc.

Table 4-7 Random Method Aggregate Calculation Summary (Taxiway)

Annular Region #	Rel Conc.	Excl. Angle (deg)	Inner Rad. (m)	Outer Rad. (m)	F_{AGG}	Rel. Inv. PL_{AGG}
1	1	180	0	550	0.000	0.000
2	1	22.5	550	4200	2.586E-05	2.586E-05
3	1	0	4200	20000	8.715E-07	8.715E-07
4	1	0	20000	30837	4.120E-08	4.120E-08
Total					2.677E-05	2.677E-05

The last two columns of Table 4-7 list the regional mean aggregate received RFI factors and relative mean aggregate inverse path loss factors computed with Equations B-23 and B-24, respectively. Using the technique from 4.2.1.1 and the Table 4-7 total relative inverse path loss factor, this scenario results are 111.52 dB mean aggregate path loss and -86.52 dBW/MHz mean aggregate received RFI power density.

4.5.2 Discrete Aggregate ATCt Base Station Fundamental RFI Effect Analysis (Taxiway)

The discrete method mean aggregate received RFI is computed as per Equation B-26 in Section B.4.3 The median path loss model used is the Hata model as all ranges are beyond 1 km. A single grid point at a radius of 2.91 km was used for the exclusion zone (u=-1 and v=2 in Section B.4.3). The mean aggregate power spectral density is determined to be -88.76 dBW/MHz while the corresponding aggregate path loss is 113.77 dB.

4.6 High Altitude Enroute Scenario Analysis

This scenario, described in Section 3.1, is represented by a limiting case for high altitude flight. The aircraft is at 18,000 feet altitude (the lowest jet route level). The specific aircraft location is above South-central Pennsylvania where several large metro areas with planned ATCt deployment are within the aircraft antenna's radio horizon. The flight level and approximate location were chosen similar to an analysis case in RTCA/DO-235B. The two ATCt base location methods are applied in scenarios analyses as above. However in this scenario, the path loss is deterministic and the only probabilistic element is the uniformly-distributed, random source position in the Random Method.

The ATCt base station antenna height is 30 m as before and the aircraft antenna height is 5490 m. Free-space propagation is assumed between them with the antenna height difference of 5460 m and the radio horizon radius to an ATCt base antenna is 328.2 km. The base station fundamental EIRP spectral density at antenna beam center is 25 dBW/MHz (Phase 0) over a 5 MHz channel bandwidth centered at 1552.7 MHz. ATCt base stations are deployed around the metro centers as generally depicted in Figure 2-10. However, each location method analyzes the deployment zones somewhat differently. Table 3-2 indicates that the aircraft location (39.819° N, 77.573° W) is within radio line-of-sight of 4 large metro areas (with surrounding suburban rings) and 3 smaller metro areas (30 km deployment radius assumed).

4.6.1 Random Aggregate ATCt Base Station Fundamental RFI Effect Analysis (Enroute)

The Random Location Method models the ATCt base concentrated deployment areas as annular segments within a low-concentration, rural background that has 40 km average base station spacing. The combined aggregate RFI computation proceeds in two steps:

©2011 RTCA, Inc.

a. Computing the low concentration background level while assuming the several metro zones are source-free (i.e.; their defining annular segments are exclusion zones)

b. Computing each high concentration zone aggregate RFI level separately and adding those to the aggregate background RFI level to determine the combined aggregate.

4.6.1.1 Rural Concentration Zone Random Aggregate RFI Analysis

The rural ATCt base station aggregate effect computation is performed with the help of a set of composite integration (metro hotspot) zones (Appendix B), each treated as source-free for the rural background case. Table 4-8 lists the dimensions and results from the integration for each of the eight zones.

Table 4-8 Composite Integration Zone Model –Rural Results

Zone #	Inner Rad. (km)	Outer Rad. (km)	Full Angle (deg.)	Agg. Factor F_{AGG}
1	62.752	77.289	23.57	7.783 E-06
2	77.289	119.752	98.57	2.439 E-05
3	119.752	163.549	75.00	2.943 E-05
4	223.447	230.516	34.15	4.577 E-06
5	230.516	280.447	65.59	2.726 E-05
6	280.447	298.985	31.44	1.041 E-05
7*	298.985	316.776	76.44	8.256 E-06
8*	316.776	328.16	45.00	8.256 E-06

* This zone contain a source-free portion (45°) representing the Atlantic Ocean

An aggregate factor computed for Zone 0 (covering the area aircraft nadir point out to the inner Zone 1 radius) in the rural case is 7.289×10^{-6} and the resulting overall rural aggregate factor (algebraic sum of all the 9 zone factors), $F_{TOTR} = 1.2507 \times 10^{-4}$. The rural base station concentration factor $\rho_B = 7.958 \times 10^{-4}$ km^{-2} (= $10^{-9.099}$ m^{-2}) which holds everywhere except the source-free and metro hotspot zones. Therefore the rural case aggregate path loss (in dB), $PL_{AGGR}(dB) = -10 \log(\rho_B \cdot F_{TOTR}) = 130.02$ dB and the rural aggregate received RFI, $P_{SDRR}(dB)=P_{SDE}(dB)-PL_{AGG}(dB)\cdot = -105.02$ dBW/MHz. Note that this mean aggregate RFI value by itself exceeds the MOPS-related environment limit (-129.35 dBW/MHz) by 24.3 dB and the initial acquisition limit (-135.36 dBW/MHz) by 30.3 dB.

4.6.1.2 Metro Concentration Zone and Combined ATCt Base Station Aggregate Analyses

The next step is to use the defined composite zone dimensions from Appendix B to compute the hotspot aggregate components by integration over just the angular dimension of each zone which, for this pass, contains ATCt base stations. An adjustment in angular dimension is made to exclude the actual source-free ocean area portion of Zone 7. Table 4-9 lists the results of the metro zone computation.

©2011 RTCA, Inc.

Table 4-9 Composite Integration Zone Model – Metro Results

Zone #	Inner Rad. (km)	Outer Rad. (km)	Full Angle (deg.)	Agg. Factor F_{AGG}
1	62.752	77.289	23.57	5.460 E-07
2	77.289	119.752	98.57	9.200 E-06
3	119.752	163.549	75.00	7.744 E-06
4	223.447	230.516	34.15	4.805 E-07
5	230.516	280.447	65.59	6.075 E-06
6	280.447	298.985	31.44	9.947 E-07
7	298.985	316.776	31.44*	2.244 E-06

* The Atlantic Ocean source-free portion (45°) was removed from this zone

The overall metro aggregate factor (algebraic sum of all the 7 metro zone factors), F_{TOTM} = 2.5954 x 10^{-5}. The metro base station concentration factor ρ_M = 0.263 km^{-2} (= $10^{-6.58}$ m^{-2}) holds everywhere except the source-free zones. The overall metro zone aggregate path loss (in dB), $PL_{AGGM}(dB) = -10 \log(\rho_M \cdot F_{TOTM})$ = 111.66 dB and the metro aggregate received RFI, $P_{SDRM}(dB)=P_{SDE}(dB)-PL_{AGGM}(dB)\cdot$= -86.66 dBW/MHz

The combined aggregate path loss (in dB), $P_{AGG}(dB) = -10 \log(\rho_M \cdot F_{TOTM} + \rho_B \cdot F_{TOTR})$. Inserting the results for the rural and metro areas yields $P_{AGG}(dB)$ = 111.60 dB. Using again the simple aggregate formula for the combined aggregate received RFI yields $P_{SDR}(dB)=P_{SDE}(dB)-PL_{AGG}(dB)$ = -86.60 dBW/MHz. The combined aggregate results are clearly dominated by the larger metro aggregate components.

4.6.2 Discrete Aggregate ATCt Base Station Fundamental RFI Effect Analysis (Enroute)

From the defined aircraft position (39.819° N, 77.573 W, 5.49 km alt.), aggregate RFI elements were computed for seven metropolitan areas within the radio horizon. Those areas were, Baltimore, Washington DC, Richmond VA, Harrisburg, Philadelphia, Pittsburgh and Allentown PA. A grid structure (see Section B.4.3, Figure B-11) was placed at each of the metropolitan areas with the grid origin at the center of each city.

As before, each metro area is assumed to contain up to three annular rings each populated with hexagons of the appropriate cell size. The analysis assumes a planar earth with the distance from aircraft nadir to the center of each metropolitan area denoted by s_o. Interference is computed for each metro area as shown in Table 4-10 and summed to get the composite aggregate RFI from all areas. No ATCt base station RFI was assumed from outside the metro zones.

©2011 RTCA, Inc.

Table 4-10 Enroute Scenario Discrete Method Results

Metro Area	# Rings Used	s_o (km)	Rcv PSD (dBW/MHz)	Agg Path Loss (dB)
Baltimore	2	122.25	-93.81	118.81
Washington	2	118.58	-92.99	117.99
Harrisburg	1	91.25	-95.69	120.69
Philadelphia	1	268.80	-97.31	122.31
Allentown	1	249.84	-96.79	121.79
Richmond	2	254.06	-96.33	121.33
Pittsburgh	1	278.49	-97.57	122.57
Total			-87.01	112.01

4.7 Summary Results

The ATCt base station fundamental aggregate RFI effect analysis results for the five aviation operational scenarios are shown below (Table 4-11). The results are for a complete set of ATCt base stations within view of the aircraft GPS antenna. Those stations are operating at the LightSquared Phase 0 deployment plan center frequency of 1552.7 MHz with a 5 MHz channel bandwidth, 32 dBW EIRP (25 dBW/MHz (Phase 0) EIRP spectral density) at beam center and peak channel loading (peak 100%).

Table 4-11 ATCt Base Station Fundamental RFI Effect Aggregate Results Summary

Case	A/C Ant. Ht. (m)	Random Rcv PSD (dBW/MHz)	Random Agg. PL (dB)	Discrete Rcv PSD (dBW/MHz	Discrete Agg. PL (dB)
Surface	4.0	-86.52	111.52	-88.76	113.77
Cat. II DH	25.94	**-76.03**	101.03	**-79.09**	104.10
Cat. I DH	53.34	**-75.92**	100.92	**-77.63**	102.64
FAF WP	535.2	**-73.55**	98.55	**-73.60**	98.61
High Alt.	5490	-86.60	111.6	-87.01	112.01

Note: All the received power spectral densities exceed the GPS MOPS limit of -129.35 dBW/MHz at 1552.7 MHz. Those shown in bold font are cases that exceed the limit by the largest amounts.

The mean aggregate received RFI values above are to be compared with the GPS receiver MOPS tracking limit (in dBW/MHz): -129.35 dBW/MHz at the ATCt base transmit center frequency. They all exceed the limit by 42.7 to 55.8 dB (random method). Even the ATCt rural backgound RFI alone exceeds the MOPS-related tracking limit by 24.3 dB and the initial acquisition limit (-135.36 dBW/MHz) by 30.3 dB in the high altitude scenario (Section 4.6.1.1). If all ATCt base stations were operating at a 60% loading factor the range of scenario values would be 40.5 to 53.6 dB above the MOPS-related tracking limit. These large mean aggregate received RFI power levels are expected to cause complete loss of aviation GPS receive function. The results are driven primarily by the high transmit power and the close proximity of ATCt carrier frequency to the GPS receiver passband edge. ATCt base station deployment concentration also contributes directly to the results.

Analysis results for the ATCt mobile station aggregate unwanted RFI effect are given (Table 4-12) for three operational scenarios where the effect is thought to be the largest. Because of some uncertainty on the number of mobile stations operating per ATCt cell, a range of values were used in the computation: 100, 300, and 1000 mobiles per cell. Each mobile, whether transmitting or idling, is assumed to be emitting -90 dBW/MHz EIRP in the GNSS L1 band (1559-1610 MHz).

©2011 RTCA, Inc.

Table 4-12 ATCt Mobile Station Unwanted RFI Effect Aggregate Results Summary

Case	A/C Ant. Ht. (m)	100 UE/cell Rcv PSD (dBW/MHz)	300 UE/cell Rcv PSD (dBW/MHz)	1000 UE/cell Rcv PSD (dBW/MHz)	Baseline Rcv PSD (no UE) (dBW/MHz)
Surface	4.0	-	-	-	-
Cat. II DH	25.94	-164.98	-160.21	-154.98	-149.86
Cat.I DH	53.34	-166.23	-161.46	-156.23	-151.11
FAF WP	535.2	-166.16	-161.39	-156.16	-151.04
High Alt.	5490	-	-	-	-

The mean aggregate received RFI values for the ATCt mobiles above are to be compared with the GPS receiver environment limit: -146.5 dBW/MHz at the GPS L1 center frequency 1575.42 MHz ± 10 MHz. All the values, including those for a general set of RFI sources described in Section 4.2.2 above are within the environment limit. Since the baseline value is assumed to exist in all the scenario cases, the addition of the ATCt mobile RFI raises the overall environment mean by nominally 9% for 300 UEs/cell (up to 31% for 1000 UEs/cell). Even though the increased mean is still within the safety margin, the probability of exceeding the receiver MOPS test limit (i.e. using the entire safety margin) is increased [4-2].

Although the effect was not analyzed specifically in this report, comparison of the results in Table 4-11 with Table 4-12 suggests that the aggregate RFI contribution from a small number of ATCt mobile stations operating onboard an aircraft parked on the ground[1] will not be significant compared to the ATCt base station aggregate RFI effect.

4.8 References

[4-1] SC-159, "Assessment of Radio Frequency Interference Relevant to the GNSS L1 Frequency Band," RTCA Document No. RTCA/DO-235B, 13 Mar. 2008

[4-2] Rec. ITU-R M.1477, *Technical and Performance Characteristics of Current and Planned Radionavigation-Satellite Service (space-to-Earth) and Aeronautical Radionavigation Service Receivers to Be Considered in Interference Studies in the Band 1 559-1 610 MHz.*

[1] Operation of ATCt mobile units on board an aircraft in flight is considered highly unlikely, as any such use is disallowed unless the aircraft operator has determined that it will not cause harmful interference. See 14 CFR 91.21 and 14 CFR 121.306.

©2011 RTCA, Inc.

This page intentionally left blank.

©2011 RTCA, Inc.

5 POSSIBLE RFI MITIGATION TECHNIQUES

Two different mitigation categories for LightSquared ATCt RFI are considered in this report: mitigation at the ATCt base or mobile station, and mitigation at the GPS receiver.

5.1 Interference Mitigation at the Source

From an aviation perspective, mitigation at the RFI source is, in general, the preferable method. Regulatory limits on the source are a principal type in this category. Source mitigation is generally preferred if there are many more receivers that may be impacted compared to the number of emitting sources, all other considerations being equal.

5.1.1 ATCt Frequency Shift

One possible means to mitigate the aggregate ATCt base station fundamental RFI problem at the 1552.7 MHz transmit center frequency is to shift the transmit center frequency to near the lower band limit, 1525 MHz. This shift takes advantage of the minimum required GPS receiver selectivity curve (Figure C-1). The shift would gain 64.2 dB of extra rejection at a center frequency of 1528.8 MHz and 58.3 dB at 1531 MHz compared to 1552.7 MHz. That move overcomes the current maximum shortfall of 55.8 dB (Section 4.7) and allows margin for future changes. If channels are further away from the 1559 MHz allocation boundary and chosen properly, the frequency shift also eliminates potential third- or higher-order intermodulation products from falling within the GPS receiver passband.

5.1.2 ATCt Power Reduction

Since the fundamental ATCt base station emission is the source of the primary RFI effect, reducing the EIRP might be another means of mitigation. This reduction would most likely need to be combined with a frequency shift and proper channel center frequency selection (to avoid third- or higher-order intermodulation). However, the power restriction at the upper 5 MHz channel center would be quite stringent (~-23 dBW EIRP max.) to make it compatible. The estimated maximum transmit power versus frequency offset for compatibility is shown below (Figure 5-1).

The estimated maximum transmit power limit curve (Figure 5-1) is derived from the lowest aggregate path loss value versus frequency (~98.5 dB for Low Altitude /Terminal Area (FAF WP) scenario) and the receiver MOPS-based susceptibility limit used in this report. A preliminary check of path loss around the 535.2 m scenario antenna height suggests the 98.5 dB value may not be the overall minimum. Therefore, further study is needed to determine and validate the path loss values used in the derivation. The antenna height for minimum path loss is expected to be between 535 m and 1 km for a single city ATCt base station deployment. The path loss is not likely to be more than 2 dB lower than the 535 m value. Since the path loss values used in the power limit curve are mean values, the further study should also include computation of the path loss cumulative probability distribution function. Further work to confirm the receive system susceptibility to broadband RFI near 1528 MHz is also needed.

©2011 RTCA, Inc.

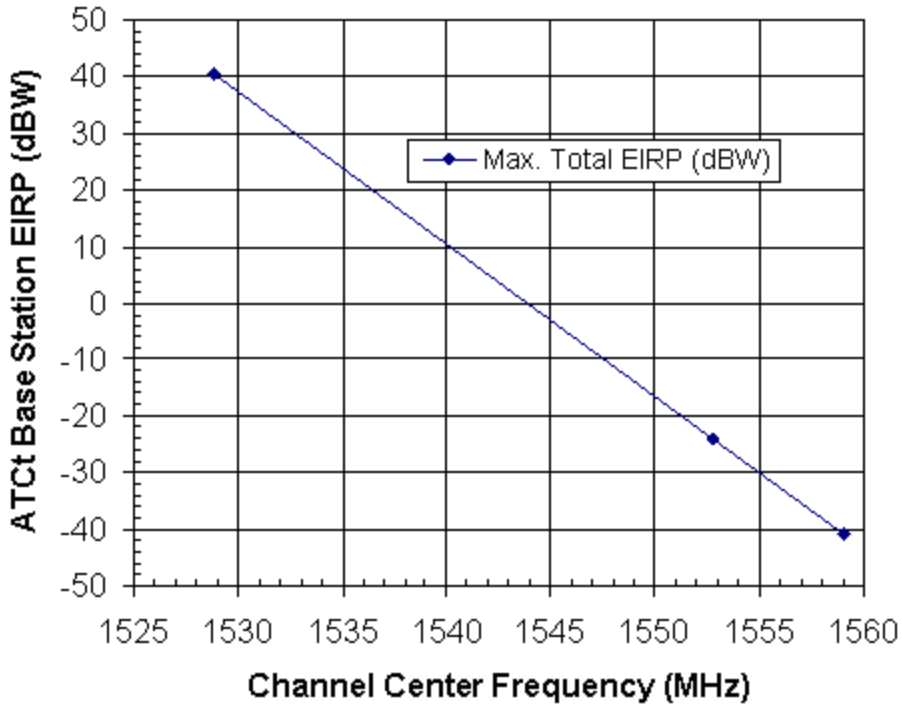

Figure 5-1 Estimated Max. ATCt Base Station EIRP versus Channel Center Freq.

5.2 GPS Receiver Susceptibility Reduction

Fielded airborne GPS, GPS/LAAS, and GPS/WAAS receivers and antennas were designed and certified to meet applicable performance standards in the presence of an assumed interference environment defined in RTCA Minimum Operational Performance Standards (RTCA/DO-316, DO-253C, DO-229D [5-1]) and corresponding FAA Technical Standard Orders. As discussed in Section 2.2.2.2, these MOPS only require that the installed equipment meet the applicable performance standards in the presence of interference levels of up to -86.4 dBm when the interference has the characteristics of the LightSquared ATCt base station 5-MHz emissions centered at 1552.7 MHz. This subsection briefly examines potential means of reducing GPS receiver susceptibility to near-band interference.

5.2.1 Improved Preselection

Most airborne installations use active antennas, built to RTCA/DO-301 [5-2] or the earlier RTCA/DO-228 (with change 1) MOPS [5-3]. DO-301 requires filtering (pre-selection and/or post-selection), but the required attenuation at the upper LightSquared 5-MHz ATCt emission center frequency of 1552.7 MHz is small – only around 6 dB. It would be very difficult to achieve much greater attenuation within an active antenna considering current commercially–available, aviation-grade filters, while simultaneously meeting the DO-301 performance requirements including:

- Differential group delay over L1 +/-10.23 MHz shall not exceed 25 ns
- Noise temperature requirements that dictate a maximum preselection insertion loss on the order of 2 dB or less. This is a typical design requirement, after accounting for the insertion loss of protector circuitry (e.g., to meet the burnout protection and lightning susceptibility requirements) and typical low noise amplifier noise figure.

©2011 RTCA, Inc.

- Minimum 3-dB bandwidth of 15 MHz.

Although not specified in DO-301, form factor requirements are also important. The ARINC 743A [5-4] form factor (4.7 × 2.9 × 0.75 in^3) is most commonly invoked for transport-category aircraft, whereas business or general aviation aircraft often utilize either ARINC 743A or a smaller tear-drop form factor. Increasing the size of the antenna package over the standard form factors may make retrofitting antennas difficult. Higher profile antennas will result in increased drag and icing accumulation.

The antenna performance and form-factor requirements are most typically met through a combination of pre- and post-selection ceramic filters. Such filters are not easily found with 3-dB bandwidths less than 24 MHz. Although advances have been made in recent years with low insertion-loss surface acoustic wave and bulk acoustic wave filters, those available commercially today also do not offer a solution to significantly increase selectivity at the LightSquared upper carrier frequency.

The only technology available today that can provide significantly greater selectivity over that found within a DO-301 compliant antenna is a cavity filter. Cavity filters, however, are far too large to fit within the antenna unit. Typical dimensions are on the order of 6 × 2 × 3 in^3 for a cavity filter providing 25 dB of attenuation at 1552.7 MHz.

New filter designs are being studied that may be able to solve the RFI compatibility problem of an ATCt carrier up to 1555.2 MHz. Vendors involved have predicted potential availability within the next several years.

The preferred approach for increasing selectivity in the long-term would be through the invocation of new performance standards for the combined antenna/receiver combination that would allow the manufacturers the ability to optimally layer filtering throughout the front-end. This approach would take many years, since it would require new standards to be developed, and installed within the fleet of aircraft that operate within U.S. airspace. Building to increased selectivity standards would also correct other potential coupling mechanisms such as reciprocal mixing, etc.

5.2.2 Adaptive Spatial (Antenna) Processing

Adaptive antenna processing is used for some military high-value platforms as a means to suppress interference. This technology requires the use of multi-element antenna arrays with typically 4 – 7 elements spaced an appreciable fraction of a wavelength apart. The physical antenna is thus very large, heavy, and expensive. There are limitations to the number of interference sources that can be simultaneously suppressed, which would likely be surpassed by the LightSquared network where hundreds of ATCt base stations could be simultaneously visible. The FAA has dismissed the use of such technologies for civil aircraft since they are export-controlled, which combined with the above high costs makes this technology impractical for civil aviation.

5.2.3 Improved Receiver Tracking Processes

As discussed in RTCA/DO-235B, the most vulnerable GPS/WAAS receiver functions in the presence of interference are carrier phase tracking and WAAS data demodulation. There are no commercially-available technologies to improve either of these functions substantially. Vector-tracking has been explored to improve the robustness of both carrier phase and code tracking, but is not yet mature to the point where it can be found in any civilian GPS products. WAAS data demodulation, as discussed in DO-235B, is currently performed to within 1.5 dB of the theoretical C/N_0 limits. Very slight improvements in C/N_0 margin would require great improvements in oscillator phase noise, which is impractical given that this solution would require new receivers. If new receivers are to

©2011 RTCA, Inc.

be built then increasing receiver selectivity would be a far more promising solution to cope with LightSquared ATCt emissions.

5.3 References

[5-1] SC-159, "Minimum Operational Performance Standards for Global Position System/Wide Area Augmentation System Airborne Equipment," RTCA Document No. RTCA/DO-229D, 13 Dec. 2006.

[5-2] SC-159, "Minimum Operational Performance Standards for Global Navigation Satellite System (GNSS) Airborne Active Antenna Equipment for the L1 Frequency Band," RTCA Document No. RTCA/DO-301, 13 Dec. 2006.

[5-3] SC-159, "Minimum Operational Performance Standards for Global Navigation Satellite System (GNSS) Airborne Antenna Equipment," RTCA Document No. RTCA/DO-228, 20 Oct. 1995, (with Change 1), 1 Nov. 2000.

[5-4] AEEC, "GNSS Sensor Characteristics," ARINC Characteristic 743A, May, 2009

©2011 RTCA, Inc.

6 SUMMARY AND CONCLUSIONS

6.1 Summary Overview

This report documents a study conducted by RTCA Special Committee 159 in response to an FAA request to address the issue of compatibility between the operation of a terrestrial wireless broadband network in the bands 1525-1559/1626.5-1660.5 MHz by LightSquared, pursuant to its FCC license, and GPS receivers onboard aircraft. To address a specific FAA-requested study aspect, the study determined analytically the mean aggregate received RFI from a distribution of LightSquared terrestrial base and mobile units within view of an aircraft GPS receiver in five operational situations. To address the other specific aspect, the study investigated aircraft GPS receiver RFI susceptibility to the planned LightSquared signals by a combination of modeling using existing domestic and international standards and laboratory testing of four certified aircraft GPS receivers. The study also briefly addressed RFI source and GPS receiver mitigation methods. From that effort and other study results, a modification was proposed for the LightSquared terrestrial network radio spectrum deployment to allow RFI compatibility with aircraft GPS receiver operations.

6.2 Assessment Element Summaries

The following sub-sections summarize the basic analysis framework and parameters for the GPS receiver, propagation path loss models, and ATCt sources (6.2.1); the RFI analysis scenarios (6.2.2); the aggregate RFI analyses (6.2.3); and the possible RFI mitigation options (6.2.4).

6.2.1 Aeronautical RFI Effect Analysis Methodology and Element Models

As described in Section 2, the RFI effects analyses in this report use the classic source-path-receiver method as the basic framework similar to previous RTCA SC-159 analyses. Each of the three framework elements is modeled by a set of key parameters. For potential RFI sources the method prescribes collection of key parameters such as effective isotropic radiated power (EIRP) (both fundamental and unwanted) and carrier frequency, antenna gain pattern, and modulation type and spectral shape. Key characteristics collected for the “path” element include scenario-specific distances and directions from the receiver to the RFI sources, type of radio wave propagation (free-space or other type), and propagation statistics. Basic propagation path models (i.e.; isotropic attenuation versus distance) can be described independent of the RFI scenario. Key characteristics for the GNSS receiver generally include signal sensitivity, selectivity, RFI susceptibility, receive antenna gain patterns, and minimum performance requirements.

6.2.1.1 ATCt Source Model Summary

Key ATCt source power parameters used in this study are 32 dBW total base station fundamental EIRP per channel and -90 dBW/MHz (1559-1610 MHz) unwanted/unintentional mobile unit EIRP spectral density. ATCt base station channel center frequencies are 1552.7 MHz (Phase 0 deployment), 1528.8 and 1552.7 MHz (Phase 1), and 1531 and 1550.2 MHz (Phase 2). The base station channel modulation is the 3GPP LTE (orthogonal frequency division multiplex) which has essentially a rectangular spectrum shape either 5 MHz wide (Phases 0 and 1) or 10 MHz wide (Phase 2). Mobile units transmit low fundamental power (-7 dBW EIRP) with 3GPP LTE

©2011 RTCA, Inc.

modulation on paired 5 or 10 MHz wide channels centered 101.5 MHz above the corresponding base station channels.

The base station transmit antenna main beam has wide horizontal plane beamwidth and narrow vertical plane beamwidth to cover a 120° wide sector. The antenna pattern is modeled for analysis by a parabolic fit to the vertical pattern main beam and constant, low-gain limit levels for the side- and back-lobes. Mobile units are assumed to have a 0 dBi omni-directional pattern for unwanted /unintentional emissions. Average base station tower-to-tower spacing values in a given metropolitan deployment zone (e.g., 2.2 km in the metro high density central zone) help define base station locations and average cell diameters for the ATCt base and mobile unit aggregate RFI analyses.

6.2.1.2 Isotropic Propagation Path Model Summary

All the RFI propagation path loss models used in this study are based on the flat-earth approximation in which the ground under the aircraft is assumed to be essentially smooth and flat out to a radio horizon radius from the point directly under the aircraft. This radio horizon value depends, in general, on the heights of the aircraft GNSS and RFI source antennas and the amount of atmospheric refraction along the path. This report uses the 4/3 Earth radius approximation to account for the refractive effect on the radio horizon.

The isotropic propagation path model in four of the five RFI scenarios in this study is a probabilistic model to address random phenomena of scattering, reflections, and blockage prior to arriving at an aircraft's GPS antenna. These propagation environments were the subject of much research during the development of cellular radio systems. As a result, the cellular radio community has over the years developed propagation models which for the most part are applicable to the present RFI evaluation scenarios. The probabilistic model for the median isotropic path loss in this study is a blend of three segment models: a two-ray model for short ranges, a Hata-Okumura model for long ranges, and one of two medium range models to connect the short- and long-range segments for a continuous function. For the ATCt base station analyses, the medium range path segment is a constant-slope logarithmic fit function. For ATCt mobile unit analyses, due to antenna height limitations, it is a modified Erceg/Greenstein model. The deterministic isotropic path loss model for the high altitude enroute scenario is the free-space model (attenuation proportional to the square of the distance).

6.2.1.3 GNSS Airborne Receiver Model Summary

The L1 band GPS receiver system model used in the analyses consists of an active antenna unit[1] connected via coaxial cable to a receiver-processor unit. The receiver system model s a “minimum operational performance” model, i.e.; the least complex configuration needed to meet current generation GPS L1 MOPS performance requirements (e.g., GPS and SBAS signal tracking and data demodulation). The receiver system is tested to meet the performance requirements at minimum rated desired signal levels in the presence of various amounts of RFI. The two principal receiver RFI test conditions which form the bases for analyzing receiver susceptibility to the LightSquared ATCt emissions are the adjacent band CW RFI limit versus frequency and the maximum wideband non-aeronautical RFI power spectral density within the GPS receiver passband. Consistent with standard spectrum management practice, these maximum test limits are adjusted downward by 6 dB for the analyses to provide a safety margin for environment uncertainties.

[1] A passive radiating antenna element and low noise amplifier with pre- and post-selector RF filters

©2011 RTCA, Inc.

The principal effect mechanism of strong near-band RFI signals from ATCt base stations is overload of the receiver selectivity that results in receiver RF/IF gain compression for the desired signal. Other degradation mechanisms are possible but overload was chosen for simplicity. This effect mechanism is modeled for this report as a function of total received RFI power at a center frequency essentially independent of RFI signal bandwidth. The ATCt base station received RFI is compared to the safety margin-adjusted, MOPS adjacent band CW susceptibility limit versus frequency (e.g., -122.35 dBW total received power at 1552.7 MHz, the upper 5 MHz wide base station channel center frequency).

The principal effect mechanism for low level unwanted /unintentional RFI emissions received from ATCt mobile units is an increase of the baseline broadband RFI present within the GPS receiver passband that reduces the carrier to noise density ratio. The derived limit in this case is -146.5 dBW/MHz within the GPS passband 1575.2 ± 10 MHz. These RFI values are referenced to the GPS passive receive antenna output terminals. The receive antenna gain upper and lower hemisphere patterns used in these analyses have been developed within RTCA SC-159 for previous analyses.

6.2.2 Aeronautical RFI Encounter Scenario Development

As detailed in Section 3, five general operational scenarios have been selected from among normal aircraft operations for the ATCt aggregate RFI evaluations in this report:

- high altitude enroute,
- low altitude enroute / terminal area (FAF waypoint),
- Category I precision approach,
- Category II/III precision approach, and
- airport surface movement (taxiway) operations.

GPS-based navigation and/or position reporting is in use now or is in development for the operations represented by these scenarios. Basic RFI encounter scenarios for the operations have been developed within SC-159 for previous RFI assessments and have been adapted to address the ATCt base station sources. Each RFI encounter scenario places the aircraft at a certain representative location and height above ground. Table 6-1 summarizes for the five RFI encounter scenarios the key antenna height and radio horizon parameters assumed and calculated for use in the RFI analysis.

Table 6-1 Aeronautical Scenario Antenna Height and Radio Horizon Parameters

Scenario Case	Aircraft Ant. Ht. (m)	ATCt Base Ant. Ht (m)	ATCt Mobile Ant. Ht. (m)	Radio Horiz. to Base (km)	Radio Horiz. to Mobile (km)
Surface	4.0	30	N/A	30.84	N/A
Cat. II DH	25.94	30	1.8	43.59	26.54
Cat. I DH	53.34	30	1.8	52.71	35.65
FAF WP	535.2	30	1.8	118.00	100.94
High Altitude	5490	30	N/A	328.16	N/A

Generic locations at or near metropolitan airports are used in the RFI evaluation for the first four cases in Table 6-1. A specific case location over South-Central Pennsylvania is used to evaluate aggregate RFI that may be encountered in a high altitude scenario. This case is believed to be representative of enroute operations near densely populated coastal regions of the United States. An aircraft flying at 5490 m (18,000 feet) altitude over the indicated location will have seven different metropolitan areas within its radio horizon. Table 3-2 lists key parameters for the High Altitude Enroute specific case.

©2011 RTCA, Inc.

Table 6-2 Metropolitan Areas Visible in High Altitude Enroute Specific Case

Location	Lat. (°N)	Long. (°W)	Distance to aircraft (km)	City Radius (km)
Aircraft	39.819	77.573	N/A	N/A
Baltimore, MD	39.291	76.610	122.26	45.4
Washington, DC	38.899	77.036	118.58	45.4
Harrisburg, PA	40.260	76.882	91.25	30.0
Philadelphia, PA	39.952	75.162	268.80	45.4
Pittsburgh, PA	40.438	79.997	278.49	45.4
Allentown, PA	40.603	75.470	249.84	30.0
Richmond, VA	37.541	77.434	254.06	30.0

FAA airport and approach layout guidelines contain various limitations on structure height and presence of objects on or near airport operational areas. Those guidelines are used in this report to determine location restrictions on the ATCt base station antennas and mobile units (source exclusion zones). Table 6-3 summarizes the scenario RFI source exclusion zone parameters used in the aggregate RFI evaluations.

Table 6-3 Aeronautical Scenario ATCt Source Exclusion Zone Parameters

Scenario Case	Base Inner Rad. (m)	Base Outer Rad. (m)	Annular Half-Ang. (deg)	Mobile Inner Rad. (m)	Mobile Outer Rad. (m)	Annular Half-Ang. (deg)
Surface (Taxiway)	0 550	550 4200	180 22.5	N/A	N/A	N/A
Cat. II DH	0 420 840	420 840 4470	180 60 10	449.3	2842	25
Cat. II DH	0 350 570	350 570 5500	180 40 12	488	5830	17
Term. Area (FAF WP)	N/A	N/A	N/A	N/A	N/A	N/A
High Alt. Enroute	298985*	328160*	45*	N/A	N/A	N/A

* This high altitude exclusion zone annular segment represents the Atlantic Ocean off New Jersey and the Delmarva Peninsula (45° full angular extent).

Initial and warm-start signal acquisition are important receiver modes in several of the operational scenarios. However for this ATCt RFI assessment, the GPS aircraft receiver mode with the highest RFI test limits, signal tracking and data demodulation, is the chosen assessment basis.

6.2.3 Aggregate ATCt Base and Mobile Station RFI Analysis Summary

6.2.3.1 ATCt Location Methods Summary

Aggregate RFI effects for ATCt base stations have been analyzed assuming both random and fixed grid station locations while mobile units are assumed to be randomly located within a cell. Three different values are analyzed for the number of mobile units per average cell area. Both location methods share common features of median path loss to a given radial location and the radio horizon for a given RFI scenario (Table 6-1). They also share a measure of the relative ATCt base station tower spacing but use it somewhat differently. The random location method uses the tower spacing within a given

©2011 RTCA, Inc.

deployment zone to determine an average value of source concentration (probabilistic parameter). The fixed discrete method, however, uses the spacing to set the fixed hexagonal grid size. The random method aggregate RFI calculation is performed by integration of a specified continuous function of location radius from zero to the radio horizon, while the discrete method calculation is performed by summing a similar function at specific discrete locations out to the radio horizon.

Source exclusion zones (Table 6-3) in the vicinity of airports are incorporated in the analysis for several of the operational scenarios as discussed in Section 3.6. The exclusion zones for the random emitter location method are implemented in the form of annular sectors with particular angular and radial size parameters. For the discrete location method an exclusion zone is implemented by simply removing one or more of the grid points from the sum. An ocean exclusion zone is used in the high altitude scenario to represent the Atlantic Ocean off the eastern U.S. shore.

6.2.3.2 Aggregate ATCt Base Station RFI Analysis Summary

For each of the five RFI scenarios Table 6-4 shows the aggregate mean received RFI power spectral density and aggregate path loss for ATCt base station fundamental emissions as determined by the random and fixed discrete source location methods. The results are for the full distribution of ATCt base stations within view of the aircraft GPS antenna at the indicated antenna heights. Those ATCt base stations are operating at the LightSquared Phase 0 deployment plan center frequency of 1552.7 MHz with a 5 MHz channel bandwidth, 32 dBW EIRP (25 dBW EIRP spectral density) at beam center, and peak channel loading. The single-city ATCt base station deployment concentration (Figure 2-9) is used for the surface through FAF WP scenarios and the multi-city concentration (Figure 2-10) is used for the high altitude scenario.

Table 6-4 ATCt Base Station Fundamental RFI Effect Aggregate Results Summary

Case	A/C Ant. Ht. (m)	Random Rcv PSD (dBW/MHz)	Random Agg. PL (dB)	Discrete Rcv PSD (dBW/MHz	Discrete Agg. PL (dB)
Surface	4.0	-86.52	111.52	-88.76	113.77
Cat. II DH	25.94	**-76.03**	101.03	**-79.09**	104.10
Cat. I DH	53.34	**-75.92**	100.92	**-77.63**	102.64
FAF WP	535.2	**-73.55**	98.55	**-73.60**	98.61
High Alt.	5490	-86.60	111.60	-87.01	112.01

Note: All the received power spectral densities exceed the GPS MOPS limit of -129.35 dBW/MHz at 1552.7 MHz. Those shown in bold font are cases that exceed the limit by the largest amounts.

The Table 6-4 aggregate mean received RFI values are to be compared with the GPS receiver MOPS-related environmental limit: -129.35 dBW/MHz at the ATCt base station Phase 0 transmit center frequency (1552.7 MHz). Depending on the scenario, the mean RFI results from the random location method exceed that limit by 42.7 dB (high altitude) to 55.8 dB (FAF). If the base stations were all operating at a nominal 60% loading factor, all the scenario mean received power results would decrease by 2.2 dB. These results are driven primarily by the high transmit power, the station deployment concentration, and the close proximity to the GPS aviation receiver passband edge. These large mean aggregate received RFI power levels are expected to cause complete loss of aviation GPS receive function.

©2011 RTCA, Inc.

6.2.3.3 Aggregate ATCt Mobile Station RFI Analysis Summary

Table 6-5 summarizes the ATCt mobile unit (UE) aggregate results for the combined unwanted (transmitting) and unintentional (idling) RFI emission effects. The scenarios analyzed here are believed to have the largest RFI impact. Regardless of UE operating mode, the RFI emission assumed for this report is -90 dBW/MHz in the GNSS L1 band, 1559-1610 MHz (i.e.; the ATCt license OOBE limit). Within the range for numbers of UE's/cell, the 300 unit count RFI values are thought to be most representative. The reference cell size has a 2.2 km average diameter (3.8 square kilometers area).

Also listed in Table 6-5 for the three scenario cases are aggregate values for a baseline set of general portable and mobile electronic devices (not including ATCt UE's) previously described in Section 4.2.2 and taken from RTCA/DO-235B [6-1]. The DO-235B model baseline devices are assumed to be emitting -81.1 dBW/MHz (unwanted or unintentional RFI EIRP) with average surface concentration of 1 per 10^4 square meters (= 380 devices in an average ATCt metro cell area). The baseline aggregate RFI values are calculated with the same method as the ATCt mobile unit values for each scenario.

Table 6-5 ATCt Mobile Station Unwanted RFI Effect Aggregate Results Summary

Case	A/C Ant. Ht. (m)	100 UE/cell Rcv PSD (dBW/MHz)	300 UE/cell Rcv PSD (dBW/MHz)	1000 UE/cell Rcv PSD (dBW/MHz)	Baseline Rcv PSD (no UE)
Surface	4.0	-	-	-	-
Cat. II DH	25.94	-164.98	-160.21	-154.98	-149.86
Cat.I DH	53.34	-166.23	-161.46	-156.23	-151.11
FAF WP	535.2	-166.16	-161.39	-156.16	-151.04
High Alt.	5490	-	-	-	-

When Table 6-5 aggregate mean results are compared to the GPS L1 MOPS receiver environment limit, -146.5 dBW/MHz over 1575.42 ± 10 MHz, all the individual results are within the MOPS-related environment limit. However, the baseline value in each scenario is always assumed to be present. Thus the presence of the additional ATCt mobile units increases the overall non-aeronautical RFI environment mean power spectral density.

The extra ATCt mobile station RFI does not have as significant an effect on the aviation GPS receiver (increase over baseline RFI level is nominally 9% for 300 UEs per cell to 31% for 1000 UEs per cell) as the base station fundamental RFI effect. However it still poses some increased probability risk over the baseline situation of exceeding the safety margin.

6.2.4 Possible Mitigation Techniques

RFI Source mitigation options discussion (Section 5.1) suggests a frequency shift to the lowest ATCt base station channel (1528.8 MHz) would allow compatibility as long as station deployment concentrations do not increase over the assumed levels. An initial estimated maximum transmit power limit curve (Figure 5-1) as a function of ATCt base station channel center frequency has been derived as a guide for assessing RFI compatibility. Since it is based on a minimum aggregate path loss value from the 5 RFI scenarios and may not be the actual minimum value, more study is needed to refine the limit curve. Aviation GPS receiver wide bandwidth RFI susceptibility performance near 1528 MHz also needs further validation work.

©2011 RTCA, Inc.

Receiver mitigation options discussion (Section 5.2) suggests the only viable option in the long term is through invocation of new performance standards for the combined antenna/receiver combination that would allow the manufacturers the ability to optimally layer filtering throughout the receiver front-end. This approach would take many years, since it would require new standards to be developed, and installed within the fleet of aircraft that operate within U.S. airspace. No viable short term options based on changes to GPS receivers or antennas have been identified.

6.3 Conclusions and Recommendations

The study concludes that the current LightSquared terrestrial authorization would be incompatible with the current aviation use of GPS, however modifications could be made to allow the LightSquared system to co-exist with aviation use of GPS. The following conclusions and recommendations are strictly based on the operational parameters for the LightSquared terrestrial wireless broadband network described in Section 2.4 and source mitigations identified in Section 5. These operational parameters would produce less RFI than if LightSquared were to operate at its fully-authorized limits.

In addition, the analysis is based upon the assumption that all equipment is minimally compliant with the interference rejection requirements in harmonized domestic and international standards. Additionally, since GPS is an aviation safety service, the analysis includes a 6 dB safety margin as is standard practice (see e.g., ITU-R M.1477 [6-2]). Results from the four receivers tested (see Appendix D) show that these receiver models are significantly more resilient to interference from the LightSquared ATCt base stations than limits derived from the standards.

The impact of a LightSquared terrestrial base station upper channel spectrum deployment is expected to be complete loss of GPS receiver function. Because of the size of the single-city station deployment, GPS-based operations below about 2000 feet will be unavailable over a large radius from the metro deployment center (assuming no other metro deployments are nearby). Given the situation in the high altitude U.S. East Coast scenario, GPS-based operations will likely be unavailable over a whole region at any normal aircraft altitude.

The results of this study indicate that terrestrial base station operation at the lower 5 MHz wide channel (1526.3 – 1531.3 MHz) is compatible with aviation GPS operations for all the representative scenarios (including both signal tracking and initial acquisition). The study indicates that for ATCt base stations using only the lower 10 MHz wide channel (1526-1536 MHz), there is a small positive margin for GPS tracking (but not necessarily initial acquisition) in the presence of mean aggregate terrestrial network RFI.

The main recommendations from this aviation GPS receiver operational assessment are:

1. From an aviation perspective, LightSquared upper channel operation should not be allowed.
2. Further study is recommended to more carefully determine a refined terrestrial base station power versus frequency limit considering:
    a. determination of the lowest path loss for the low altitude enroute scenario,
    b. confirmation of acceptable receiver susceptibility for GPS initial acquisition and signal tracking in the presence of the 10 MHz bandwidth terrestrial network interference,
    c. computation of the cumulative probability distribution function for the aggregate path loss.

©2011 RTCA, Inc.

6.4 References

[6-1] SC-159, “Assessment of Radio Frequency Interference Relevant to the GNSS L1 Frequency Band,” RTCA Document No. RTCA/DO-235B, 13 Mar. 2008

[6-2] Rec. ITU-R M.1477, Technical and Performance Characteristics of Current and Planned Radionavigation-Satellite Service (space-to-Earth) and Aeronautical Radionavigation Service Receivers to Be Considered in Interference Studies in the Band 1 559-1 610 MHz.

©2011 RTCA, Inc.

MEMBERSHIP
(corrected as of 06/15/2011)

Special Committee 159

Global Positioning System

SC-159 Chairman

Christopher Hegarty	The MITRE Corporation
George Ligler	Project Management Enterprises Inc.

SC-159 Secretary

Young Lee	The MITRE Corporation

Working Group 6 Members

Hamza Abduselam	Federal Aviation Administration
Kenneth Alexander	Federal Aviation Administration
John Ashley	The MITRE Corporation
Chad Baber	FAA/WAAS
Michael Biggs	Federal Aviation Administration
Mark Cato	Air Line Pilots Association
David Choi	The MITRE Corporation
Paul Christopher	PFC Associates
Barbara Clark	Federal Aviation Administration
Milton Clary	Overlook Systems Technologies, Inc.
Charlie Daniels	Overlook Systems Technologies, Inc.
James Davis	FreeFlight Systems
George Dimos	Volpe National Transportation Systems Center
Joe Dorfler	DORS International
Santanu Dutta	LightSquared
Swen Ericson	ZETA Associates
Robert Erlandson (Co-Chair)	NISC III
John Foley	Garmin Ltd.
Robert Frazier (Co-Chair)	Federal Aviation Administration
Joe Grabowski	ZETA Associates
Matt Harris	The Boeing Company
Tom Hayden	Telecomm Strategies
Jens Hennig	General Aviation Manufacturers Association
Bruce Jacobs	Pillsbury, Winthrop, Shaw, Pittman
Sai Kalyanaraman	Rockwell Collins, Inc.
E.F. Charles LaBerge	EFC LaBerge Engineering & Analysis, LLC
Vladimir Latev	Universal Avionics Systems Corporation
Bob Lehman	Honeywell International, Inc.
Frank Lorge	Federal Aviation Administration
Daryl McCall	Fastek International
Harold Moses	RTCA, Inc.

©2011 RTCA, Inc.

Timothy Murphy	The Boeing Company
Gustavo Nader	INMARSAT
Orville Nyhus	Honeywell International, Inc.
Ajay Parikh	LightSquared
Kenneth Peterson	NISC III
Brian Ramsey	National Aeronautics and Space Administration
Patrick Reddan	ZETA Associates
Marc Revol	Thales Avionics
Michael Richmond	Federal Aviation Administration
David Robinson	Federal Aviation Administration
Raul Rodriguez	Leventhal, Senter & Lewman
John Savoy	Honeywell International, Inc.
Mike Simmons	Garmin Ltd.
Bernald Smith	Soaring Society of America
John Tepper	Federal Aviation Administration
Timothy Totten	United Parcel Service
Michael Tran	The MITRE Corporation
A.J. Van Dierendonck	AJ Systems
Tom Walsh	Aerospace Corporation
Jim Young	Honeywell International, Inc.

SC-159 Members

Steven Aab	Rockwell Collins, Inc.
Hamza Abduselam	Federal Aviation Administration
Raghavendra Achanta	Advanced Management Technology Inc.
Wayland Adams	Honeywell International, Inc.
Mark Ahlbrecht	Honeywell International, Inc.
Jeffrey Aimar	The Boeing Company
Dennis Akos	GPB HEPL
Kenneth Alexander	Federal Aviation Administration
Khalifa Ali	Federal Aviation Administration
Rob Anderson	Federal Aviation Administration
Robert Anoll	Federal Aviation Administration
Douglas Arbuckle	Federal Aviation Administration
Jean-Pierre Arethens	Thales Avionics
John Ashley	The MITRE Corporation
Laurent Azoulai	Airbus SAS
Chad Baber	FAA/WAAS
Phillip Baker	Overlook Systems Technologies, Inc.
Michael Ball	Northrop Grumman Corporation
Clayton Barber	Garmin Ltd.
Terrence Barrett	UCI
Chris Bartone	Ohio University - Avionics Engineering Center
Steve Baruch	LSL-LAW
Frederic Bastide	Sofreavia

©2011 RTCA, Inc.

Michael Beamish	Analysis Unlimited
Kevin Bean	The MITRE Corporation
Steven Bellingham	NAV Canada
Don Benson	MITRE
Knute Berstis	NOAA
Gerhard Berz	Skyguide Magazine
Michael Biggs	Federal Aviation Administration
Juan Blanch	Stanford University
John Borden	NAVSYS Corporation
Kathleen Boseley	Honeywell International, Inc.
Phil Boughton	DORS International
Michael Braasch	Ohio University - Avionics Engineering Center
Ronald Braff	The MITRE Corporation
Benjamin Brandt	The MITRE Corporation
Mats Brenner	Honeywell International, Inc.
Kevin Bridges	Federal Aviation Administration
Ned Brokloff	The Johns Hopkins University
Alison Brown	NAVSYS Corporation
Steve Brown	National Business Aviation Association
Sam Buckwalter	ARINC Incorporated
Deane Bunce	Federal Aviation Administration
Jason Burns	Federal Aviation Administration
Bob Buschette	Rockwell Collins, Inc.
Hank Cabler	Federal Aviation Administration
Curtis Call	Honeywell International, Inc.
Alan Cameron	JM Telecom Consultants
Alessandro Capretti	ICAO
Tim Cashin	The MITRE Corporation
Shawn Casler	FAA - Wm. J. Hughes Technical Center
Rick Cassell	Engility Corporation
Mark Cato	Air Line Pilots Association
Fang-Chenh Chan	IIT Research Institute
Eric Chatre	Galilec Support Structure
Jean Chenebault	Alcatel Space Industries
Lawrence Chesto	1 Grp of Consultants & Independents
Laura Cheung	Raytheon Systems Company
David Choi	The MITRE Corporation
Thomas Christein	SAIC
Paul Christopher	PFC Associates
Barbara Clark	Federal Aviation Administration
Gregory Clark	Advanced Management Technology Inc.
Milton Clary	Overlook Systems Technologies, Inc.
Kim Class	Honeywell International, Inc.
Richard Cooley	Honeywell International, Inc.
John Croft	Flight International

©2011 RTCA, Inc.

David Crosser	Raytheon Systems Company
Jim D'ottavi	FAA William J Hughes Technical Center
Charlie Daniels	Overlook Systems Technologies, Inc.
Steven Davies	Raytheon Systems Company
James Davis	FreeFlight Systems
Jerry Davis	Airbus Industries
Bruce DeCleene	Federal Aviation Administration
Thomas Dehel	Federal Aviation Administration
Michael DiBenedetto	Ohio University - Avionics Engineering Center
George Dimos	Volpe National Transportation Systems Center
Yi Ding	Esterline CMC Electronics
Mike Dion	Alion Science and Technology
Maria Dipasquantonio	Federal Aviation Administration
James Doherty	Institute for DEF Analyses
Daniel Domey	Esterline CMC Electronics
Joe Dorfler	DORS International
Christopher Douglas	Sierra Nevada Corporation
JR Dreier	JM Telecom Consultants
Ed Drocella	U. S. Department of Commerce
Santanu Dutta	LightSquared
Kevin Dutton	Honeywell International, Inc.
Glen Dyer	ITT Corporation
David Eicher	Rockwell Collins, Inc.
Bakry El-Arini	The MITRE Corporation
Joe Elchynski	Honeywell International, Inc.
Leo Eldredge	Federal Aviation Administration
Per Enge	Stanford University
Swen Ericson	ZETA Associates
Robert Erlandson	NISC III
Russ Etheridge	Overlook Systems Technologies, Inc.
Sohel Fares	Esterline CMC Electronics
Richard Farr	American Airlines, Inc.
James Fernow	The MITRE Corporation
Harold Fink	JM Telecom Consultants
Bill Flathers	Sparrow-Tech Inc.
John Foley	Garmin Ltd.
JoAnn Ford	Federal Aviation Administration
Thomas Foster	SAIC
Robert Frazier	Federal Aviation Administration
Amy Fritz	The MITRE Corporation
Sally Frodge	Federal Aviation Administration
Peter Fyfe	The Boeing Company
Paul Galyean	Navcom Technology
Robert Geary	Titan Corporation

©2011 RTCA, Inc.

Michael Geyer	Department of Transportation
Joseph Gillespie	FAA - Wm. J. Hughes Technical Center
David Girts	Honeywell International, Inc.
Russell Gollnick	Rockwell Collins, Inc.
Pamela Gomez	Federal Aviation Administration
Joe Grabowski	ZETA Associates
Sylvie Grand-Perret	EUROCONTROL
Robert Grappel	MIT Lincoln Laboratory
Charisse Green	Federal Aviation Administration
Btett Greenwalt	Federal Communications Commission
Duncan Greer	Queensland University of Technology
Dieter Guenter	ISI, Inc.
Herve Guichon	Thales Avionics
Gondo Gulean	EUROCONTROL
Alan Hankin	ISI, Inc.
Joseph Hansen	Sierra Nevada Corporation
Matt Harris	The Boeing Company
Randolph Hartman	Honeywell International, Inc.
Tom Hayden	Telecomm Strategies
Christopher Hegarty	The MITRE Corporation
Mark Hemstad	NAUTAC
Jens Hennig	General Aviation Manufacturers Association
Stephen Heppe	Telenergy
Nobuo Hiroe	NEC Corporation, Radio Applications Division
Philip Holmer	Titan Corporation
Steven Horvath	Garmin AT, Inc.
Kris Hutchison	Aviation Spectrum Resources, Inc. (ASRI)
Peter Hwoschinsky	Federal Aviation Administration
Victor Iatsouk	Federal Space Agency "ROSCOSMOS"
Richard Idiens	FDC Belgium
Jean-Luc Issler	CNES
Steven Jackson	Federal Aviation Administration
Bruce Jacobs	Pillsbury, Winthrop, Shaw, Pittman
Merlin James	Garmin Ltd.
James Jameson	Aerospace Corporation
Don Jeckell	Comant Industries, Inc.
Jeff Kacirek	Honeywell International, Inc.
Rudolph Kalafus	Trimble Military and Advanced Systems
Sai Kalyanaraman	Rockwell Collins, Inc.
Elliott Kaplan	The MITRE Corporation
Robert Kelly	Kelly Systems Engineering
Taehwan Kim	The MITRE Corporation
Stephen Kong	AeroConnex LLC
Steve Kuhar	Federal Express Corporation
E.F. Charles LaBerge	EFC LaBerge Engineering & Analysis, LLC

©2011 RTCA, Inc.

John Lacey	Lockheed Martin Corporation
Jonathan Lai	Rockwell Collins, Inc.
Jarrett Larrow	Federal Aviation Administration
Vladimir Latev	Universal Avionics Systems Corporation
Deborah Lawrence	Federal Aviation Administration
Jiyun Lee	AMTI
Young Lee	The MITRE Corporation
Bob Lehman	Honeywell International, Inc.
Roland Lejeune	The MITRE Corporation
Michael Lemke	Department of Defense
George Ligler	Project Management Enterprises Inc.
Andreas Lipp	EUROCONTROL
Fan Liu	Honeywell International, Inc.
Gary Livack	Federal Aviation Administration
Robert Loh	Innovative Solutions International, Inc.
Mark Lorenz	ITT Corporation
Frank Lorge	Federal Aviation Administration
Ming Luo	Stanford University
Mikael Mabilleau	Egis Avia
Larry MacDonald	Federal Aviation Administration
Alberto Madrazo-Fernandez	GMV Aerospace and Defence, S.A.
Paul Magno	Helicopter Association International
Catherine Majauskas	Federal Aviation Administration
Robert Mallet	Technology Planning Inc.
Ian Mallett	CASA Central Authority
Christophe Marionneau	Thales Avionics
Kelly Markin	The MITRE Corporation
Daryl McCall	Fastek International
Jim McDonald	Honeywell International, Inc.
Keith McDonald	NavtechGPS
Edward McGann	Megapulse, Inc.
Gary McGraw	Rockwell Collins, Inc.
Thomas McKendree	Raytheon Systems Company
Jeff Meyers	Federal Aviation Administration
Calvin Miles	Federal Aviation Administration
Barry Miller	Federal Aviation Administration
Bradford Miller	Federal Aviation Administration
James Miller	National Aeronautics and Space Administration
Steve Molina	Joint Spectrum Center
Frederick Moorefield	U. S. Air Force
Kenneth Morgan	Honeywell International, Inc.
Tadashi Moriya	(Limited Company) Moriya Engineering Consultants
Joseph Morrissey	The MITRE Corporation
Thomas Morrissey	ZETA Associates

©2011 RTCA, Inc.

Harold Moses	RTCA, Inc.
Campbell Motley	Innovative Solutions International, Inc.
Joel Murdock	Federal Express Corporation
Timothy Murphy	The Boeing Company
Arun Murthi	AERO&SPACE USA INC
Gustavo Nader	INMARSAT
Prasad Nair	Project Management Enterprises Inc.
Mitchell Narins	Federal Aviation Administration
Robert Nelson	Satellite Engineering research Corporation
Pierre Neri	ENAC
Tien Ngo	U. S. Navy
Elisabeth Nguyen	The Aerospace Corporation
Paul Novak	SAIC
Orville Nyhus	Honeywell International, Inc.
Daniel O'Laughlin	The MITRE Corporation
John Oelschlaeger	JM Telecom Consultants
Frank Olic	Raytheon Systems Company
Larry Oliver	Advanced Management Technology Inc.
David Olsen	Federal Aviation Administration
A.J. Oria	Overlook Systems Technologies, Inc.
Rick Packard	Adacel Systems, Inc.
Timothy Padden	
Mike Palmer	Transport Canada
Ajay Parikh	LightSquared
Patrice Pasturel	Garmin AT, Inc.
Kenneth Peterson	NISC III
William Petruzel	BP Associates
Eric Phelts	Stanford University
Michael Philippakis	Cobham Tech. Service
Brian Pierce	U. S. Air Force
Ryan Porisch	Honeywell International, Inc.
Paul Prisaznuk	ARINC Incorporated
Sam Pullen	Stanford University
Patrick Quach	Langley Research Center
Srini Raghavan	Aerospace Corporation
Brian Ramsay	National Aeronautics and Space Administration
B. Rao	The MITRE Corporation
Patrick Reddan	ZETA Associates
Patrick Reines	Honeywell International, Inc.
Marc Revol	Thales Avionics
Michael Richmond	Federal Aviation Administration
Lionel Ries	CNES
David Robinson	Federal Aviation Administration
Mike Rockwell	ARINC Incorporated
Carlos Rodriguez	Federal Aviation Administration

©2011 RTCA, Inc.

Raul Rodriguez	Leventhal, Senter & Lewman
Glyn Romrell	Sierra Nevada Corporation
Linn Roth	Locus, Inc.
Benoit Roturier	DGAC, France
Steve Rowson	Thales ATM, Inc.
Jason Rudisill	Honeywell International, Inc.
Dean Rudy	Sierra Nevada Corporation
William Ruhl	Esterline CMC Electronics
William Russell	Russell Systems
Takeyasu Sakai	Electronic Navigation Research Institute
Jim Savage	Innovative Solutions International, Inc.
John Savoy	Honeywell International, Inc.
Albert Sayadian	Federal Aviation Administration
Michael Scales	U. S. Air Force
Joseph Scheitlin	Honeywell International, Inc.
Tim Schempp	Raytheon Systems Company
Les Schroeppel	SAIC
Ron Schroer	SAIC
David Scull	OPTIMUS Corporation
Mark Settle	Federal Communications Commission
Ralph Sexton	Innovative Solutions International, Inc.
Ranjeet Shetty	Advanced Management Technology Inc.
Curtis Shively	The MITRE Corporation
Paul Siegmund	Federal Aviation Administration
C. Sigler	Advanced Management Technology Inc.
Mike Simmons	Garmin Ltd.
Trent Skidmore	Ohio University - Avionics Engineering Center
Bernald Smith	Soaring Society of America
Dusty Somerville	JetBlue Airways
George Sotolongo	The Boeing Company
Craig Spence	Aircraft Owners and Pilots Association
Cary Spitzer	AvioniCon
Thomas Stansell	Stansell Consulting
Geoff Stearn	LightSquared
Jeff Stevens	Old North Bridge Consulting
Bob Stimmler	Raytheon Systems Company
Alex Stratton	Rockwell Collins, Inc.
Bruce Stucky	Garmin Ltd.
John Studenny	Esterline CMC Electronics
Mark Sturza	3C Systems Company
Mahesh Surathu	Rockwell Collins, Inc.
Ann Swanson	DowLohnes
Thomas Taffner	JM Telecom Consultants
Aziz Tazi	Transport Canada

©2011 RTCA, Inc.

Michael Teems	The Johns Hopkins University
Tom Teetor	Defense Concept Associates, Inc.
John Tepper	Federal Aviation Administration
Marcus Tittiger	Transport Canada
Timothy Totten	United Parcel Service
Michael Tran	The MITRE Corporation
Ted Urda	Federal Aviation Administration
A.J. Van Dierendonck	AJ Systems
Karen Van Dyke	Volpe National Transportation Systems Center
Frank Van Graas	Ohio University - Avionics Engineering Center
Kevin Vanderwerf	Honeywell International, Inc.
Michael Vaujin	Honeywell
Javier Ventura-Traveset	European Space Agency
Paul Volk	Adaptive Aerospace Group
Matthew Wade	Federal Aviation Administration
James Waid	Honeywell International, Inc.
Tom Walsh	Aerospace Corporation
Todd Walter	Stanford University
Rick Walton	Lockheed Martin Corporation
Mike Webb	Federal Aviation Administration
Michael Whitehead	Satloc
Joel Wichgers	Rockwell Collins, Inc.
Larry Wiederholt	MITRE
Heidi Williams	Aircraft Owners and Pilots Association
Jeffrey Williams	University of Houston
Robert Williams	Joint Spectrum Center
Christopher Wolf	Federal Aviation Administration
Jorge Woods	Civil Aviation Safety Authority
Sandra Wright	Alion Science and Technology
Victor Wullschleger	Federal Aviation Administration
Rui Xue	Aviation Data Communication Corporation
Tin Yau Ying	U. S. Air Force
David York	Helicopter Association International
Jim Young	Honeywell International, Inc.
Tom Zalesak	U. S. Navy
Nestor Zarraoa-Lopez	GMV (Spain)
David Zeigler	Spectralux Corporation

©2011 RTCA, Inc.

This page intentionally left blank.

©2011 RTCA, Inc.

Appendix A

MOPS-Based GNSS Receiver Broadband RFI Test Procedure

©2011 RTCA, Inc.

This page intentionally left blank.

©2011 RTCA, Inc.

A MOPS-BASED GNSS RECEIVER BROADBAND RFI TEST PROCEDURES

The objective of the following tests is to evaluate the overload and desensitization impact of the LightSquared transmissions on the GNSS receiver. This impact is verified by evaluating GPS receiver performance metrics (critical to a certified aviation receiver) in the presence of LightSquared 3GPP Interferers.

A.1 MOPS-based GPS Receiver Overload RFI Effect Test Procedures

The intent of the following test procedures is to evaluate the impact of LightSquared's LTE (3GPP) signal transmissions on the GPS receiver's performance. The following test procedures focus on the application of Continuous Wave (CW) and broadband interferers at specific frequency ranges and varying power levels.

The simulation conditions used for the measurement accuracy tests in RTCA/DO-229D (Section 2.5.8) are used as a baseline for the purposes of evaluating the GNSS receiver's performance in the presence of these transmissions. Based on available information, it is observed that LightSquared's LTE (3GPP) transmission bandwidths will be 10 MHz wide (2 channels across 1526 – 1536 MHz and 1545.5 – 1555.2 MHz) during their final phase 2 deployment. The LTE downlink closest to the GPS band will be centered at 1550.5 MHz (1550.5 +/- 5 MHz). However, during the initial phase zero deployment, the LTE downlink is centered on 1552.7 and is 5 MHz wide (1550.2 to 1555.2 MHz).

For the purposes of the preliminary evaluation the total transmit power in the downlink band is assumed to be concentrated at a single frequency point (for e.g. at 1552.7 MHz). At the outset, the LightSquared signal is not expected to correlate with the GNSS signal. To validate this, the test will initially be performed with CW interference (CWI). The next step would be to utilize a signal generator to replicate the LightSquared transmissions and compare the receiver impact of these transmissions at varying power levels to that of the CWI. This will aid towards obtaining a correction factor between CWI and the LTE modulations. It will also help provide a reference point for the range accuracy SBAS message loss rate tests. The initial power levels of the LightSquared transmissions (for the baseline test conditions explained below) would be set at the same level as the GPS Receiver's CW Interference mask RTCA/DO-229D Appendix C).

The reported Carrier to Noise ratio (CNR) from the GPS Receiver is used as a yardstick of receiver performance. In addition, the pseudorange measurement accuracy (which reflects a critical receiver performance metric) and SBAS Message failure rates (for applicable units) will be evaluated at specific 3GPP Interferer signal levels. However, for a given receiver architecture, the range measurement accuracy is typically tied to the CNR.

A.1.1 Carrier-to-Noise Ratio (CNR) Degradation Baseline Test

The following depicts the test conditions used for comparison of relative impact of the CW interference versus the 3GPP LTE interferers.

A.1.1.1 CNR Degradation Baseline Test Satellite Simulator and Interference Conditions

The simulator and interference conditions shall conform to the following requirements:

a. For all test scenarios, the broadband GNSS test noise and Nsky,antenna (-172.5 dBm/Hz) shall be simulated. A broadband external interference noise (IExt,Test) has a spectral density equal to -173.5 dBm/Hz at the antenna port.

©2011 RTCA, Inc.

The CW power and frequencies are listed in Table A-1. These CW frequencies are the mid band frequencies of the 5 and 10 MHz LTE 3GPP BTS bands that would be rolled out across Phases 0, 1A and 2.

The GNSS test noise depends on the number, power, and type of satellites simulated during the test. The power spectral density of the total GNSS Noise (I_{GNSS}) is -171.9 dBm/Hz (RTCA/DO-235B, Appendix F.2.3). This GNSS Noise was derived for GPS tracking but is used in the test for both GPS and SBAS tracking to allow simultaneous testing of GPS and SBAS thereby reducing test time. However it is acceptable to run the SBAS testing separately using a total GNSS Noise (I_{GNSS}) of -172.8 dBm/Hz for collection of the SBAS message loss rate data. The effective noise power spectral density (I_{Test}) of the satellites present in the simulator scenario may be removed from the total GNSS Noise; to do so, the satellite equivalent power spectral density specified in Table A-2 (I_{GH}, I_{GL}, I_{SH}, and I_{SL}) is removed for each satellite present. The number of maximum power GPS satellites is N_{GH}, the number of minimum power GPS satellites is NGL, the number of maximum power SBAS satellites is N_{SH}, and the number of minimum power SBAS satellites is N_{SL}. The GNSS test noise is determined by removing I_{Test} from I_{GNSS} as follows:

$$I_{GNSS,Test} = 10log10[10^{-171.9//10} - 10^{I_{Test}/10}]; \text{ where:}$$
$$I_{Test} = 10log10[(N_{GL})10^{I_{GL}/10} + (N_{GH})10^{I_{GH}/10} + (N_{SL})10^{I_{SL}/10} + (N_{SH})10^{I_{SH}/10}]$$

Note: The indicated power levels (both signal and noise) are for the steady-state portion of the tests; power levels are set to the required values once steady state navigation has been achieved. Refer to Appendix M of RTCA/DO-229D for an explanation of how I_{Test} is derived and examples of the computation of $I_{GNSS,Test}$ and how it may be applied. This appendix also provides guidance on how the test can be setup.

Simulated GPS and SBAS RF shall be at the minimum power level for the equipment. One GPS satellite shall be set to the maximum power level (including maximum transmit power and maximum combined satellite and aircraft antenna gain). At least two SBAS satellites shall be used.

When the setup uses an external amplifier to simulate the impact of the GNSS Antenna preamplifier (RTCA/DO-301 equivalent antenna), it is recommended that a net 30dB gain (to simulate maximum antenna pre-amp gain and minimum cabling loss) is implemented in order to evaluate the worst case impact of the 3GPP Interferers.

Table A-1 Steady State Accuracy Test CWIValues*

Frequency (MHz)	Power (dBm)	I/S (dB)
1528.8	-22.2	111.8
1531	-28.1	105.9
1550.2	-79.6	54.4
1552.7	-86.4	47.6

* The CWI power is specified at the antenna port. The actual level used during testing is reduced by the minimum frequency selectivity of the active antenna adjusted for any filtering in the test set-up itself. When demonstrating compatibility with a minimum standard antenna, the frequency selectivity is specified in RTCA/DO-301. When using a specific antenna, its minimum frequency selectivity can be used when determined in accordance with RTCA/DO-301. A block diagram of an example test setup is shown Figure A-1.

©2011 RTCA, Inc.

Note: Care should be taken when applying non-L1 CW frequencies so that the L1 CW and broadband specifications are not exceeded.

Table A-2 Satellite Equivalent Power Spectral Density

Satellite Type	Maximum Power Satellite	Minimum Power Satellite
GPS	I_{GH} = -183.5 dBm/Hz	I_{GL} = -196.5 dBm/Hz
SBAS	I_{SH} = -179.8 dBm/Hz	I_{SL} = -198.3 dBm/Hz

Note: These values of equivalent power spectral density were computed using the same assumptions as were used to determine the total GNSS Noise in Appendix C of RTCA/DO-229D.

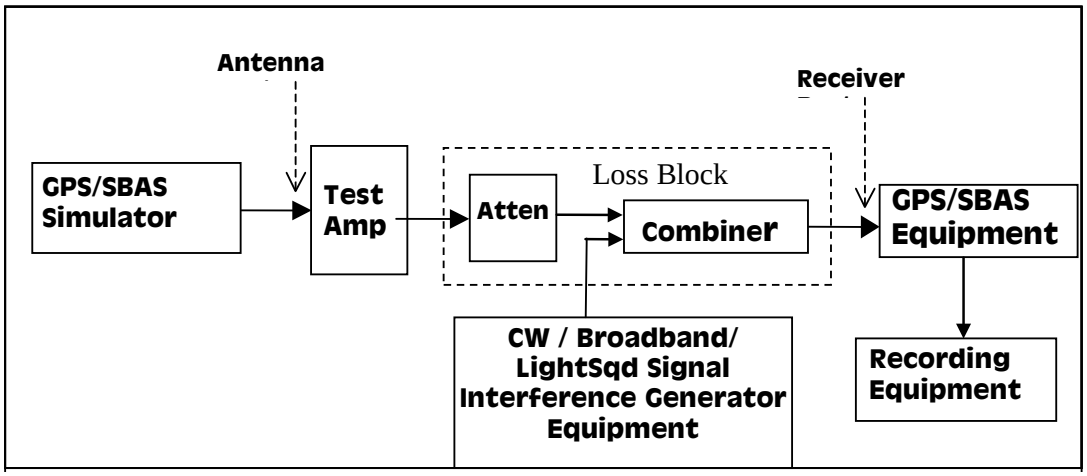

Figure A-1 Example Test Set-up and Compensation of Signals, Noise and Interference

A.1.1.2 CNR Degradation Baseline Test Procedure

a. The test unit is connected to the RF signal and interference source.

b. The simulator scenario shall be engaged and the satellites RF shall be turned on.

c. The equipment under test shall be powered and initialized. It is assumed that the receiver has obtained a valid almanac for the simulator scenario to be tested prior to conducting these tests.

d. When the unit is navigating, the interference to be applied shall be applied to the equipment under test, and the power of the signal and interference shall be adjusted to the required level (at the appropriate frequency as seen in Table A-1).

e. At this base power level ensure that the unit meets the MOPS requirements per RTCA/DO-229D. Record the CNR's of individual satellites (SBAS and GPS).

f. Increase the level of the CWI by 2 dB (this step size may be varied) and hold this level for 60 seconds.

g. Record the CNR's of the individual GPS SV's and the CWI level.

   1. If the CNR's on the SV's have not degraded go back to step f.

   2. If the CNR is reduced by > 1dB, record the result for that RFI level and go back to the previous CWI level, ensure the unit attains the original CNR level and increase the CWI in smaller steps (in order to capture the CWI level that cause a 1dB degradation).

©2011 RTCA, Inc.

3. Proceed to the next step.

h. Repeat steps e, f and g at the other CWI frequencies listed in Table A-1.

i. Replace the CWI interference source with a signal generator that would replicate a 5 MHz bandwidth LTE (3GPP) signal transmission and repeat the test procedure (from step a) for the 1528.8 and 1552.7 MHz frequencies.

j. Replace the CWI interference source with a signal generator that would replicate a 10 MHz bandwidth LTE (3GPP) signal transmission and repeat the test procedure (The starting point may be a I/S value somewhat less than in step i, and using only center frequencies 1531.0 and 1550.2 MHz).

Note:

1. *A comparison of the unit's CNR degradation across both types on interference sources is helpful to verify the assumptions in interference analyses. The value from steps i and j are also used in subsequent higher level receiver performance tests in A.1.2 and A.1.3 below. Any receiver margin above the interference mask is considered as design margin.*
2. *As an option, the comparison test of A.1.1.2 above may be performed for higher CNR degradation values.*

A.1.2 Measurement Accuracy Test

The purpose of this Accuracy Test is to evaluate the equipment's accuracy performance under specific interference levels that have been ascertained from the CNR degradation test procedure (see A.1.1.2). It is not intended to verify the accuracy of the atmospheric corrections; these corrections need not be included in the test. In order to meet the RTCA/DO-229D MOPS requirements, the equipment must meet the accuracy requirements of Section 2.1.2.1, 2.1.3.1, and 2.1.4.1.3 of RTCA/DO-229D.

Note: This evaluation method is based on the assumption that a least-squares position algorithm (per Section 2.1.4.1.4 of RTCA/DO-229D) is implemented. If a different form of positioning is used, this evaluation method may not be appropriate.

A.1.2.1 Measurement Accuracy Test Satellite Simulator and Interference Conditions

The measurement accuracy test shall be performed under the following test conditions:

a. The baseline test condition (at the MOPS interferer levels) used in A.1.1.2 with a modification to $I_{Ext,Test.}$ Use $I_{Ext,Test}$ of -170.5 dBm/Hz vs. -173.5 dBm/Hz.

b. The equivalent LTE (3GPP) broadband RFI signal level at which the receiver's estimated CNR is lower by 1dB from the baseline used in Section 2. (option: higher level CNR degradation values may be used as desired)

The total duration of each test case test shall be based upon sampling intervals required to obtain samples that are statistically independent. Independent samples collected during the initial acquisition and before steady-state operation are used for the validation of σnoise overbounding. The samples collected prior to steady-state operation should not be used for the steady-state RMS accuracy evaluation and the steady-state evaluation of $\left(\sigma_{noise}^2[i]+\sigma_{divg}^2[i]\right)^{1/2}$.

©2011 RTCA, Inc.

Note: It would be advantageous to extend the duration of this test to support evaluation of SBAS Message Loss Rate (for applicable receivers).

This test is performed for following cases (with the listed order of priority)

a. 5 MHz 3GPP Interferer BW at 1552.7 MHz

b. 5 MHz 3GPP Interferer BW at 1528.8 MHz

c. 5 MHz 3GPP Interferer BW's at both 1552.7 and 1528.8 MHz

d. 10 MHz 3GPP Interferer BW at 1531 MHz

e. 10 MHz 3GPP Interferer BW at 1550.2 MHz

f. 10 MHz Interferer BW's at both 1531 and 1550.2 MHz

It is recommended that the Doppler/delta range metrics on the tracked satellites (if available) be evaluated alongside the pseudorange accuracy procedure. This includes evaluation of the accuracy degradation of the Doppler/delta range measurement from the receiver, the Doppler/Delta range validity flag and available loss of code/carrier lock indicators. The measurement type (Doppler/delta range) and validity flag information is available on Label 060 (bits 21 and 22) on the ARINC standard 429 GNSS data bus. The measurement is found on Label 063/064 on this bus.

A.1.2.2 Measurement Accuracy Test Procedure

a. Perform steps a through e of A.1.1.2. Sampling should begin for each satellite immediately after it is included in the navigation solution for the σnoise overbounding evaluation described in paragraph d below.

b. When steady-state accuracy is reached, data are recorded as follows:

c. Initially, 50 independent samples of pseudorange data are recorded at the required sampling interval (see note below).

Note: The sampling interval will be two times the integration interval used for carrier phase smoothing of pseudoranges. For example, if the integration interval used for carrier smoothing of the pseudoranges is 100 seconds, the sampling interval will be 200 seconds. If ten pseudoranges are collected per sampling interval (nine independent measurements), the duration of the initial data collection period will be 20 minutes.

d. The normalized RMS range error statistic, RMS_PR, is computed according to the following formula, using all collected samples (including those prior to steady-state operation):

$$\mathrm{RMS_PR}(M) \equiv \sqrt{\frac{\sum_{j=1}^{M}\left\{\sum_{i=1}^{N_j}\frac{Z_{ij}^2}{\left[\sigma_{norm,ij}^2 N_j\right]}\right\}}{M}}$$

where:

$$Z_{ij} \equiv PR_{ij} - R_{ij} - (c\Delta t)_j$$

$$(c\Delta t)_j \equiv \frac{1}{N_j}\sum_{i=1}^{N_j}\left(PR_{ij} - R_{ij}\right)$$

©2011 RTCA, Inc.

$$\sigma^2_{norm,ij} = \frac{\left[\left(N_j - 1\right)^2 \sigma^2_{noise,ij} + \sum_{\substack{k=1 \\ k \neq i}}^{N_j} \sigma^2_{noise,kj} \right]}{N_j^2}$$

where:

PR_{ij} = smoothed pseudo-range, channel i, time j
R_{ij} = true range, satellite i, time j (includes extrapolation)
N_j = number of satellites at time j
M = number of sampling intervals
$\sigma_{noise,ij}$ = satellite i, time j (refer to Appendix J.2.4 of the DO-229D MOPS)

Note:

1. *Interchannel biases on the simulator may impede the accuracy test specified herein. It may be necessary to determine this bias and inflate the test threshold based upon equipment calibration. If two receivers are used to remove this bias (via double-differencing), the test must account for potential interchannel biases in the receivers themselves and cannot simply remove all bias components.*

2. *Since code-carrier divergence is not simulated in this test, the σ_{divg} term is not used in this normalization. Validation of σ_{divg} should be accomplished by analysis.*

e. Verification of σnoise overbounding: The error statistic is compared to the 110% Pass Threshold of Table 2-25 of RTCA/DO-229D based on the Number of Independent Samples (NIS), where NIS is given by:

$$NIS(M) \equiv \sum_{j=1}^{M} \left(N_j - 1\right)$$

If RMS_PR is below the pass threshold (Table A-3), the result is a pass. If the RMS_PR is not below the pass threshold, additional data may be collected. In this case, the RMS_PR shall include the initial independent samples plus all additional data, and the formulas and pass criteria of this section (which apply for an arbitrary number of samples) shall be used.

Note: It is expected that the pass criteria will not be met with the initial data collection (only the initial acquisition and 50 steady-state operation independent samples due to the limited sample size. Development of the test criteria, and the associated pass probabilities are described in Appendix M of RTCA/DO-229D.

f. Steady-state value of $\left(\sigma^2_{noise}[i] + \sigma^2_{divg}[i]\right)^{1/2}$: Using only those samples collected during steady-state, the average $\left(\sigma^2_{noise}[i] + \sigma^2_{divg}[i]\right)^{1/2}$ output values for each satellite are compared to the requirements of Appendix J.2.4 of RTCA/DO-229D. The output values must be less than or equal to the required accuracy values for the designator of the equipment.

©2011 RTCA, Inc.

g. Verification of RMS accuracy: The steps defined in paragraph c and d are repeated using only those samples collected during steady-state operation and using the required RMS accuracy (section 2.1.4.1.3 of RTCA/DO-229D) (minus any steady-state value of σ_{divg}) instead of the output $\sigma_{noise,i,j}$ in the computation of $\sigma_{norm,i,j}$. The pass criteria defined in paragraph d applies.

Table A-3 Pass Threshold Table

NIS	110% Pass Threshold	125% Pass Threshold
25-50	N/A	1.084
50-75	0.954	1.137
75-100	0.981	1.159
100-150	0.998	1.172
150-200	1.017	1.187
200-300	1.028	1.196
300-400	1.042	1.206
400-500	1.050	1.212
500-750	1.055	1.216
750-1000	1.063	1.222
1000-1250	1.068	1.226
1250-1500	1.072	1.229
1500-2000	1.074	1.231
> 2000	1.078	1.233

Note: The 110% pass threshold yields a 10% probability of passing equipment with a true accuracy of 110% of the required accuracy. The 125% pass threshold yields an 80% probability of failing equipment with a true accuracy of 125% of the required accuracy.

A.1.3 SBAS Message Loss Tests

The purpose of this test is to evaluate the loss rate of SBAS messages at degraded CNR's as a result of the LightSquared 3GPP LTE transmissions. Typically, SBAS Message Loss Rate requirements in Section 2.1.1.3.2 of RTCA/DO-229D will need to be met at the minimum operating conditions (RTCA/DO-229D Section 2.1.1.10) in the presence of RTCA/DO-229D Appendix C interference conditions. In this case, the Message Loss rate requirement (Message Loss Rate < 1 in 1000 messages) is evaluated under interference conditions that also include the 3GPP interferers. This test will help evaluate 3GPP power levels at which the receiver does not meet the SBAS message loss requirement. Data necessary for this test may be collected concurrently during the tests in A.1.2.2 (by extending the period of time for the test in A.1.2.2).

Notes:

1 *SBAS message loss information is typically not provided on the standard ARINC data outputs from a GNSS receiver. Instrumentation data from the GPS receivers may need to be used to obtain this information from the GPS receiver.*

2 *It is expected that the SBAS message loss rate threshold would be exceeded prior to exceeding the pseudorange accuracy threshold.*

©2011 RTCA, Inc.

A.2 References

[A-1] SC-159, “Minimum Operational Performance Standards for Global Position System/Wide Area Augmentation System Airborne Equipment,” RTCA Document No. RTCA/DO-229D, 13 Dec. 2006

©2011 RTCA, Inc.

Appendix B

Aggregate RF Interference Computation Method

©2011 RTCA, Inc.

This page intentionally left blank.

© 2011 RTCA, Inc.

B AGGREGATE RF INTERFERENCE COMPUTATION METHOD

B.1 Introduction

This appendix contains a derivation of the analytic statistical aggregate received Radio Frequency Interference (RFI) model (B.2) used in the random RFI source location method and in part in the discrete RFI source location method (B.4.3). RF propagation path loss models used in the aggregate computation are described (B.3). Detailed aggregate computations are then described that use each of the two RFI source location methods (B.4) which are referenced in the report main body.

B.2 Derivation of Analytic Statistical Aggregate Received RFI Model

Consider a circular region as shown in Figure B-1 with a radius R_o and an RFI source exclusion zone as shown. The circle depicts the region on the ground around a metropolitan airport in which RFI sources are located during an aircraft approach operation but it can be generalized to other operational cases. Geometric factors are shown for an RFI source exclusion zone and radio horizon (outer limit, R_o, of RFI source radius). The central point (WP) refers to the aircraft nadir point along its ground track.

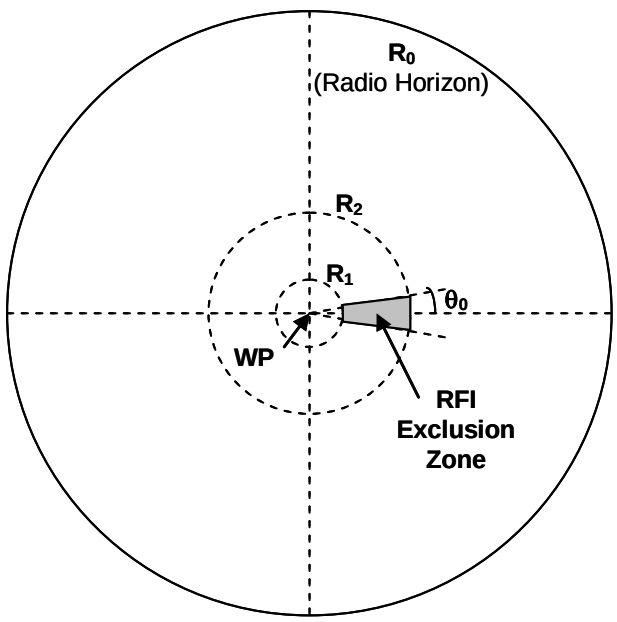

Figure B-1 Generic Runway Approach Geometry-Top View

B.2.1 Derivation of RFI Emitter Source Probability Factors

B.2.1.1 RFI Source Number and Location Factors

An unknown number of active emitters are assumed to be uniformly distributed throughout the allowed region with a particular surface concentration ρ_E (average number of active emitters per sq. meter). The range from aircraft nadir to each emitter is unknown but modeled with a known probability distribution function. Each emitter radiates energy with a power density of P_o Watts/MHz. This radiation undergoes scattering, reflections, and shadow loss prior to reaching the airborne GPS receiver. The propagation environment is modeled probabilistically with a median path loss given by one of several possible models discussed in Appendix B.3.

© 2011 RTCA, Inc.

The aggregate received RFI power spectral density, P_I, at the aircraft GPS receive antenna can be written as $P_I = \sum_{k=0}^{n} X_k(r_k)$; Equation B-1

where the random variable X_k is the received RFI power (or power spectral density) due to emitter k, and r_k is the emitter's radial location with respect to aircraft nadir point. The random number of emitters n, is appropriately described by the Poisson distribution (see for example [B-1]). Thus if ξ denotes the number of active emitters present in a circle of radius R_o, then

$$P(\xi = n) = [(\bar{n})^n / n!]\exp(-\bar{n})\,; \qquad \text{Equation B-2}$$

where $\bar{n}$ denotes the mean number of active emitters in the circular region. Note from B-1 that n = 0 implies there are no emitters present, hence $X_0 = 0$, but from B-2 this occurs with probability $\exp(-\bar{n})$. Thus the probability distribution function for P_I is discontinuous at $P_I = 0$.

The random radial distance r_k is described by a probability density function, f(r), that is identical for each emitter independent of the index k. For an aircraft operational scenario that has no emitter exclusion zone,

$$f(r) = 2r / R_o^2,\ 0 \le r \le R_o\,. \qquad \text{Equation B-3}$$

In a scenario that includes an annular segment exclusion zone as shown in Figure B-1,

$$f(r) = \begin{cases} 2\pi r / (\pi R_o^2 - \theta_o(R_2^2 - R_1^2)), & 0 \le r < R_1 \\ 2(\pi - \theta_o) r / (\pi R_o^2 - \theta_o(R_2^2 - R_1^2)), & R_1 \le r < R_2 \\ 2\pi r / (\pi R_o^2 - \theta_o(R_2^2 - R_1^2)), & R_2 \le r \le R_o \end{cases}; \qquad \text{Equation B-4}$$

where θ_0 is the annulus half-angle and R_1 and R_2 are, respectively, the inner and outer annular radii.

B.2.1.2 Median Single-Source Received Power Probability Factors

Research done by the cellular radio community showed that path loss statistics taken over large areas exhibited two different fading components described as fast fading and slow fading [B-2]. The slow fading component is very well approximated by a log-normal distribution while the fast fading is best described using the Rayleigh distribution. This implies that if γ(t) denotes the received envelope arriving at an antenna from a single emitter, we may write $\gamma(t) = \alpha(t)\beta(t)$ where α(t) and β(t) are independent. The term α(t) denotes the fast fading envelope and β(t) the slow fading log-normal component with a standard deviation ranging from 4 to 12 dB. As discussed in [B-2], the envelope γ(t) can be shown to have a Suzuki distribution.

If the envelope power, X(t), is defined as $X(t)=\gamma^2(t)$, the probability distribution associated with X can be approximated by a log-normal distribution [B-2] to make it mathematically easier to handle. The log-normal distribution is described by two parameters, μ and σ, which can be determined from the mean and variance of the distribution. This distribution has a density function given by

$$f(X) = [1/(\sqrt{2\pi}\sigma_X)]\exp[-(\ln(X) - \mu_X)/(2\sigma_X{}^2)]\,. \qquad \text{Equation B-5}$$

© 2011 RTCA, Inc.

In applying these results to interference analysis, the parameter μ_X becomes the median interference power from a single emitter in natural log terms while σ_X is the standard deviation of that power also in natural log terms. The median power parameter, μ_X, will be a function of the ground distance, *r*, between the interfering emitter and the receiving antenna, while σ_X is customarily range-independent. Since each emitter transmits the same power, $P_k = P_o$, the median power received from each emitter is determined by a product of the isotropic median propagation path loss from the individual source, the transmit antenna gain, and the receive antenna gain. Therefore the median power received from each emitter described by the common parameter $\mu_X(r)$ given by:

$$\mu_X(r) = \ln[10^{-0.25} P_o G_{xmt}(\theta_{elev}(r)) PL(r) G_{rcv}(\varphi_{elev}(r))]; \qquad \text{Equation B-6}$$

where P_0 is the interfering source emitted power, $PL(r)$ the isotropic median path loss, $G_{xmt}(\ )$ the interfering emitter antenna gain, $G_{rcv}(\ )$ the receive antenna gain, $\theta_{elev}(r)$ the elevation angle to the receive antenna, and $\phi_{elev}(r)$ the elevation angle to the interfering emitter antenna. The factor $10^{-0.25}$ is associated with the log-normal approximation of the Suzuki distribution [B-2].

Similarly, the standard deviation, σ_X of this single source median received power is identical for each emitter, since it is determined by the standard deviation associated with path loss [B-2]. The standard deviation of the path loss (8.48 dB for this report) requires the substitution, $\sigma_X = (\ln(10)/10)\sigma_{dB}$ for computation. Note that since the emissions are assumed to be independent from emitter to emitter, the received signals X_k are independent and identically distributed random variables each having a log-normal distribution with parameters $\mu_X(r)$ and σ_X. These features enable computation of the mean aggregate received RFI power.

B.2.2 Mean Aggregate Received RFI Derivation

To determine the mean aggregate received power we make use of the relation,

$$\overline{P_I} = E(P_I) = E[E(P_I \mid n)] \qquad \text{Equation B-7}$$

where E( ) represents the expectation operator. Since the X_k are independent, identically-distributed, random variables, there is no dependence on k and, for a given number of sources, n,

$$E(P_I \mid n) = nE(X(r)). \qquad \text{Equation B-8}$$

Thus, since the number of sources, n, is actually an independent random variable,

$$E(P_I) = E(n)E(X(r)) = \overline{n}E(X(r)). \qquad \text{Equation B-9}$$

Then, since X is log-normally distributed,

$$E(X(r)) = E[E(X(r) \mid r)] = E[\exp(\mu_X(r) + \sigma_X{}^2/2)]. \qquad \text{Equation B-10}$$

By combining B-6, B-9, and B-10, the mean aggregate received power becomes

$$\overline{P_I} = \overline{n}P_o 10^{-0.25} \exp(\sigma_X{}^2/2) \int_0^{R_o} PL(r) G_{xmt}(r) G_{rcv}(r) f(r) dr. \qquad \text{Equation B-11}$$

The value for $\overline{n}$ depends on the whether the scenario includes an exclusion zone. If there is no exclusion zone, $\overline{n} = \rho_E \pi R_o^2$; Equation B-12

where ρ_E = average number of sources per unit area (same dimensions as $1/R_0^2$). For a scenario with an exclusion zone, $\overline{n} = \rho_E(\pi R_o^2 - \theta_o(R_2^2 - R_1^2))$. Equation B-13

© 2011 RTCA, Inc.

Equation B-11 can be modified to compute mean aggregate received power spectral density by dividing both sides by a reference bandwidth (e.g., the necessary bandwidth of the representative RFI source emission with power P_0).

B.3 RFI Propagation Isotropic Path Loss Models

B.3.1 General Isotropic Path Loss Model Methodology

All the RFI propagation path loss models used in this report are based on the flat-earth approximation. In other words, the ground under the aircraft is assumed to be essentially smooth and flat out to a radio horizon radius from the point on the ground directly under the aircraft. In line-of-sight propagation conditions at radio frequencies near the GPS L1 carrier, this radio horizon value depends, in general, on the aircraft GNSS and RFI source antenna heights and the amount of atmospheric refraction along the path. This report uses the 4/3 Earth radius approximation for the refractive effect on the radio horizon. More details are found in Section B.4

Various propagation models are used in evaluating the impact of LightSquared ATCt base and mobile unit RFI to airborne GPS receivers. In the broad sense, two categories of models are needed. For most of the RFI scenarios a probabilistic path loss model is required however there is one scenario in which free space path loss is most appropriate. Those scenarios where blockage is a factor are typically evaluated using probabilistic models while clear line of sight scenarios are analyzed using free space path loss. As free space path loss is discussed in a multitude of textbooks, this appendix will focus primarily on probabilistic propagation models.

The majority of scenarios described in Section 3 of this report involve environments in which emissions from LightSquared equipment undergo scattering, reflections, and absorption prior to arriving at an aircraft's GPS antenna. The analysis of these scenarios must incorporate propagation models that adequately address such random propagation phenomena. These propagation environments were the subject of much research during the development of cellular radio systems. As a result, the cellular radio community has over the years developed propagation models which for the most part are applicable to the present RFI evaluation scenarios.

B.3.1.1 Isotropic Path Loss Model for Aircraft Antenna Height Below 550 Meters

The median isotropic path loss model for aircraft antenna height values below 550 meters consists in general of 3 segments appropriately blended together. They form a continuous function of the lateral separation radius, *r* (in meters) between the aircraft and RFI source antennas. For radii less than a few hundred meters, conventional 2-Ray propagation is chosen. That model assumes a direct path ray between the 2 antennas interacts with one other ray reflected from the ground between antennas. For radii greater than about 1 km, the Hata suburban propagation model is chosen. At radii beyond 20 km, a long-distance extension is made to the standard Hata formulation. If necessary to achieve path loss continuity, the 2-Ray and Hata model segments are connected together by one of two means. One means is by a constant-slope logarithmic fit function that covers radius values in between the segment ranges. The other means used in ATCt mobile station scenarios with aircraft heights below 80 m is by a modified Erceg/Greenstein path loss segment. Since the median isotropic path loss is generally a function of the aircraft and RFI source antenna heights, the path loss model is adapted to each specific RFI scenario.

© 2011 RTCA, Inc.

B.3.1.1.1 Two-Ray Isotropic Path Loss Model

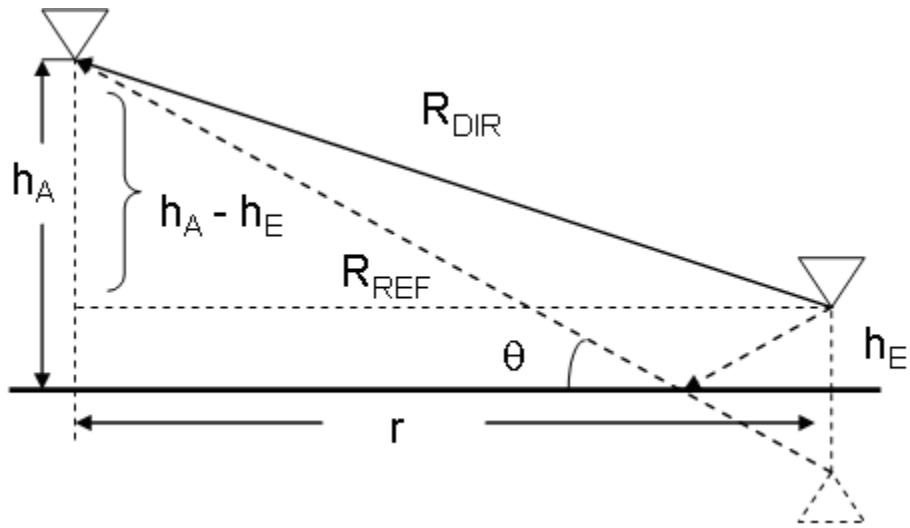

Figure B-2 Two-Ray Path Loss Model Geometry (Profile View)

From the 2-Ray model geometry, depicted in Figure B-2, the isotropic path loss can be derived in the following way. Define the direct ray path length, R_{DIR}, and reflect ray length, R_{REF}, as $R_{DIR}(r)=\sqrt{r^2+\left(h_A-h_E\right)^2}$ and $R_{REF}(r)=\sqrt{r^2+\left(h_A+h_E\right)^2}$; where h_A and h_E are the aircraft and RFI source antenna heights, respectively. Then by simple trigonometry, the ground reflection angle, θ(r), is given as: $\theta(r)=\sin^{-1}\left(\frac{h_A+h_E}{R_{REF}}\right)$.

For radio waves the ground reflection surface can be characterized by its electrical constituent parameters, ε_r, (relative dielectric constant), and σ_c (electrical conductivity). For vertically polarized waves, assumed to be emitted by the RFI sources in this evaluation, the complex wave reflection coefficient, $\rho_v(f_c, r)$, is determined by:

$\rho_v(f_c,r)=\frac{(\varepsilon_r-ix)\sin(\theta(r))-\sqrt{(\varepsilon_r-ix)-\cos^2(\theta(r))}}{(\varepsilon_r-ix)\sin(\theta(r))+\sqrt{(\varepsilon_r-ix)-\cos^2(\theta(r))}}$; where the electrical dissipation ratio parameter, x, at the RFI source center frequency, f_c, is defined as $x=\frac{\sigma_c}{2\pi f_c\varepsilon_0}$, ε_0 is the free-space permittivity, and i, the imaginary constant $=\sqrt{-1}$.

The longer reflected ray path length compared to the direct ray results in a relative phase delay, $\phi(r)=\frac{2\pi}{\lambda_c}\left(R_{REF}(r)-R_{DIR}(r)\right)$; where λ_c is the wavelength at the RFI source center frequency. The interaction between direct and reflected rays at the aircraft receive antenna is given by the complex field factor $P_v(r)=1+\rho_v(r)\cdot e^{-i\phi(r)}$. Combining the relations for vertical polarization reflection coefficient, relative phase delay, and multi-path field factor results in the 2-Ray model isotropic path loss equation (in dB):

$$PL_{2-Ray}(r)=20\log\left(\frac{4\pi}{\lambda_c}\cdot\frac{R_{DIR}(r)}{\left|P_v(r)\right|}\right) \qquad \text{Equation B-14}$$

© 2011 RTCA, Inc.

This model should be reasonably accurate out to a lateral radius where the direct ray launch angle toward the aircraft antenna is above about 6 degrees. For radii much beyond that point, more complex scattering, blockage, and shadowing effects become significant. The reflection surface chosen for this report is concrete ($\varepsilon_r = 7$, $\sigma_c = 0.15$).

B.3.1.1.2 Hata-Okumura Isotropic Median Path Loss Model

For propagation from RFI sources at distances beyond about 1 km from the aircraft antenna, we use the well-known Hata-Okumura path loss model [B-2]. It was originally developed for predicting UHF cellular mobile telephone propagation at distances beyond 1 km from the base station for various types of terrain. In this report the suburban terrain parameters are used to represent the environment around a large metropolitan airport.

The suburban environment median path loss (in dB), (lengths in m, frequency in MHz), is

$$PL_{HSE}(r) = 69.12 + 26.16 \cdot \log(f_c) - 2 \cdot \log^2\left(\frac{f_c}{28}\right) - AF(h_A, h_E) + \beta_{dB}(r, h_A) \cdot \log\left(r/1000\right) \quad ; \quad \text{Equation B-15}$$

where the antenna factor, $AF(\ )$, and propagation exponent factor, β, are given by:

$$AF(h_A, h_E) = 13.82 \cdot \log(h_A) + 3.2 \cdot \log^2(11.75 h_E)\,, \qquad \text{Equation B-16}$$

and

$$\beta_{dB}(r, h_A) = \left(44.9 - 6.55\log(h_A)\right) F(r, h_A)\,. \qquad \text{Equation B-17}$$

For $r \leq 20$ km, $F(r,h_A) = 1$; otherwise,

$$F(r, h_A) = 1 + \left(0.014 + 1.87 \cdot 10^{-4} f_{c,MHz} + \frac{1.87 \cdot 10^{-3} h_A}{1 + 7 \cdot 10^{-6} h_A^{\,2}}\right) \log\left(\frac{r}{20000}\right)^{0.8}. \qquad \text{Equation B-18}$$

The path loss model above incorporates the ITU-R extension to the conventional Hata model for lateral separations more than 20 km (Equation B-18). Over ranges from 1 to 100 km, the Hata model median path loss equation set can be used up to an h_A (taller antenna height) value around 550 m with less than 2.3 dB path loss error compared to Okumura's measurements. That error is deemed acceptable for this analysis.

B.3.1.1.3 Erceg/Greenstein Isotropic Median Path Loss Model (ATCt Mobile)

For ATCt mobile station RFI scenarios a modified Erceg-Greenstein path loss model is applied to intermediate medium ranges when aircraft antenna heights are less that 80 m. The standard Erceg/Greenstein model [B-3] has a median path loss that varies with both range and frequency and an additive term that describes the random variation about that median. The general equation (in dB) is:

$$PL_{E-G}(r) = \left[A + 10\left(a - bh_A + c/h_A\right) \cdot \log(r / r_0)\right] + \left[\text{random variation terms}\right].$$

The intercept term, A, is the free-space path loss at reference distance, r_0, and wavelength λ_c. That is $A = 20\log(4\pi r_0/\lambda_c)$; where r_0 is nominally 100 m. The median path loss propagation exponent terms, a, b, and c, are empirically derived from measurements and depend on the type of propagation environment. The second square bracket contains terms that include a range-dependent standard deviation. Terrain model C (flat, light tree cover) is used in this report.

© 2011 RTCA, Inc.

The modified Erseg-Greenstein model in this report incorporates the median path loss but the additive term describing the variation about that median has a standard deviation that is invariant with range. The modified median isotropic path loss (in dB) for terrain model C becomes:

$$PL_{EG,\mathrm{mod}}(r) = \left[A + 10\left(a - bh_A + {}^{c}\!/_{h_A} \right) \cdot \log(r / r_0) \right], \qquad \text{Equation B-19}$$

where *a*, *b*, and *c* are, respectively, 3.6, 0.005, and 20. The standard deviation used here (8.48 dB) is taken from [B-2] but is within the range of standard deviations for terrain category C used in the Erceg/Greenstein model.

The Erceg/Greenstein model is derived from data taken at 1900 MHz with an emitter antenna height of 2 meters [B-3]. We use this model at the GPS L1 frequency band (1575.42 MHz) with an assumed emitter antenna height of 1.8 meters. As per the model, the decrease in path loss at the lower GPS frequency is 1.63 dB, which is within 1 dB of the measured difference in path loss due to frequency differences by Okumura [B-2]. For this reason we have chosen to use the Erceg-Greenstein median path loss model even at the lower GPS L1 frequency

The difference in emitter antenna heights results in a slightly lower path loss prediction by the standard Erseg/ Greenstein model than would be expected for a 1.8 meter height [B-3]. Use of the standard model, therefore, would yield a slightly larger estimate of the mean interference power density. Based on Okumura's measurements, however, this difference should be on the order of only 0.2 dB.

The outer radius limit to which the modified Erseg/ Greenstein path loss model applies depends on GPS receive antenna height. It is chosen to achieve a smooth transition to the long range model as described in above (Section B.3.1.1.2). For receive antenna heights greater than 80 meters, a different medium range model with a fixed propagation exponent value and intercept is used (Section B.3.1.1).

B.3.1.2 Isotropic Path Loss Model for Aircraft Antenna Height Above 550 Meters

The median isotropic path loss model for aircraft antenna height values below 550 meters is considered inappropriate for extension to greater aircraft heights. The reason is that supporting propagation modeling studies have antenna height limits that would be significantly exceeded and thus affect model accuracy. Instead a simple free-space propagation model is used in this report. The isotropic free-space path loss in algebraic terms is:

$$PL_{F-S}(r) = \left(\frac{4\pi r}{\lambda_c} \right)^2; \qquad \text{Equation B-20}$$

where λ_c is the RF wavelength at the RFI source center frequency.

B.3.2 RFI Scenario-Specific Isotropic Path Loss Models

As described in Section B.3.1 above, all the path loss models depend on the aircraft and RFI source antenna heights. Table B-1 lists the antenna heights used for each of the five operational scenarios.

© 2011 RTCA, Inc.

Table B-1 Aircraft and RFI Source Antenna Heights

Scenario	Aircraft Antenna Height (m)	ATCt Base Ant. Height (m)	ATCt Mobile Ant. Height (m)
Surface (Taxiway)	4	30	1.8
Cat. II DH	25.94	30	1.8
Cat. I DH	53.34	30	1.8
Low Altitude / Terminal Area (FAF WP)	535.2	30	1.8
High Altitude Enroute	5490	30	1,8

B.3.2.1 Generic Terminal Area (FAF WP) Scenario Isotropic Path Loss

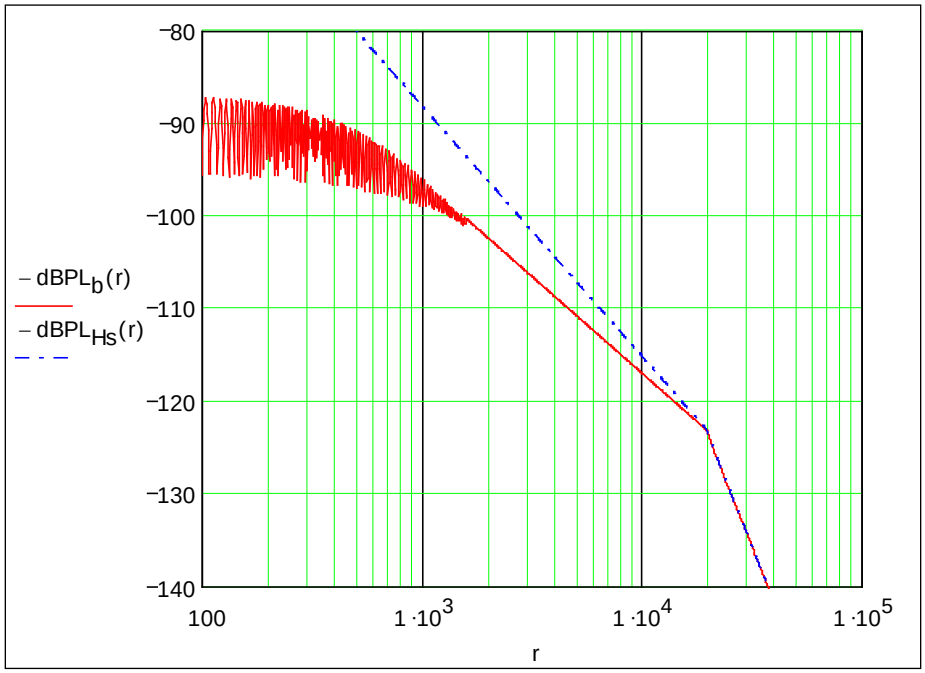

Figure B-3 Terminal Area Isotropic Median Path Loss (Base Station Case)

From the scenario values in Table B-1, the aircraft antenna is above the ATCt base station antenna by 505.2 m and the mobile antenna by 533.4 m. The isotropic path loss equations for ATCt base station fundamental emission are figured at 1552.7 MHz, the uppermost 5 MHz channel center frequency. For the mobile station the isotropic path loss equations for the unwanted emissions are figured at 1575.42 MHz, (the GPS L1 carrier frequency).

In the ATCt base station case, the 2-Ray path loss is applied out to a 1597 m lateral separation redius (direct ray launch angle = 17.6°) where the reflected ray grazing angle (18.45°) is just above the point for minimum reflection coefficient magnitude. A constant-slope logarithmic fit equation (loss slope = 2.089) is applied between 1597 m and 20 km. Beyond that point the extended range Hata model is used. Figure B-3 above shows the composite path loss (-$dBPL_b(r)$) versus lateral separation radius, r, for the ATCt base station case.

© 2011 RTCA, Inc.

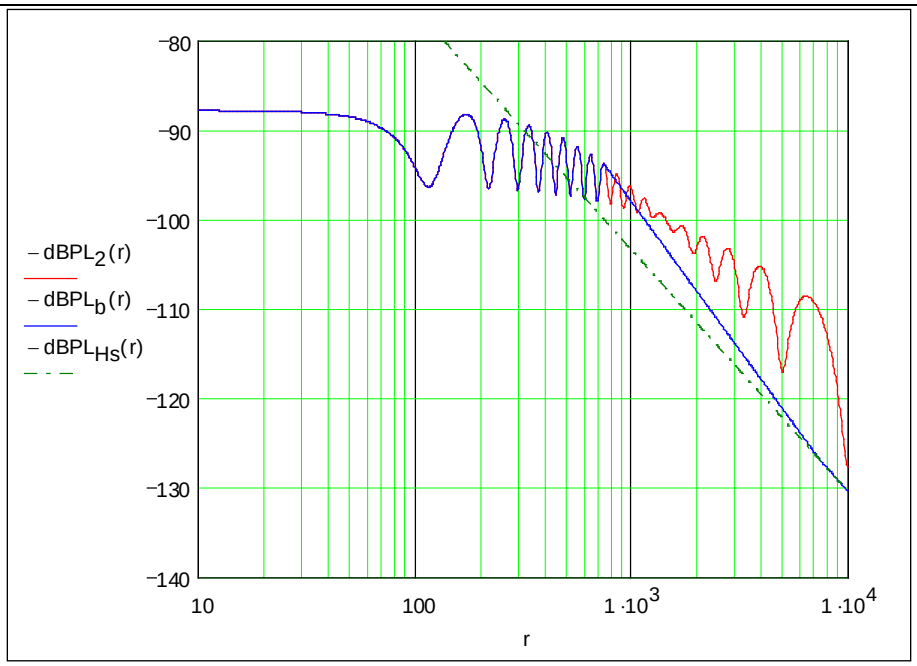

Figure B-4 Terminal Area Isotropic Median Path Loss (Mobile Station Case)

In the ATCt mobile case, the 2-Ray path loss is applied out to 750.23 m. A constant-slope logarithmic fit equation (loss slope = 2.320) is applied between 750.23 m and 7.502 km and the extended range Hata model is used beyond that point (Figure B-4). The smaller lateral separation cut-off of the 2-Ray model for the mobile case is appropriate because of geometry relative to the shorter mobile antenna.

B.3.2.2 Generic Category I Decision Height Waypoint Path Loss

From the scenario values in Table B-1, the aircraft antenna is above the ATCt base station antenna by 23.34 m and the mobile antenna by 51.54 m. As in the terminal area (FAF WP) scenario above, the path loss equations for ATCt base and mobile stations are figured at 1552.7 MHz and 1575.42 MHz, respectively.

In the ATCt base station case, the 2-Ray path loss is applied out to a 222.9 m lateral separation. A constant-slope logarithmic fit equation (loss slope = 2.923) is applied between 222.9 and 1000 m. Beyond that point the extended range Hata model is used. The Cat. I DH base station example of the vertical polarization reflection coefficient magnitude and phase (Figure B-5) and the composite path loss ($-dBPL_b(r)$) for the ATCt base station case (Figure B-6) are shown below.

In the ATCt mobile case, the 2-Ray path loss is applied out to 101.38 m. The Erceg/ Greenstein model is applied between 101.38 m and 11.288 km and the extended range Hata model is used beyond that point.

© 2011 RTCA, Inc.

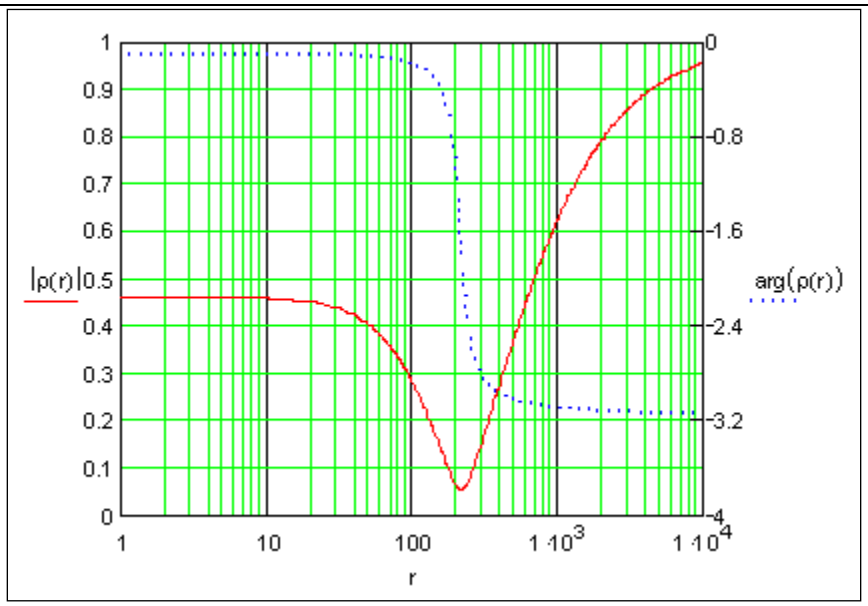

Figure B-5 Vertical Polarization Wave Reflection Coefficient (1552.7 MHz)

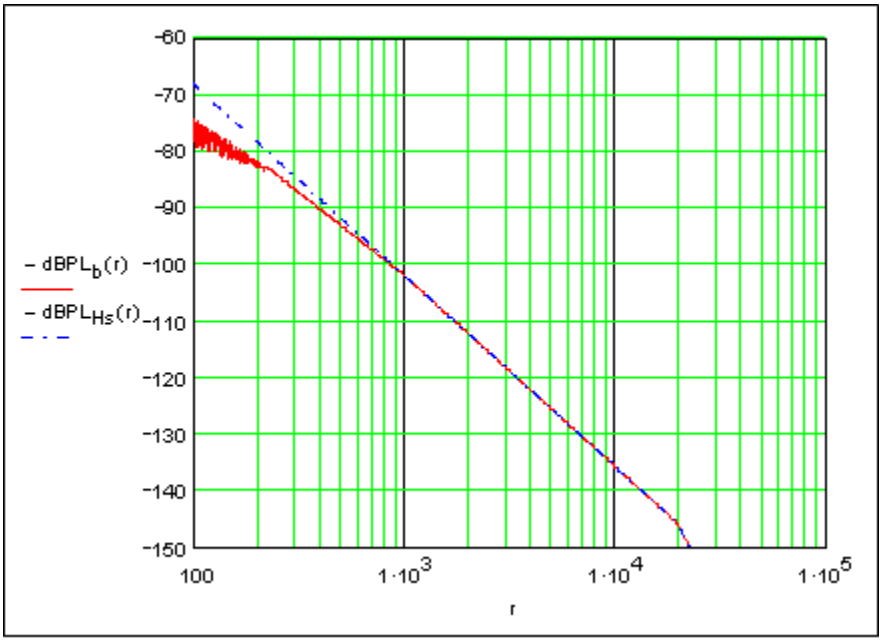

Figure B-6 Category I DH Isotropic Median Path Loss (Base Station Case)

B.3.2.3 Generic Category II Decision Height Waypoint Path Loss

The Table B-1 scenario values indicate the aircraft antenna is below the ATCt base station antenna by 4.06 m and above the mobile antenna by 24.14 m. As in the scenarios above, the path loss equations for ATCt base and mobile stations are figured at 1552.7 MHz and 1575.42 MHz, respectively.

In the ATCt base station case, the 2-Ray path loss is applied out to a 190.18 m lateral separation radius. No constant-slope fit segment is needed since the extended Hata path loss intersects at that point. The roles of the aircraft antenna (height = h_A) and ATCt base antenna (height = h_B) are reversed in the extended range Hata model to keep them within

© 2011 RTCA, Inc.

the appropriate value limits. The composite path loss (-dBPL$_b$(r)) for the ATCt base station case (Figure B-7) is shown below.

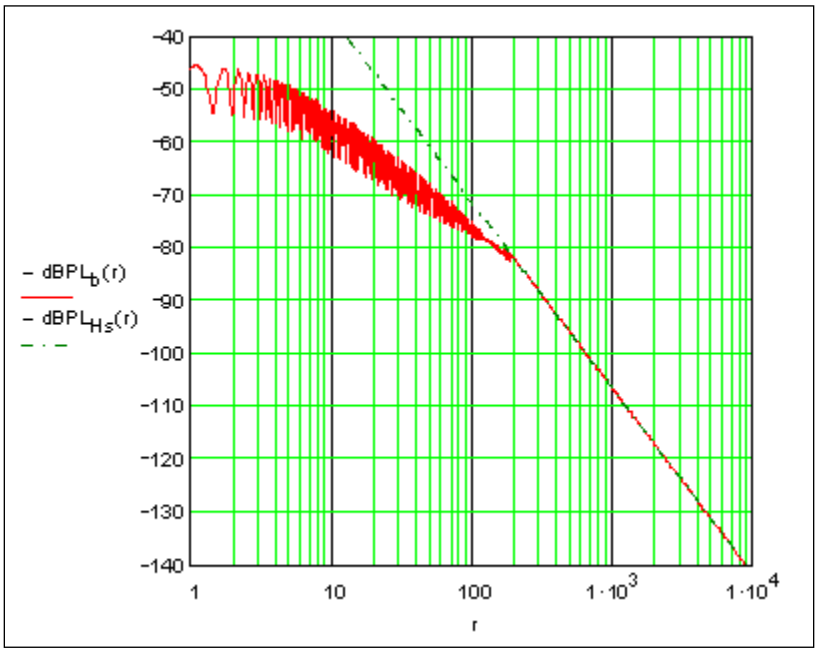

Figure B-7 Category II DH Isotropic Median Path Loss (Base Station Case)

In the ATCt mobile case, the 2-Ray path loss is applied out to 114.77 m. The Erceg/ Greenstein path loss model is then applied out to 2.475 km and the extended range Hata model is used beyond that point.

B.3.2.4 Generic Surface (Taxiway) Path Loss

The scenario values in Table B-1, indicate the aircraft antenna is below the ATCt base station antenna by 26 m. The ATCt base station path loss equations for are figured at 1552.7 MHz as in the previous scenarios. No analysis was made on the mobile station aggregate effect due to the relatively small number mobiles estimated to be nearby.

In the ATCt base station case, the 2-Ray path loss is applied out to a 97 m lateral separation radius. A constant-slope logarithmic fit equation (loss slope = 3.983) is applied between 97 and 1000 m. The roles of the aircraft antenna (height = h_A) and ATCt base antenna (height = h_B) are reversed in the extended range Hata model to keep them within the appropriate value limits. The composite path loss (-dBPL$_b$(r)) for the ATCt base station case (Figure B-8) is shown below.

© 2011 RTCA, Inc.

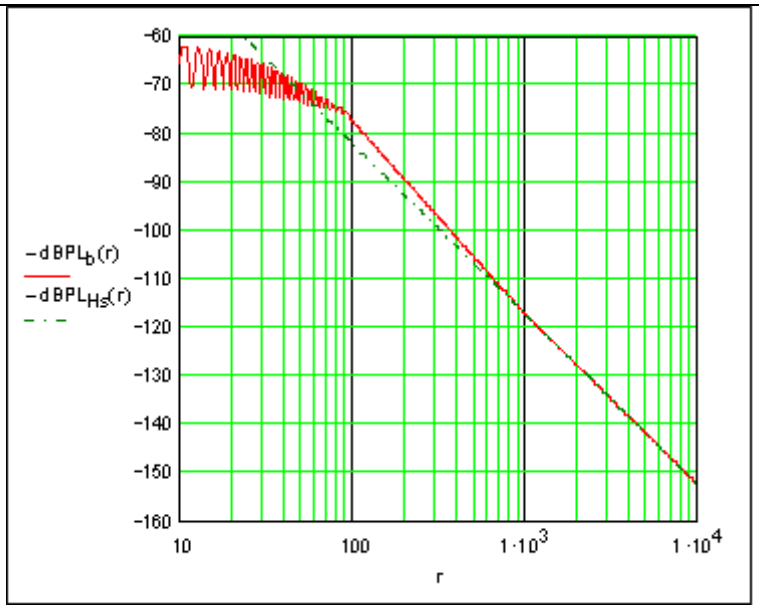

Figure B-8 Surface (Taxiway) Isotropic Median Path Loss (Base Station Case)

B.4 Scenario-Specific Aggregate Received RFI Detailed Computations

In the following subsections two different ATCt base station location methods are described: "Random" and "Fixed Discrete". Base and mobile station location constraints in the airport vicinity are briefly discussed. Using the two location methods and airport constraints, ATCt base and mobile station aggregate RFI computations are then performed for the five operational scenarios developed in Section 3 using the RFI source and receiver parameters from Section 2.

B.4.1 ATCt RFI Source Location Methods and Location Constraints

B.4.1.1 Random and Fixed Discrete Location Methods – General Description

The locations of deployed ATCt base stations relative to each other and to the aircraft are neither likely to be completely random with some average spacing nor are the locations likely to be on a regular grid structure with fixed spacing. Instead, the locations will probably be represented by some arrangement between these two limits. To determine reasonable bounds on the aggregate RFI, both of the two limiting-case location methods are used for computing the ATCt base station mean aggregate received RFI in this report. Since ATCt mobile stations are likely oriented randomly within each cell, only the random location method is used in the aggregate mobile station RFI computation.

Both location methods share common features of median path loss to a given radial location and the radio horizon for a given RFI scenario. They also share a measure of the relative ATCt base station tower spacing but use it somewhat differently. The random location method uses the tower spacing within a given deployment zone to determine an average value of source concentration (probabilistic parameter). The fixed discrete method, however, uses the spacing to set the fixed hexagonal grid size.

B.4.1.2 ATCt RFI Source Location Constraints

Although it is not strictly a limit on the placement of sources, the radio horizon for a given aircraft antenna height is a constraint on the location of ATCt sources that can affect the aggregate received RFI. The estimated radio horizon, R_0 (in meters), between

© 2011 RTCA, Inc.

the aircraft antenna (height = h_A, in meters) and the RFI emitter antenna (height = h_E) is: $R_0 = 1000\left(\sqrt{17.008h_A} + \sqrt{17.008h_E}\right)$, based on the 4/3 Earth radius approximation. The radio horizon values to ATCt base station and mobile antenna for each aircraft operational scenario are listed below (Table B-2).

Table B-2 Radio Horizon from Aircraft to ATCt Base and Mobile Stations

Scenario	A/C Ant. Height (m)	ATCt Base Ant. Ht. (m)	ATCt Mobile Ant. Ht. (m)	Radio Horiz. to Base (km)	Radio Horiz. to Mobile (km)
Surface	4.0	30	1.8	30.84	13.78
Cat. II DH	25.94	30	1.8	43.59	26.54
Cat.I DH	53.34	30	1.8	52.71	35.65
FAF WP	535.2	30	1.8	118.00	100.94
High Alt.	5490	30	1.8	328.16	311.10

Certain other constraints exist in the vicinity of airports that are related to heights of structures. Airport runway and approach layout guidelines [B-4] prescribe height limitations for structures underneath and around an aircraft final approach path by an obstacle clearance surface (Table B-2).

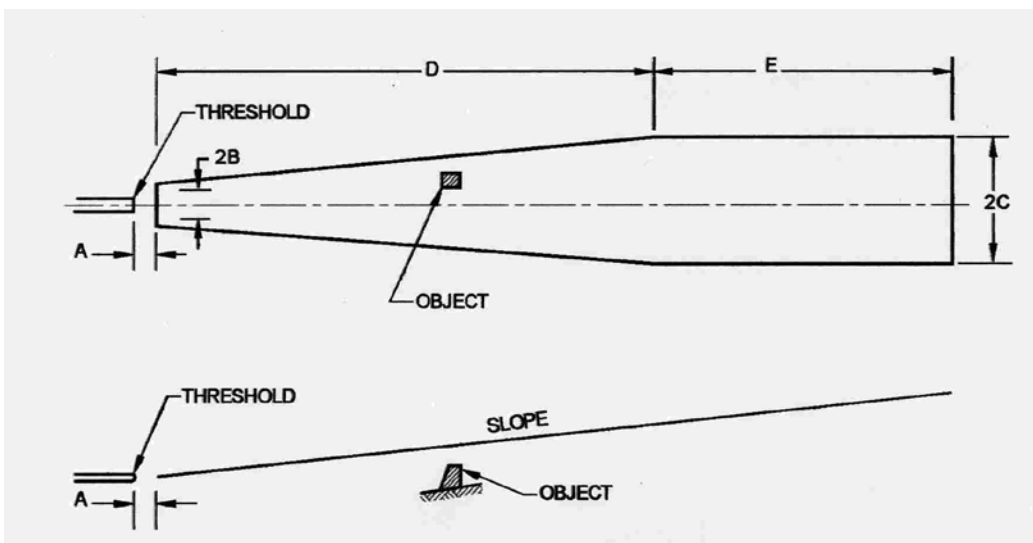

Figure B-9 Approach Obstacle Surface (Top and Side Views)
(Dimensions (feet): A = 200, B = 400, C = 1900, D = 10,000 (nom.), E = 0, Slope = 1:34)

Another airport layout guideline, the runway object-free zone (Figure B-9) constrains objects of any height in the immediate vicinity of runways. The relatively tall ATCt base station antenna (30 m) encounters more location limitations near airports than the shorter mobile unit (1.8 m).

© 2011 RTCA, Inc.

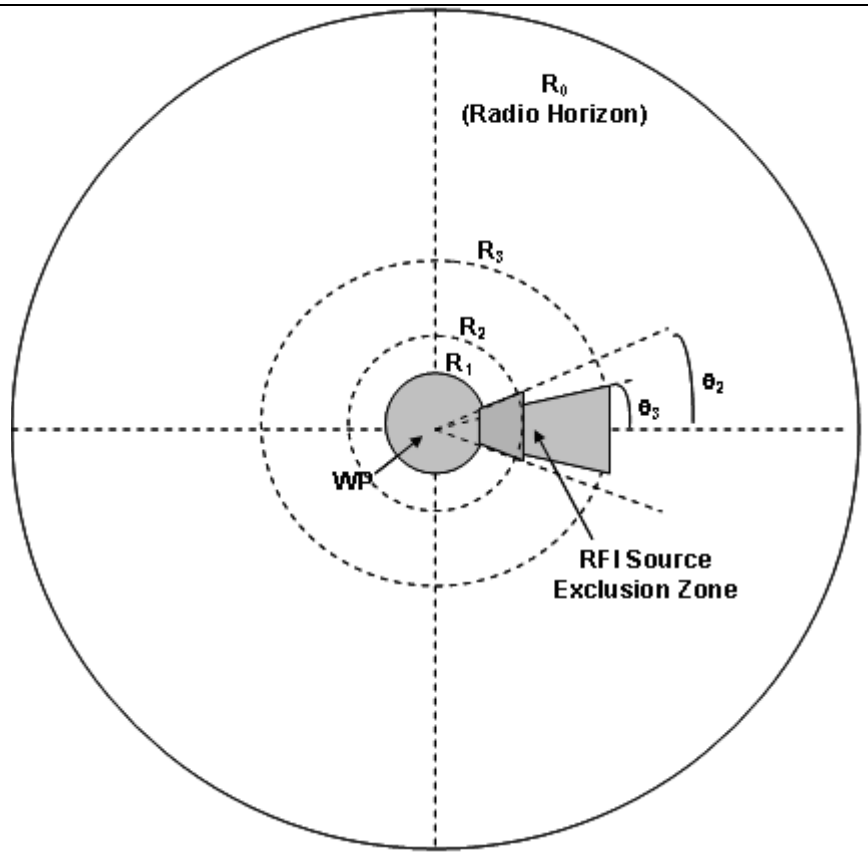

Figure B-10 Random Method Exclusion Zone Example Diagram (Top View)

The combination of these factors results in ATCt source exclusion zones for several operational scenarios. The basic runway layout assumed for this report is a 10,000 foot single runway with approaches designated for both runway ends. This assumption simplifies the exclusion zone definition and makes it more generic for analyses in this report. More complex, specific cases for multiple-runway airports would likely have additional RFI source exclusion zones for the other runways as well. Those specific cases would require further study and are beyond the scope of this report.

The exclusion zone shapes are modeled slightly differently between the two source location methods. The random method models an overall zone shape as a combination of one or more annular segments (see Figure B-10) and, in some cases, a complete circular segment. The fixed discrete method simply excludes an ATCt base station source from a given cell or cells in the aggregate RFI summation over the grid pattern to achieve essentially the same RFI effect within the exclusion zone area.

Airport-related exclusion zones are eliminated from certain scenarios since they are either undefined (as in the High Altitude Enroute) or rather small due to large distance from the runway (Terminal Area (FAF WP)).

Table B-3 summarizes the random location method RFI source exclusion zone parameters for ATCt base and mobile stations in each scenario case.

© 2011 RTCA, Inc.

Table B-3 Aeronautical Scenario ATCt Source Exclusion Zone Parameters

Scenario Case	Base Inner Rad. (m)	Base Outer Rad. (m)	Annular Half-Ang. (deg)	Mobile Inner Rad. (m)	Mobile Outer Rad. (m)	Annular Half-Ang. (deg)
Surface (Taxiway)	0 550	550 4200	180 22.5	N/A	N/A	N/A
Cat. II DH	0 420 840	420 840 4470	180 60 10	449.3	2842	25
Cat. II DH	0 350 570	350 570 5500	180 40 12	488	5830	17
Term. Area (FAF WP)	N/A	N/A	N/A	N/A	N/A	N/A
High Alt. Enroute	298985*	328160*	45*	N/A	N/A	N/A

* This high altitude exclusion zone annular segment represents the Atlantic Ocean off New Jersey and the Delmarva Peninsula (45° full angular extent).

B.4.2 Random ATCt Base Station Location Method Computations

The random base station location method uses the principles of the analytic statistical aggregate RFI model described in Section B.2. The ATCt base stations are modeled as randomly located within some outside radius consistent with a uniform probability distribution. That distribution is defined by a specified average source-to-source spacing. The actual number of base stations within the outside radial constraint is a random number defined by a Poisson distribution. The isotropic path loss for a source at a given radial separation, *r*, from the aircraft nadir point is characterized as a log-normal random variable with parameters μ_X and σ_X.

Since the ATCt base station fundamental emission is broadband and can be represented by a specified EIRP spectral density, P_{SDE} (in W/MHz), received RFI is computed as a mean aggregate power spectral density, P_{SDR}. The mean aggregate received RFI power spectral density is computed with the basic Equation (11) in Section B.2.2. After modification for power spectral density, Equation (11) can be further simplified by substituting definitions for $\bar{n}$ and *f(r)*, to yield a simpler, more intuitive, algebraic form. That is:

$$P_{SDR} = \rho_E P_{SDE} F_{AGG} \; ; \qquad \text{Equation B-21}$$

where ρ_E is the average base station concentration factor (= 1/(average cell area) in m^{-2}) and the aggregate factor, F_{AGG} (in m^2), (no exclusion zone) is given in algebraic form by:

$$F_{AGG} = 2\pi \cdot 10^{\eta} \int_0^{R_o} PL(r) G_{xmt}(r) G_{rcv}(r) \cdot r \cdot dr \; , \qquad \text{Equation B-22}$$

in which the log-normal mean exponent factor, η, is: $0.5\log(e)\left(0.1\sigma_{X,dB}\ln(10)\right)^2 - 0.25$

Inspection of Equation B-21 suggests that the mean aggregate received RFI, P_{SDR}, is directly related to the single source EIRP spectral density, P_{SDE}, by the product, $\rho_E F_{AGG}$. This product can be used to define the mean aggregate path loss in algebraic form as

$$PL_{M,AGG} = 1 \big/ \rho_E F_{AGG} \; . \qquad \text{Equation B-23}$$

© 2011 RTCA, Inc.

The "fixed discrete" method result can be expressed in similar form except that the factor equivalent to the explicit parameter ρ_E is contained in the implicit fixed grid size.

Generalizing Equation B-22 to handle cases with any number of exclusion zones yields:

$$F_{AGG} = 2 \cdot 10^{\eta} \sum_{i=1}^{N} \left[\left(\pi - \Theta_i \right) \int_{Rin_i}^{Rout_i} PL(r) G_{xmt}(r) G_{rcv}(r) \cdot r \cdot dr \right]; \qquad \text{Equation B-24}$$

where N is the number of exclusion zones and Θ_i, (in radians) $R_{in,i}$, and $R_{out,I}$ (in meters) are the annular zone half-angle, the inner and outer radii of the *i*-th zone, respectively. Note in Equation (B-24) that if $\Theta_I = 0$, there is no source exclusion in the zone and if $\Theta_I = \pi$, there is complete exclusion. Note also that the outermost zone outer radius is R_0, the radio horizon. For certain scenarios when the ρ_E value changes beyond a certain radius or for a particular annular segment, the F_{AGG} is computed for that particular area and the overall mean aggregate received RFI is determined by the sum of products as

$$P_{SDR} = P_{SDE} \sum_{j=1}^{M} \rho_{E,j} F_{AGG,j} \ . \qquad \text{Equation B-25}$$

B.4.2.1 Terminal Area (FAF WP) Aggregate ATCt Base Station RFI (Random Method)

As described in Section 3.2, the RFI scenario for a generic low altitude / terminal area GNSS receiver operation is represented by an aircraft nominally at the FAF waypoint (aircraft antenna height = 535.2 m). The nadir point on its ground track is roughly centered within a metropolitan ATCt base station deployment (average tower spacing = 2.2 km out to 45.4 km radius, then 6.2 km out to 70.3 km radius). The radio horizon to a 30 m high ATCt antenna is 118.00 km (Table B-2). No source exclusion zone around the airport is used since its effect is insignificant (large distance to the runway threshold). The isotropic path loss is described in Section B.3.1. The three deployment zone ρ_E values are 0.26307 km^{-2} ($10^{-6.580}$ m^{-2}), 0.03312 km^{-2} ($10^{-7.480}$ m^{-2}) and 3.93 x 10^{-3} km^{-2} ($10^{8.406}$ m^{-2}). The relative values shown are with respect to the highest ρ_E value. Table B-4 lists the regional mean aggregate received RFI factors and relative inverse path loss factors are computed with Equations B-23 and B-24.

Table B-4 Terminal Area (FAF) Aggregate RFI Results (Random Method)

Annular Region #	Rel Conc.	Excl. Angle (deg)	Inner Rad. (m)	Outer Rad. (m)	F_{AGG}	Rel. Inv. PL_{AGG}
1	1	0	0	20000	4.137E-04	4.137E-04
2	1	0	20000	45400	1.170E-04	1.170E-04
3	0.1259	0	45400	70300	4.254E-06	5.356E-07
4	0.0149	0	70300	117996	6.580E-07	9.829E-09
Total					5.356E-04	5.312E-04

By extension of Appendix B Equations B-23 and B-25, the mean aggregate path loss, PL_{AGG}(dB), and mean aggregate received RFI power density, P_{SDR}(dB), are given as:

$PL_{AGG}(dB) = -10 \log(\rho_E \, IPL_{AGG})$, and $P_{SDR}(dB) = P_{SDE}(dB) - PL_{AGG}(dB)$;

where IPL_{AGG} is the total relative inverse path loss factor for the scenario, ρ_E is the central metro base station concentration and P_{SDE} is the ATCt base station EIRP spectral density (25 dBW/MHz for these scenarios). Using these equations and the Table B-4 total relative path loss factor, this scenario results are 98.55 dB mean aggregate path loss and -73.55 dBW/MHz mean aggregate received RFI power density.

© 2011 RTCA, Inc.

B.4.2.2 Category I Decision Height Aggregate ATCt Base Station RFI (Random Method)

As described in Section 3.3, the RFI scenario for a generic Category I GNSS receiver precision approach operation is represented by an aircraft nominally at the Category I DH waypoint (aircraft antenna height = 53.34 m). The nadir point on its ground track is again roughly centered within a metropolitan ATCt base station deployment (average tower spacing = 2.2 km out to 45.4 km radius). The radio horizon to a 30 m high ATCt antenna is 52.71 km (Table B-2). A source exclusion zone around the airport runway is used (parameters listed below). The isotropic path loss is described in Section B.3.2. Two deployment zone ρ_E values are assumed: 0.26307 km^{-2} ($10^{-6.580}$ m^{-2}) and 0.03312 km^{-2} ($10^{-7.480}$ m^{-2}). The relative values shown are with respect to the highest ρ_E value. Table B-5 lists the regional exclusion zone parameters and the resulting regional mean aggregate received RFI and aggregate path loss factors (computed with Equations B-23, B-24 and B-25).

Table B-5 Cat. I Decision Height Aggregate RFI Results (Random Method)

Annular Region #	Rel Conc.	Excl. Angle (deg)	Inner Rad. (m)	Outer Rad. (m)	F_{AGG}	Rel. Inv. PL_{AGG}
1	1	180	0	350	0.000	0.000
2	1	40	350	570	7.053E-05	7.053E-05
3	1	12	570	5500	2.220E-04	2.220E-04
4	1	0	5500	20000	1.406E-05	1.406E-05
5	1	0	20000	45400	8.071E-07	8.071E-07
6	0.125911	0	45000	52708	9.500E-09	1.196E-09
Total					3.074E-04	3.074E-04

Using the technique from B.4.2.1 and the Table B-5 total relative path loss factor, the scenario results are 100.92 dB mean aggregate path loss and -75.92 dBW/MHz mean aggregate received RFI power density.

B.4.2.3 Category II Decision Height Aggregate ATCt Base Station RFI (Random Method)

As described in Section 3.4, the RFI scenario for a generic Category II GNSS receiver precision approach operation is represented by an aircraft nominally at the Category II DH waypoint (aircraft antenna height = 25.94 m). This scenario also represents the limiting case for Cat. III approach and landing operations. The nadir point on its ground track is again roughly centered within a metropolitan ATCt base station deployment (average tower spacing = 2.2 km out to 45.4 km radius). The radio horizon to a 30 m high ATCt antenna is 43.59 km (Table B-2). The aircraft antenna height is slightly below the ATCt tower height so the aircraft primary antenna pattern region is being illuminated by the primary base station antenna pattern. An exclusion zone around the airport runway similar to the Cat. I zone is used (parameters listed below). The isotropic path loss is described in Section B.3.2. One deployment zone ρ_E value is used: 0.26307 km^{-2} ($10^{-6.580}$ m^{-2}). Table B-6 lists the regional exclusion zone parameters and the resulting regional mean aggregate received RFI and aggregate path loss factors (computed with Equations B-21, B-23 and B-24).

© 2011 RTCA, Inc.

Table B-6 Cat. II Decision Height Aggregate RFI Results (Random Method)

Annular Region #	Rel Conc.	Excl. Angle (deg)	Inner Rad. (m)	Outer Rad. (m)	F_{AGG}	Rel. Inv. PL_{AGG}
1	1	180	0	420	0.000	0.000
2	1	60	420	840	1.751E-04	1.751E-04
3	1	10	840	4470	1.149E-04	1.149E-04
4	1	0	4470	20000	8.957E-06	8.957E-06
5	1	0	20000	43593	7.031E-07	7.031E-07
Total					2.997E-04	2.997E-04

Using the technique from B.4.2.1 and the Table B-6 total relative path loss factor, the scenario results are 101.03 dB mean aggregate path loss and -76.03 dBW/MHz mean aggregate received RFI power density.

B.4.2.4 Generic Surface (Taxiway) Scenario Aggregate ATCt Base Station RFI

As described in Section 3.4, the RFI scenario for a generic airport surface GNSS receiver operation is represented by an aircraft nominally at the end of the taxiway (aircraft antenna height = 4 m). The nadir point is again roughly centered within a metropolitan ATCt base station deployment (average tower spacing = 2.2 km out to 45.4 km radius). The radio horizon to a 30 m high ATCt antenna is 30.84 km (Table B-2). The aircraft antenna height is again below the ATCt tower height so its primary antenna pattern region is being illuminated by the primary base station antenna pattern. An exclusion zone is used around the airport runway similar to the Cat. II zone (parameters listed below). The isotropic path loss is described in Section B.3.2. One deployment zone ρ_E value is used: 0.26307 km^{-2} ($10^{-6.580}$ m^{-2}). Table B-7 lists the regional exclusion zone parameters and the resulting mean aggregate received RFI and aggregate path loss factors (computed with Equations B-21, B-23 and B-24).

Table B-7 Airport Surface (Taxiway) Aggregate RFI Results (Random Method)

Annular Region #	Rel Conc.	Excl. Angle (deg)	Inner Rad. (m)	Outer Rad. (m)	F_{AGG}	Rel. Inv. PL_{AGG}
1	1	180	0	550	0.000	0.000
2	1	22.5	550	4200	2.586E-05	2.586E-05
3	1	0	4200	20000	8.715E-07	8.715E-07
4	1	0	20000	30837	4.120E-08	4.120E-08
Total					2.677E-05	2.677E-05

Using the technique from B.4.2.1 and the Table B-7 total relative path loss, this scenario results are 111.52 dB mean aggregate path loss and -86.52 dBW/MHz mean aggregate received RFI power density.

B.4.2.5 US East Coast High Altitude Scenario Aggregate ATCt Base Station RFI

This general scenario, described in Section 3.1, is represented by a limiting case for high altitude flight. The aircraft is at 18,000 feet altitude (the lowest jet route level). The specific aircraft location is above South-central Pennsylvania where several large metro areas with planned ATCt deployment are within the aircraft antenna's radio horizon. The flight level and approximate location were chosen similar to an analysis case in RTCA/DO-235B.

© 2011 RTCA, Inc.

The random location method models the ATCt base concentrated deployment areas as annular segments within a low-concentration, rural background that has 40 km average base station spacing. The aggregate RFI computation proceeds in two steps:

1. Computing the low concentration background level while assuming the several metro zones are source-free (i.e.; their defining annular segments are exclusion zones)
2. Computing each high concentration zone aggregate RFI level separately and adding those to the aggregate background RFI level to determine the composite aggregate.

B.4.2.5.1 Low Tower Concentration Zone Aggregate RFI Analysis

Inspection of Table 3-1 containing metro center location radial separation distances from the aircraft, suggests the metro deployment concentrations could be modeled as annular segments with certain radial and angular dimensions. This feature would enable random method aggregate computation. Additionally, some of the metro centers have approximately the same radial distance.

To begin the annular zone modeling, note that Baltimore and Washington metro zone centers have almost the same radial distance to the aircraft. Because these cities are close together, their 45.4 km metro center deployment zones also overlap and the two central zones can be modeled as one larger annular segment. A similar technique can be also used to pair Philadelphia and Pittsburgh, along with Allentown and Richmond. However, in these two city-pair cases each city has its own separate angular segment. Table B-8 lists the parameters for each of the ATCt base station metro concentration zones and an actual exclusion zone for the Atlantic Ocean off the New Jersey and the DelMarVa Peninsula.

Table B-8 High Altitude East Coast Hotspot Parameters

Location	Dist. to a/c	Ave Rad	Inner Rad	Outer Rad	Total Ang
Baltimore	122.255				
Wash. DC	118.582	120.4188	77.289	163.549	75.00
Harrisburg	91.252		62.752	119.752	23.57
Philadelphia	268.799				16.00
Pittsburgh	278.493	273.6458	230.516	316.776	15.44
Allentown	249.837				17.22
Richmond	254.057	251.9471	223.447	280.447	16.93
Ocean			298.985	328.160	45.00

Table B-8 indicates that certain of the hotspot annuli overlap in radius with other hotspots. For example, the Harrisburg hotspot partially overlaps the Washington/ Baltimore. Before the aggregate integration can be performed, these overlaps need to be sorted out. From this basic definition table, a set of composite integration radial and angular zone dimensions can be formed (Table B-9).

© 2011 RTCA, Inc.

Table B-9 Composite Integration Zone Model Dimensions

Zone #	Inner Radius (km)	Outer Radius (km)	Full Angle (deg.)
1	62.752	77.289	23.57
2	77.289	119.752	98.57
3	119.752	163.549	75.00
4	223.447	230.516	34.15
5	230.516	280.447	65.59
6	280.447	298.985	31.44
7*	298.985	316.776	76.44
8*	316.776	328.16	45.00

* This zone contains a source-free portion (45°) representing the Atlantic Ocean

With the composite zone dimensions defined, the rural ATCt base station aggregate effect computation is performed with the Table B-9 zones treated as source-free. Table B-10 lists the results from the integration for each of the eight zones.

Table B-10 Composite Integration Zone Model –Rural Results

Zone #	Inner Rad. (km)	Outer Rad. (km)	Full Angle (deg.)	Agg. Factor F_{AGG}
1	62.752	77.289	23.57	7.783 E-06
2	77.289	119.752	98.57	2.439 E-05
3	119.752	163.549	75.00	2.943 E-05
4	223.447	230.516	34.15	4.577 E-06
5	230.516	280.447	65.59	2.726 E-05
6	280.447	298.985	31.44	1.041 E-05
7*	298.985	316.776	76.44	8.256 E-06
8*	316.776	328.16	45.00	8.256 E-06

The Zone 0 aggregate factor (covering the area aircraft nadir point out to the inner Zone 1 radius) in the rural case is 7.289 x 10^{-6} and the resulting overall rural aggregate factor (algebraic sum of all the 9 zone factors), F_{TOTR} = 1.2507 x 10^{-4}. The rural base station concentration factor ρ_B = 7.958 x 10^{-4} km^{-2} (= $10^{-9.099}$ m^{-2}) which holds everywhere except the source-free zones. Therefore the rural concentration aggregate path loss (in dB), $PL_{AGGR}(dB) = -10 \log(\rho_B \cdot F_{TOTR}) = 130.02$ dB and the rural aggregate received RFI, $P_{SDRR}(dB)=P_{SDE}(dB)-PL_{AGG}(dB) \cdot = -105.02$ dBW/MHz

B.4.2.5.2 Metro Concentration Zone and Combined Aggregate RFI Analysis

The next step is to use the defined composite zone dimensions (Table B-9) to compute the hotspot aggregate components from each zone. In this case the sources only occupy the annular segment previously treated as source-free. One adjustment in angular must be made, however, to exclude the actual source-free ocean area portion of Zone 7. Table B-11 lists the results of the metro zone computation.

© 2011 RTCA, Inc.

Table B-11 Composite Integration Zone Model –Metro Results

Zone #	Inner Rad. (km)	Outer Rad. (km)	Full Angle (deg.)	Agg. Factor F_{AGG}
1	62.752	77.289	23.57	5.460 E-07
2	77,289	119.752	98.57	9.200 E-06
3	119.752	163.549	75.00	7.744 E-06
4	223.447	230.516	34.15	4.805 E-07
5	230.516	280.447	65.59	6.075 E-06
6	280.447	298.985	31.44	9.947 E-07
7	298.985	316.776	31.44*	2.244 E-06

* This Atlantic Ocean source-free portion (45°) was removed from this zone

The resulting metro aggregate factor (algebraic sum of all the 7 zone factors), F_{TOTM} = 2.5954 x 10^{-5}. The metro base station concentration factor ρ_M = 0.263 km^{-2} (= $10^{-6.58}$ m^{-2}). Therefore the metro concentration aggregate path loss (in dB), PL_{AGGM}(dB) = -10 log($\rho_M \cdot F_{TOTM}$) = 111.66 dB and the metro aggregate received RFI, P_{SDRM}(dB)=P_{SDE}(dB)-PL_{AGGM}(dB)·= -86.66 dBW/MHz

The combined aggregate path loss (in dB), P_{AGG}(dB) = -10 log($\rho_M \cdot F_{TOTM}$ + $\rho_B \cdot F_{TOTR}$). Inserting the results for the rural and metro areas yields P_{AGG}(dB) = 111.60 dB. Using again the simple aggregate formula for the combined aggregate received RFI yields P_{SDR}(dB)=P_{SDE}(dB)-PL_{AGG}(dB) = -86.60 dBW/MHz The combined aggregate results are clearly dominated by the larger metro aggregate components.

B.4.3 Fixed Discrete ATCt Base Station Location Method Computations

To establish an aggregate ATCt base station RFI effect from a fixed station location grid structure, an analysis was done for base stations located along a regular hexagonal fixed grid. Figure B-11 illustrates this structure centered around a general aircraft operational ground track point within some ATCt base station deployment zone.

In Figure B-11 the non-orthogonal coordinate pair (u,v) denotes discrete ATCt base station location coordinates (centers of the hexagonal cells) as measured in integer multiples of the cell spacing, d, from the central cell. The aircraft is assumed to be on a particular flight path (dash-dotted line) with the nadir point on its ground track at the non-integer coordinates (-a/2, a) where $a = 1/\sqrt{3}$. That point is separated from the grid center by a distance of d/2. A base station is assumed to be located at the center of the grid. Other base stations are located at cell centers out to the radio horizon. For the indicated flight path in scenarios with airport exclusion zones (Table B-3), the only base station position assumed to be excluded by airport layout constraints has the coordinates (-1, 2). The radial distance between aircraft nadir point and any ATCt base station is given by $r(u,v) = d\sqrt{(u+a/2)^2 + (u+a/2)(v-a) + (v-a)^2}$, where $a = 1/\sqrt{3}$.

The density of base stations is assumed to be constant out to a radius of 45.4 Km at which point the density may change as illustrated in Figure 2-9. The interference analysis accounts for this by using hexagonal cell sizes which are unique to each of the annular rings depicted in Figure 2-9.The number of annular rings used in the analysis depends on the scenario and just where the ring limits from Figure 2-9 fall with respect to the radio horizon. The maximum number of rings needed is three.

© 2011 RTCA, Inc.

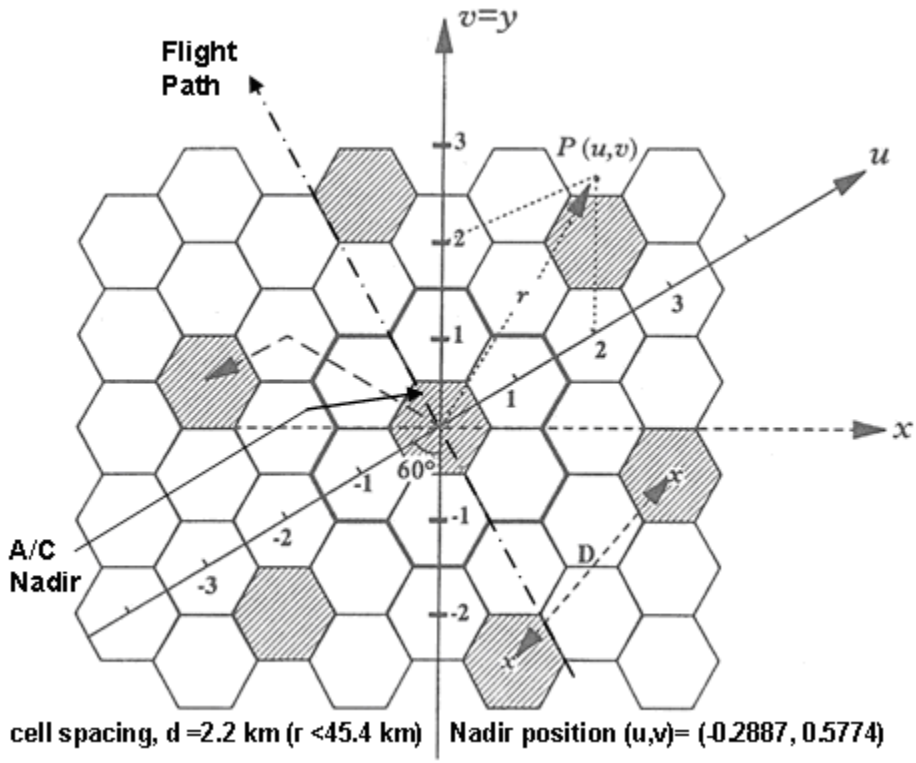

<u>Figure B-11</u> Fixed Hexagonal Cellular Grid Structure (Top View)

We begin by formulating a generic analysis that pertains to all scenarios described in Sections 3.2 through 3.5. The analysis pertinent to the enroute scenario will be described separately in Section B.4.3.5.

To this end we have the following definitions.

Let $u_{max}(i)$ denote the maximum value of the u coordinate for the ith ring.

$$u_{\max}(i) = IntegerPart[R_O / d_i - 0.5];$$

where R_o is the radio horizon.

Similarly $u_{min}(i)$ denotes the minimum value of the u coordinate for the ith ring.

$$u_{\min}(i) = -IntegerPart[(R_O / d_i - 0.5)(2/\sqrt{3})].$$

The corresponding values for the v coordinate are functions of u and given by,

$$v_{\max}(u,i) = IntegerPart[-u/2 + \sqrt{(R_O / d_i - 0.5)^2 - (3/4)u^2}]$$

and $$v_{\min}(u,i) = IntegerPart[-u/2 - \sqrt{(R_O / d_i - 0.5)^2 - (3/4)u^2}].$$

Also,

$$r_i(u,v) = d_i\sqrt{(u + a/2)^2 + (u + a/2)(v - a) + (v - a)^2}\ ;\ \text{where } a = 1/\sqrt{3}$$

To appropriately sum over a possible three rings we need the indicator functions,

$$g_1(u,v) = \begin{Bmatrix} 1, & r_1(u,v) \le \min\{45.4Km, R_O\} \\ 0, & elsewhere \end{Bmatrix},$$

© 2011 RTCA, Inc.

$$g_2(u,v) = \begin{cases} 1, & 45.4Km + d_2/2 < r_2(u,v) \le \min\{70.3Km, R_O\} \\ 0, & elsewhere \end{cases},$$

and $$g_3(u,v) = \begin{cases} 1, & 70.3Km + d_3/2 < r_3(u,v) \le R_O \\ 0, & elsewhere \end{cases}.$$

To account for whether or not the aircraft antenna height is greater than the cell tower height, we define,

$$\chi(h_A) = \begin{cases} 1, & h_A \le h_E \\ 10^{-0.23}, & h_A > h_E \end{cases}.$$

The one cell in the exclusion zone is eliminated by the function,

$$Ex(i,u,v) = \begin{cases} 0, & \{i=1, u=-1, v=2\} \\ 1, & elsewhere \end{cases}.$$

We define an elevation angle γ to account for antenna gain variations with range as,

$$\gamma_i(u,v) = \begin{cases} \pi/2, & r_i(u,v) = 0 \\ Arc\tan[(\max\{h_A, h_E\} - \min\{h_A, h_E\})/r_i(u,v)], & elsewhere \end{cases}.$$

The necessary antenna gains have been defined in Section 2 while the median path loss, PL(r), is defined in Section B.3. Using these definitions, we write the summand as,

$$Sum(i,u,v) = Ex(i,u,v)g_i(u,v)PL(r_i(u,v))G_{rcv}(\gamma_i(u,v))G_{xmt}(\gamma_i(u,v) + (\pi/90)\,\mathrm{sgn}(h_A - h_E))$$

and aggregate mean interference power density for the discrete model becomes

$$\overline{P_I} = \chi(h_A)P_O 10^{\eta} \sum_{i=1}^{3} \sum_{u_{\min}(i)}^{u_{\max}(i)} \sum_{v_{\min}(u,i)}^{v_{\max}(u,i)} Sum(i,u,v), \qquad \text{Equation B-26}$$

where η is as defined in Section B.3.

B.4.3.1 Generic Terminal Area (FAF WP) Scenario Aggregate ATCt Base Station RFI

For the Final Approach Fix (FAF) scenario the GPS antenna height is 535.2 meters, the cell tower height at 30 meters, and a radio horizon of 118 km. The ATCt emission power spectral density P_{SDE} (=P_o/ 5 MHz) was set at 25 dBW/MHz. The median path loss model used is a blending of the two-ray and Hata models as was used for the random method discussed in Appendix B.4.2.1. The number of rings for this scenario was limited to two with distances d_1=2.2 km and d_2=6.2 km. A third ring was shown to contribute no significant interference power. The results are shown in the table below.

Table B-12 Generic Terminal Area (FAF) Discrete Model Interference

Mean Aggregate Base Station Received RFI Power Density (dBW/MHz)	Mean Aggregate Base Station RFI Path Loss (dB)
-73.60	98.61

© 2011 RTCA, Inc.

B.4.3.2 Generic Category I Decision Height Scenario Aggregate ATCt Base Station RFI

For the Category I decision height scenario the GPS antenna height is 53.34 meters, the cell tower height at 30 meters, and a radio horizon of 52.708 Km. The emission power spectral density, P_{SDE}, was set at 25 dBW/MHz. The median path loss model used is the Hata model as all ranges are beyond 1 Km. The number of rings for this scenario was limited to two. The interference results are shown in the table below.

Table B-13 Generic Category I Discrete Model Interference

Mean Aggregate Base Station Received RFI Power Density (dBW/MHz)	Mean Aggregate Base Station Path Loss (dB)
-77.63	102.64

B.4.3.3 Generic Category II Decision Height Scenario Aggregate ATCt Base Station RFI

For the Category II decision height scenario the GPS antenna height is 25.94 meters, the cell tower height at 30 meters, and a radio horizon of 43.592 km. The emission power spectral density, P_{SDE}, was set at 25 dBW/MHz. The median path loss model used is the Hata model as all ranges are beyond 1 km. The number of rings for this scenario was limited to one because of the radio horizon being less than 45.4 km. The interference results are shown in the table below.

Table B-14 Generic Category II Discrete Model Interference

Mean Aggregate Base Station Received RFI Power Density (dBW/MHz)	Mean Aggregate Base Station Path Loss (dB)
-79.09	104.10

B.4.3.4 Generic Surface (Taxiway) Scenario Aggregate ATCt Base Station RFI

For the generic surface (taxiway) decision height scenario the GPS antenna height is assumed to be 4 meters, the cell tower height at 30 meters, and a radio horizon of 30.836 km. The emission power spectral density P_{SDE} was set at 25 dBW/MHz. The median path loss model used is the Hata model as all ranges are beyond 1 Km. The number of rings for this scenario was limited to one because of the radio horizon being less than 45.4 Km. The interference results are shown in the table below.

Table B-15 Generic Surface (Taxiway) Discrete Model Interference

Mean Aggregate Base Station Received RFI Power Density (dBW/MHz)	Mean Aggregate Base Station Path Loss (dB)
-88.76	113.77

B.4.3.5 US East Coast High Altitude Scenario Aggregate ATCt Base Station RFI

For the discrete model high altitude scenario, the aircraft was flown at an altitude of 5.49 Km located at 39.819^{o} North Latitude and 77.573^{o} West Longitude and flying at a bearing of 48.27^{o}. This places the aircraft approximately 120 km Northwest of the Baltimore and Washington metropolitan areas. At the altitude flown, interference was computed for seven metropolitan areas within the radio horizon. Those areas were,

© 2011 RTCA, Inc.

Baltimore, Washington DC, Richmond VA, Harrisburg, Philadelphia, Pittsburgh and Allentown PA. The grid structure shown in Figure B-11 was placed at each of the metropolitan areas with the grid origin at the center of each city. The interference analysis mimics that given in Section B.4.3.1 with certain modifications to account for the aircraft displacement. The geometry is shown in Figure B-12 below.

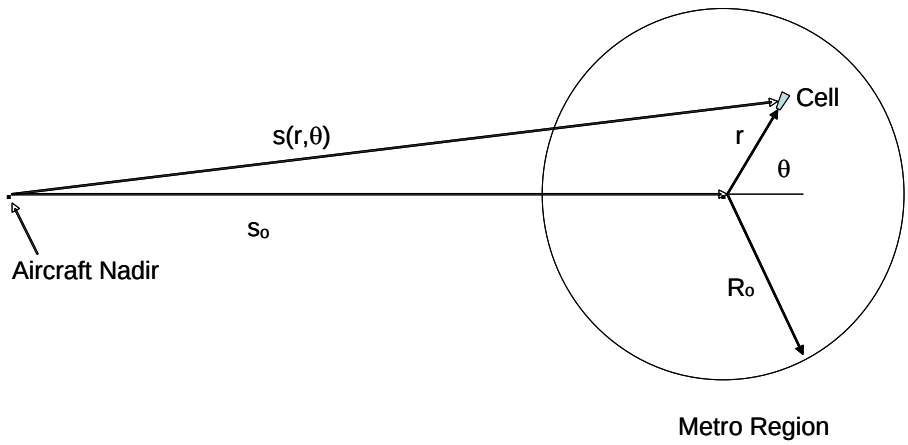

Figure B-12 Enroute Discrete Method Interference Scenario Geometry

As before, each metropolitan area is assumed to contain up to three annular rings each populated with hexagons of the appropriate size. The analysis assumes a planar earth with the u axis of the hexagonal grid co-aligned with the line depicted by s_o in Figure B-12. The distance s in the figure varies with annular ring number as well as (u,v) coordinate and is given by,

$$s_i(u,v) = \sqrt{(s_O + d_i(u + v/2))^2 + (d_i(\sqrt{3}/2)v)^2} \ .$$

A modification must then be made to the elevation angle γ as,

$$\gamma_i(u,v) = \begin{Bmatrix} \pi/2, & s_i(u,v) = 0 \\ Arc\tan[(\max\{h_A, h_E\} - \min\{h_A, h_E\}) / s_i(u,v)], & elsewhere \end{Bmatrix}.$$

Since cell towers in metropolitan areas tend be located at the highest possible point as on top of building structures, it is appropriate to assume a free space propagation model for the enroute scenario. Thus for the discrete grid analysis we have,

$$PL_i(u,v) = [(4\pi/\lambda)^2((h_A - h_E)^2 + s_i^2(u,v))]^{-1}.$$

For certain metropolitan areas, exclusion zones have been incorporated as for example in Baltimore there is an exclusion zone for the Chesapeake Bay. Also as the annular rings of cells around Baltimore and Washington DC begin to overlap, the rings are cut off so as to avoid this difficulty.

With these modifications, the expression for the mean interference power density given previously in equation (1) can be used directly. Table B-16 shows the results.

© 2011 RTCA, Inc.

Table B-16 Enroute Scenario Discrete Method Results

Metro Area	# Rings Used	s_o (km)	Rcv PSD (dBW/MHz)	Agg Path Loss (dB)
Baltimore	2	122.25	-93.81	118.81
Washington	2	118.58	-92.99	117.99
Harrisburg	1	91.25	-95.69	120.69
Philadelphia	1	268.80	-97.31	122.31
Allentown	1	249.84	-96.79	121.79
Richmond	2	254.06	-96.33	121.33
Pittsburgh	1	278.49	-97.57	122.57
Total			-87.01	112.01

B.4.4 Random ATCt Mobile Station Location Method Computations

To evaluate the magnitude of LightSquared mobile unit RFI to airborne GPS receivers, the methodology outlined in Appendix B.2.2 is used. The RF sources that populate the circular region shown in Figure B-1 are LightSquared mobile units at an assumed surface density ρ_E (mobiles per square meter). The mobile unit exclusion zone shown in Figure B-1 may or may not be present depending on the landing approach scenario. Details regarding the exclusion zones may be found in Section 3.

Each mobile unit is assumed to have an unwanted emission into the GPS L1 band. The source of this emission is customarily out of band noise generated by the final power amplifier and as such the emission level typically remains constant independent of mobile unit power control. Thus in all of the cases analyzed this mobile emission level is held at -90 dBW/MHz ($P_{SDE,}$ substituted for P_o in Appendix B.2.2 equation (11)).

The mobile units are assumed to be uniformly distributed throughout the circular region (minus the exclusion zone) each at a height of 1.8 meters. Radiation from each mobile encounters scattering, reflection, and absorption which is accounted for in the analysis by using the probabilistic path loss model described in Appendix B.3. Generally each scenario utilizes the two-ray, Erceg/Greenstein, and Hata median path loss models with range dependent blend points appropriate for the particular scenario. The exception is the FAF case which uses two-ray, log-log ($r^{-\alpha}$), and Hata models.

The results from each scenario are compared with results from a prior analysis of mobile unit interference to airborne GPS receivers in which a variety of mobile and portable unit types were assumed present including cell phones, laptop computers, PDA's, WiFi equipment, etc., but no LightSquared mobiles. These units were assumed to radiate power at -81.1 dBW/MHz, approximately 10 dB below the 47 CFR 15 limit and were distributed with a surface density ρ_E of 1 unit every 10,000 square meters.

B.4.4.1 Generic Terminal Area (FAF WP) Scenario Aggregate ATCt Mobile Station RFI

For the Final Approach Fix (FAF) scenario the GPS antenna height is 535.2 meters, the mobile height at 1.8 meters, and a radio horizon of 95.408 Km. The emission density P_{SDE} was set at -90 dBW/MHz. The median path loss model used is a blending of the two-ray and Hata models as was used for the random method discussed in Appendix B.4.2.1. Figure B-13 shows a plot of the median path loss used in this analysis case.

© 2011 RTCA, Inc.

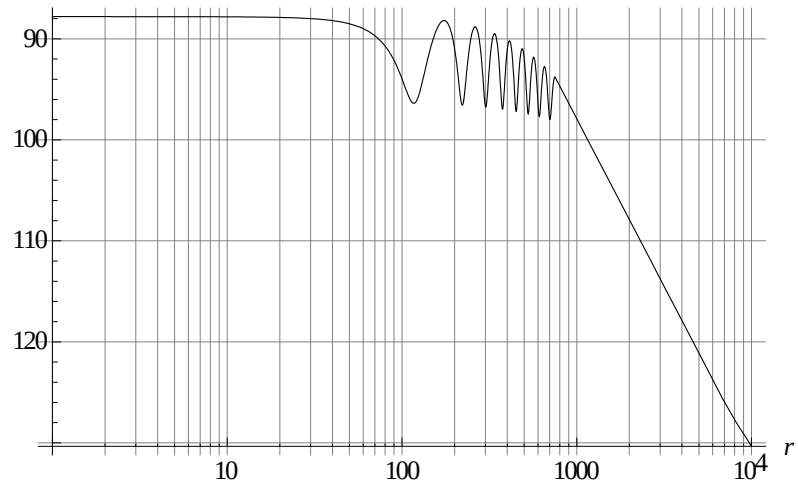

Figure B-13 Median Path Loss For Mobile Terminal Area (FAF WP) Scenario

The vertical axis in Figure B-13 shows median path loss in dB as a function of range r in meters (horizontal axis).

Analysis results are shown in the Table B-17 below. In this table, the term "cell" represents 3.80 square kilometers (area of circular region with 2.2 km average diameter).

Table B-17 Mobile Unit Terminal Area (FAF WP) Scenario Results

Case	A/C Ant Ht. (m)	Exclusion Zone Parameters	100 UE/cell Rcv PSD (dBW/MHz)	300 UE/cell Rcv PSD (dBW/MHz)	1000 UE/cell Rcv PSD (dBW/MHz)	Agg PSD w/o ATCt
FAF WP	535.2	None	-166.16	-161.39	-156.16	-151.04

B.4.4.2 Generic Category I Decision Height Scenario Aggregate ATCt Mobile Station RFI

For the Category I Decision Height scenario the GPS antenna height is 53.34 meters, the mobile height at 1.8 meters, and a radio horizon of 30.119 Km. The emission density P_o was set at -90 dBw/Mhz. The median path loss model used is a blending of two-ray, Erceg/Greenstein, and Hata models. Figure B-14 shows a plot of the median path loss used in this analysis case.

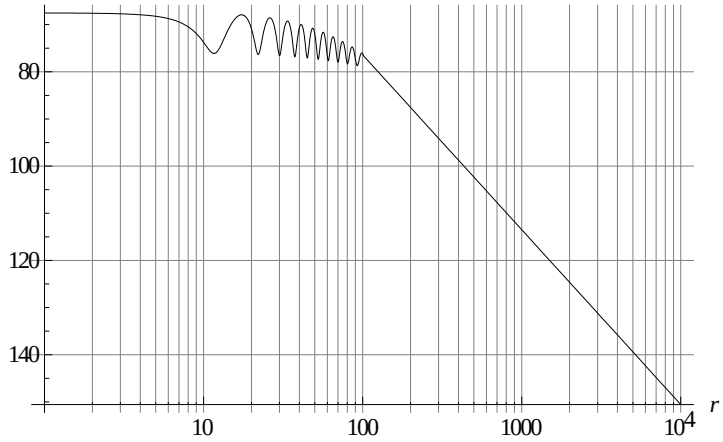

Figure B-14 Median Path Loss For Mobile Unit Category I Scenario

© 2011 RTCA, Inc.

The vertical axis in Figure B-14 shows median path loss in dB as a function of range r in meters (horizontal axis).

Analysis results are shown in the Table B-18 below. In this table, the term "cell" represents 3.80 square kilometers.

Table B-18 Mobile Unit Category I DH Scenario Results

Case	A/C Ant. Ht. (m)	Exclusion Zone Parameters	100 UE/cell Rcv PSD (dBW/MHz)	300 UE/cell Rcv PSD (dBW/MHz)	1000 UE/cell Rcv PSD (dBW/MHz)	Agg PSD w/o ATCt
Cat I DH	53.34	R_1=488m R_2=5830m θ_o=17°	-166.23	-161.46	-156.23	-151.11

B.4.4.3 Generic Category II Decision Height Scenario Aggregate ATCt Mobile Station RFI

For the Category II Decision Height scenario the GPS antenna height is 25.94 meters, the mobile height at 1.8 meters, and a radio horizon of 21.004 Km. The emission density P_o was set at -90 dBw/Mhz. The median path loss model used is a blending of two-ray, Erceg/Greenstein, and Hata models. Figure B-15 shows a plot of the median path loss used in this analysis case.

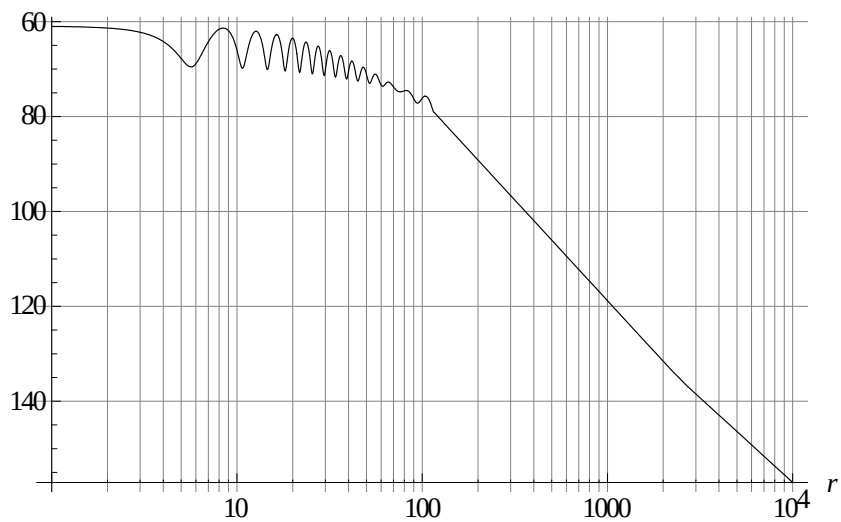

Figure B-15 Median Path Loss for Mobile Unit Category II Scenario

The vertical axis in Figure B-15 shows median path loss in dB as a function of range r in meters (horizontal axis).

Analysis results are shown in the Table B-19 below. In this table, the term "cell" represents 3.80 square kilometers.

© 2011 RTCA, Inc.

Table B-19 Mobile Unit Category II DH Scenario Results

Case	A/C Ant Ht. (m)	Exclusion Zone Parameters	100 UE/cell Rcv PSD (dBW/MHz)	300 UE/cell Rcv PSD (dBW/MHz)	1000 UE/cell Rcv PSD (dBW/MHz)	Agg PSD w/o ATCt
Cat II DH	25.94	R_1=449.3m R_2=2842m θ_o=25°	-164.98	-160.21	-154.98	-149.86

B.5 Aggregate RFI Results Comparison and Discussion

Table B-20 summarizes the results of the ATCt base station fundamental emission mean aggregate RFI computations for the random and fixed discrete location methods.

Table B-20 ATCt Base Station Fundamental RFI Aggregate Results Summary

Case	A/C Ant. Ht. (m)	Random Rcv PSD (dBW/MHz)	Random Agg. PL (dB)	Discrete Rcv PSD (dBW/MHz	Discrete Agg. PL (dB)
Surface	4.0	-86.52	111.52	-88.76	113.77
Cat. II DH	25.94	**-76.03**	101.03	**-79.09**	104.10
Cat. I DH	53.34	**-75.92**	100.92	**-77.63**	102.64
FAF WP	535.2	**-73.55**	98.55	**-73.60**	98.61
High Alt.	5490	-86.60	111.6	-87.57	112.60

Note: All the received power spectral densities exceed the GPS MOPS limit of -129.35 dBW/MHz at 1552.7 MHz. Those shown in bold font are cases that exceed the limit by the largest amounts.

The mean aggregate received RFI values in Table B-20 are to be compared with the GPS receiver MOPS-related tracking limit (in dBW/MHz): -129.35 dBW/MHz at the ATCt base transmit center frequency. They all exceed the limit by 42.7 to 55.8 dB (random method) for 100% peak channel loading. These results are driven primarily by the high transmit power and the close proximity to the GPS receiver passband edge.

Table B-21 ATCt Mobile Station Unwanted RFI Effect Aggregate Results Summary

Case	A/C Ant. Ht. (m)	100 UE/cell Rcv PSD (dBW/MHz)	300 UE/cell Rcv PSD (dBW/MHz)	1000 UE/cell Rcv PSD (dBW/MHz)	Baseline Rcv PSD (no UE)
Surface	4.0	-	-	-	-
Cat. II DH	25.94	-164.98	-160.21	-154.98	-149.86
Cat.I DH	53.34	-166.23	-161.46	-156.23	-151.11
FAF WP	535.2	-166.16	-161.39	-156.16	-151.04
High Alt.	5490	-	-	-	-

The mean aggregate received RFI values for the ATCt mobiles summarized in Table B-21 are to be compared with the GPS receiver environment limit: -146.5 dBW/MHz at the GPS L1 center frequency 1575.42 MHz. All the values, including those for a general set of RFI sources described in B.4.4 above are within the environment limit. Since the baseline value is assumed to exist in all the scenario cases, the addition of the ATCt mobile RFI raises the overall environment mean by between 9% (300 UE/Cell) and 31% (1000 UE/Cell).

© 2011 RTCA, Inc.

B.6 References

[B-1] B. V. Gnedenko, *The Theory of Probability*. New York, N.Y.: Chelsea Publishing Co., 1967

[B-2] D. Parsons, *The Mobile Radio Propagation Channel*. Chichester, England: John Wiley & Sons, 1996.

[B-3] V. Erceg, L.J. Greenstein, *et al*, "An Empirically Based Path Loss Model for Wireless Channels in Suburban Environments," *IEEE Journal on Selected Areas in Communications*, vol. 17, no. 7, July 1999.

[B-4] FAA AAS-100, "Airport Design Advisory Circular," AC 150/5300-13 (Chg. 1-15), 31 Dec. 2009

© 2011 RTCA, Inc.

Appendix C

Analytical Derivation of Maximum Tolerable Interference Levels

© 2011 RTCA, Inc.

This page intentionally left blank.

©2011 RTCA, Inc.

C Analytical Derivation of Maximum Tolerable Interference Levels

C.1 Wide Bandwidth Near-band Aggregate RFI Limit

Several GPS receiver MOPS have a test condition limit curve (Figure C) that specifies narrow bandwidth (CW) test conditions for frequencies in and near the receiver passband 1575.42 ± 10 MHz. This section will derive a wideband limit for signals with moderate bandwidth that whose spectra fall outside but near the receiver passband.

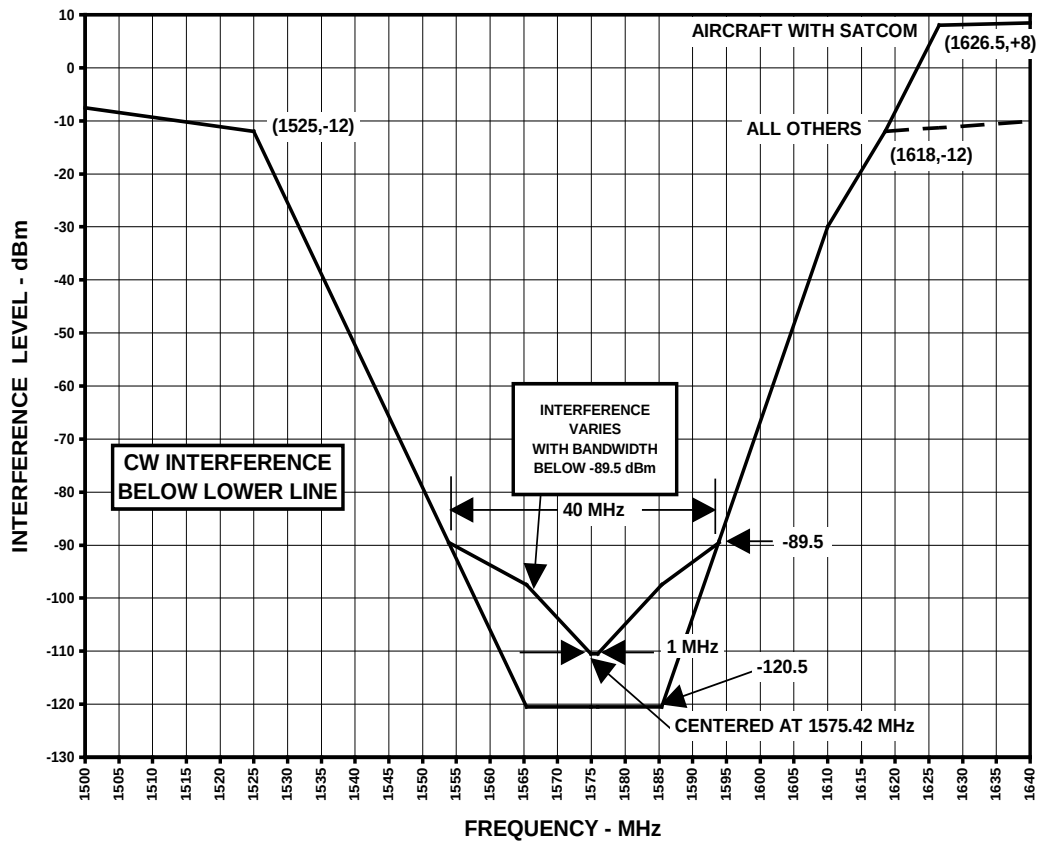

Figure C-1 Antenna Port CW Interference Limit

One particular RFI frequency range of interest for this report is 1525 - 1559 MHz. From Figure C, the CW RFI curve in that frequency range has the limit equation (in dBm):

$$P_{TEST}(f_c) = -120.5 + 2.6843\cdot(1565.42-f_c); \qquad \text{Equation C-1}$$

where f_c is the interference frequency in MHz. This limit is used as a test condition for various receiver performance tests, but frequency management strategy dictates that the RFI environment be managed to a level 6 dB below that limit. Thus the limit for non-aeronautical environmental RFI is:

$$P_{ENV}(f_c) = -126.5 + 2.6843\cdot(1565.42-f_c). \qquad \text{Equation C-2}$$

One theory is that the principal effect of a strong RFI signal outside receiver passband is likely to saturate the receiver by overcoming its RF/IF selectivity and compressing the linear gain to the desired, in-band signal. As such it should be just the total RFI power that causes the effect and not any particular RFI modulation. Thus a wideband signal with total power P_{WB} (dBm), center frequency f_c, and necessary bandwidth bw (MHz) should have a limit based on Equation C-2:

© 2011 RTCA, Inc.

$P_{WB}(f_c)$ - 10·log $(bw/1\text{MHz})$ = -126.5- 10·log$(bw/1\text{MHz})$ + 2.6843·(1565.42-f_c).

Converting this equation to dBW/MHz terms yields:

$PSD_{WB}(f_c)$ = -156.5 - 10·log$(bw/1\text{MHz})$ + 2.6843·(1565.42-f_c); Equation C-3

where $PSD_{WB}(f_c) = P_{WB}(f_c)$ -30 dB - 10·log$(bw/1\text{MHz})$

C.2 Third-Order Intermodulation RFI Effect Limit

This subsection provides an assessment of intermodulation products that may arise in airborne active antennas (see Figure 2-1) built to the requirements in RTCA/DO-301 due to LightSquared ATCt base station emissions for the Phase 1A and Phase 2 spectrum deployments (each with two channels). Intermodulation products may also arise within the receiver-processor (see Figure 2-1). This latter scenario is not addressed here, since there are many variants of front-end architectures within airborne receivers, and it would thus not be possible to develop a "representative" design to assess.

C.2.1 Active Antenna LNA Model

Consider the simple LNA system model shown in Figure C-. The LNA takes an input voltage, *x(t)*, which is typically the filtered output of a passive antenna element, and provides an output voltage, *y(t)*, with a nominal power gain of *G*. This note focuses on a representative airborne active antenna LNA that provides a nominal power gain of 34.5 dB. RTCA/DO-301 requires a minimum active antenna unit gain of 26.5 dB, and a nominal gain that it at least 3 dB higher than this. Considering that the active antenna unit also includes lossy components, assumed to be 5 dB here for the burnout protector, preselection filter, and postselection filter, this provides the justification for the 34.5 = 29.5 + 5 dB nominal gain that was selected for this analysis.

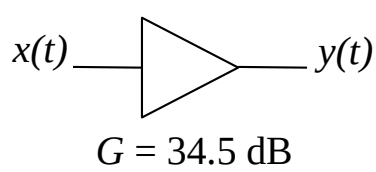

Figure C-2 Low Noise Amplifier System Model

For an ideal LNA, the input-output voltage characteristics may be described as:

$$y = a_1 x \qquad \text{Equation C-4}$$

where $a_1 = \sqrt{G}$ with *G* being the nominal power gain .

As is well-known, actual LNAs are only well-modeled by Equation C-4 for small input voltages. For larger input voltages, the output voltage saturates. A truncated Taylor series expansion is often used (see, e.g., [C-1]) as a more accurate model:

$$y = \sum_{i=1}^{N} a_i x^i \qquad \text{Equation C-5}$$

For example, Figure C- shows the voltage input-output characteristics of an LNA modeled using Equation C-5 with *N* = 5 and the following coefficients:

©2011 RTCA, Inc.

$$
\begin{aligned}
a_1 &= 53.088 \text{ (unitless)} \\
a_2 &= 0 \\
a_3 &= -997490 / R \text{ (volts}^{-2}\text{)} \\
a_4 &= 0 \\
a_5 &= 6.5e9 / R^2 \text{ (volts}^{-4}\text{)}
\end{aligned}
\qquad \text{Equation C-6}
$$

where R = 50 Ω is the resistance assumed to relate voltage to power. The a_1 coefficient was selected as $a_1 = \sqrt{G}$ to provide a nominal gain of 34.5 dB. The a_2 and a_4 coefficients were selected as zero to provide an odd-symmetric input-output voltage characteristic.

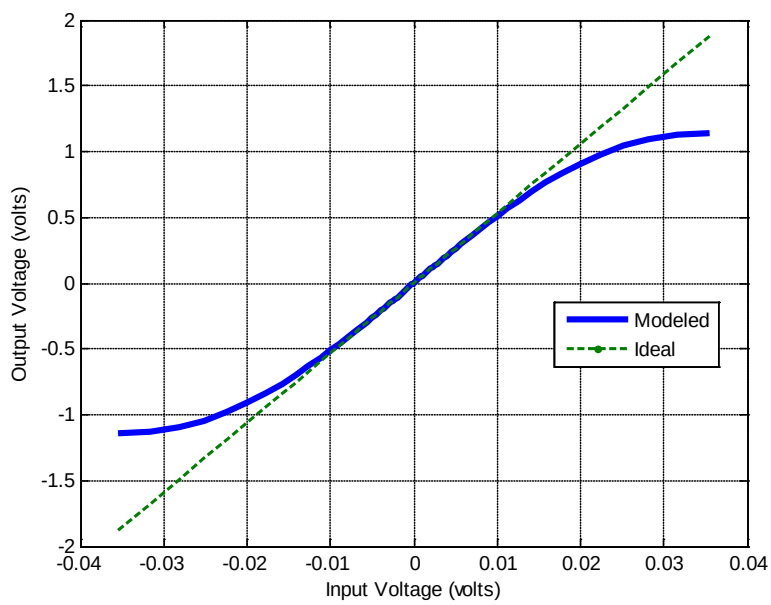

Figure C-3 Input-Output Voltage Characteristic for Modeled Airborne Active Antenna LNA

The parameter a_3 was selected to achieve a 1-dB compression point just compliant with DO-301 (-25 dBm for the active antenna subassembly), and a third-order intercept point consistent with the rule-of-thumb of being 10-15 dB above the 1-dB compression point. Figure C- shows the input-output power characteristics of the modeled LNA. The modeled LNA is consistent with the DO-301 requirements, providing an input 1-dB compression point of -22.2 dBm (see Figure C-), which would provide an input 1-dB compression point above -20 dBm for the overall active subassembly presuming combined insertion losses of 2.7 dB for the preselector filter and protection circuit.

© 2011 RTCA, Inc.

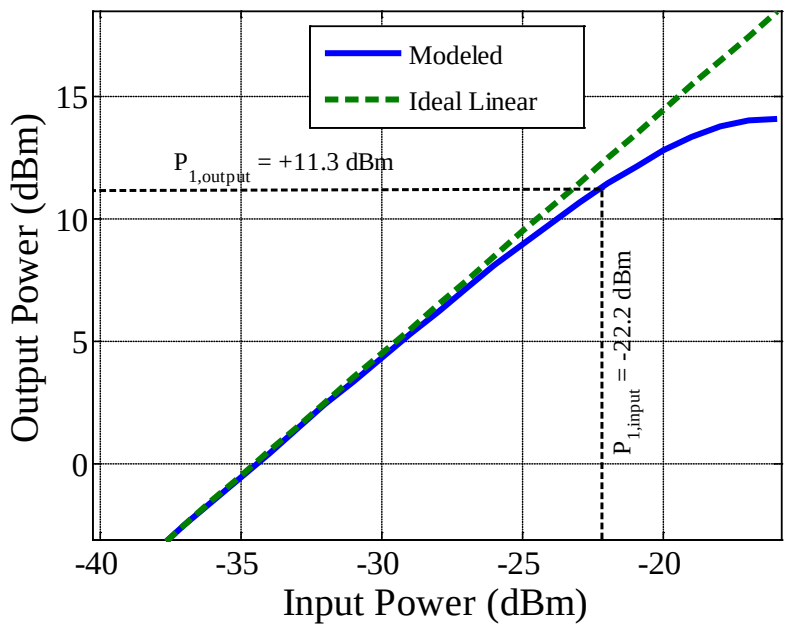

Figure C-4 Modeled LNA Input-Output Power Characteristics

C.2.2 Response of Active Antenna LNA to LightSquared Emissions

Noting that the input-output characteristics are virtually unchanged for input power levels below -20 dBm by truncating the Taylor series to N = 3, here we focus on the simpler LNA input-output voltage model:

$$y = a_1 x + a_3 x^3 \qquad \text{Equation C-7}$$

with the input voltage presumed to be well-modeled as a Gaussian, wide sense stationary random process.

The output voltage autocorrelation may be determined as:

$$\begin{aligned} R_y(\tau) &\equiv E\left[y(t+\tau)y(t)\right] \\ &= E\left[\left(a_1 x(t+\tau) + a_3 x^3(t+\tau)\right)\left(a_1 x(t) + a_3 x^3(t)\right)\right] \\ &= \left(a_1^2 + 6a_1 a_3 \sigma_x^2 + 9a_3 \sigma_x^4\right) R_x(\tau) + 6a_3^2 R_x^3(\tau) \end{aligned} \qquad \text{Equation C-8}$$

where $R_x(\tau)$ is the input voltage autocorrelation and $\sigma_x^2 = R_x(0)$ is the variance of *x(t)* (i.e., input power aside from a possible scale factor for a non-unity resistance).

From Equation C-6, the following expression may be derived to relate the output power spectrum, $S_y(f)$, of the LNA to its input power spectrum, $S_x(f)$:

$$S_y(f) = \left(a_1^2 + 6a_1 a_3 \sigma_x^2 + 9a_3 \sigma_x^4\right) S_x(f) + 6a_3^2 S_x(f) * S_x(f) * S_x(f) \qquad \text{Equation C-9}$$

where * is the convolution operator.

C.2.3 Preselector Filter Model

Figure C- shows the presumed preselector filter attenuation characteristics. This curve was derived from Figure 2-1 of DO-301.

©2011 RTCA, Inc.

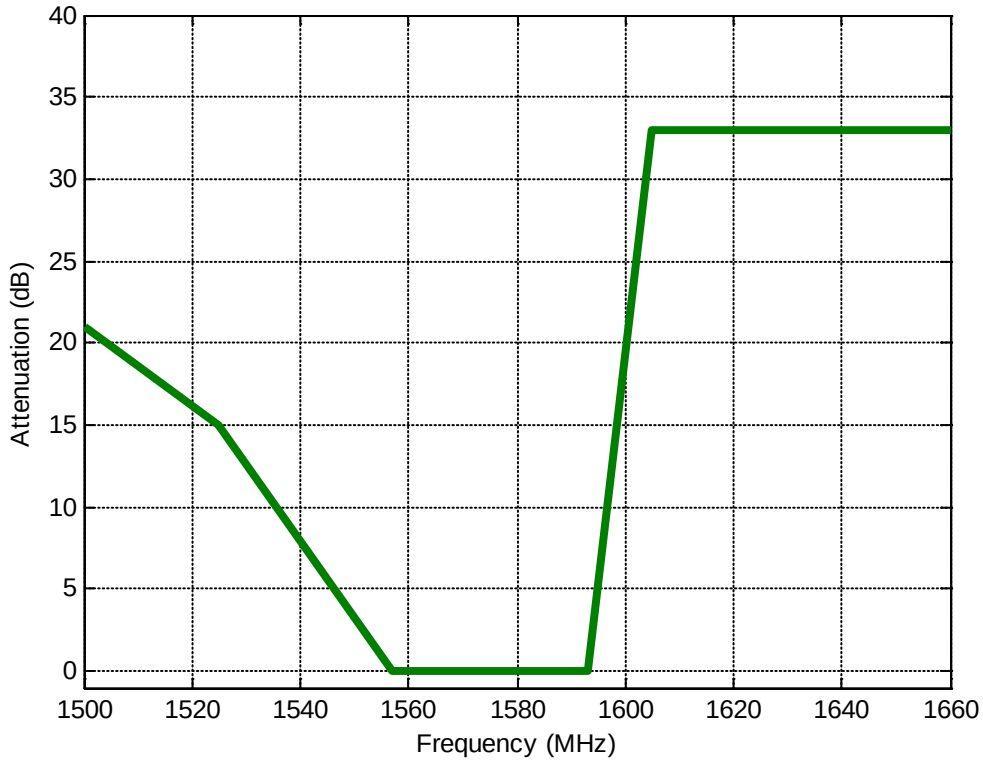

Figure C-5 Modeled Active Antenna Preselector Attenuation

C.2.4 Simulation Results

Figure C-, through Figure C- show the LNA input and output power spectra for various LightSquared received power levels, presuming no filtering prior to the LNA. Phase 1 emissions are assumed, and these emissions are very simply modeled as perfectly rectangular 5-MHz blocks centered at 1528.8 MHz and 1552.7 MHz with total input power as indicated on each figure. An input noise floor of -201.5 dBW/Hz is also included[1].

[1]This level would not truly be present at the LNA input even presuming that the overall front-end had precisely this effective N_0 value, since a good portion of the effective N_0 arises from the LNA noise figure. Nonetheless, ignoring rigor in this area does not materially affect the results presented here.

© 2011 RTCA, Inc.

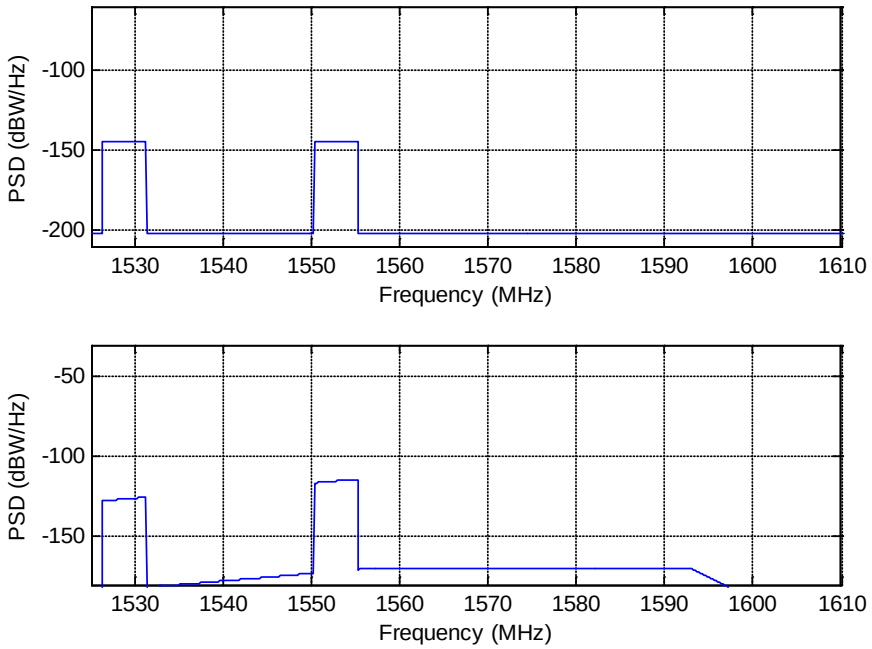

<u>Figure C-6</u> Input (top) and Output (bottom) Power Spectrum of Modeled LNA; LightSquared Signal Power at Antenna Output Port is -45 dBm (LNA in Linear Region)

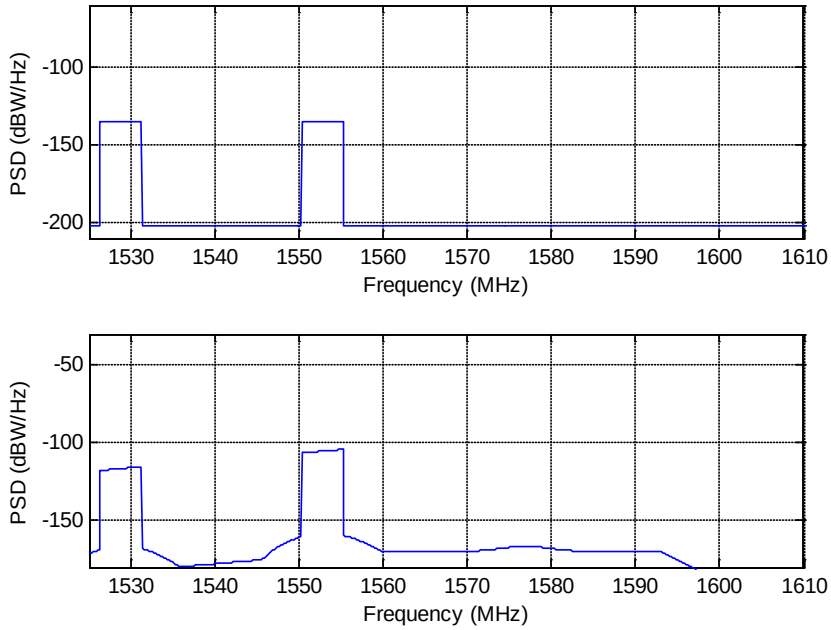

<u>Figure C-7</u> Input (top) and Output (bottom) Power Spectrum of Modeled LNA; LightSquared Signal Power at Antenna Output Port is -35 dBm (LNA Entering into Compression)

©2011 RTCA, Inc.

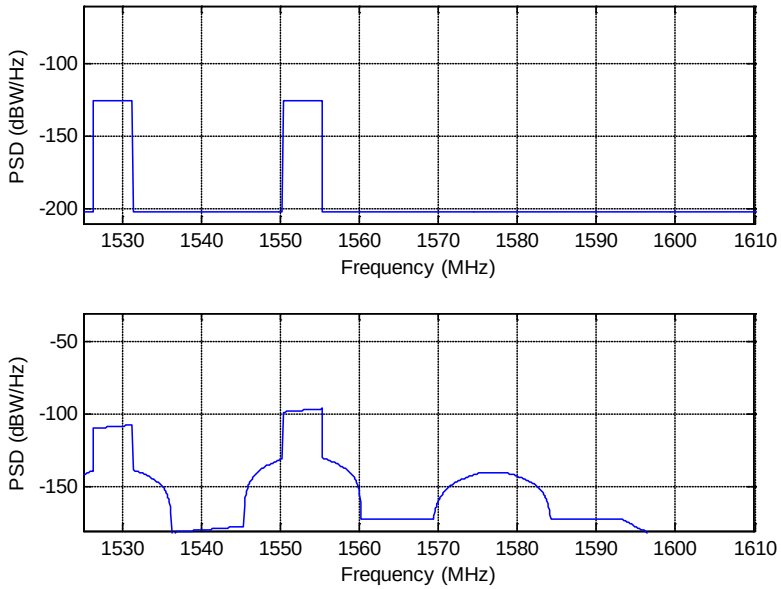

Figure C-8 Input (top) and Output (bottom) Power Spectrum of Modeled LNA; LightSquared Signal Power at Antenna Output Port is -25 dBm (LNA Entering Deeper into Compression)

Figure C- shows the degradation to the effective N_0 for a C/A-code receiver due to the third-order intermodulation product, presuming that the remainder of the receiver front-end is perfectly linear and perfectly bandlimited to 20 MHz[1]. The plot was produced by computing the inner product of the LNA output power spectrum, referred back to the passive antenna port by scaling by the true LNA gain and assumed 2.7 dB insertion loss (for the preselector filter and protection circuity), against the normalized power spectrum of the C/A-code. The inner product was computed over L1 +/-10 MHz under the presumption that the fundamental LightSquared emissions would be suppressed completely by later filtering within the receiver. A 1 dB degradation is seen at a LightSquared received power level of -36.7 dBm (-39.7 dBm/channel) for the Phase 0 signals, and -35.0 dBm (-38.0 dBm/channel) for the Phase 1 signals.

[1]These are obviously big assumptions that are not likely to be true for most fielded receivers. Saturation is likely to occur in later receiver components such as LNAs or mixers within receivers where accumulated front-end gain outpaces attenuation of the fundamental LightSquared emissions.

© 2011 RTCA, Inc.

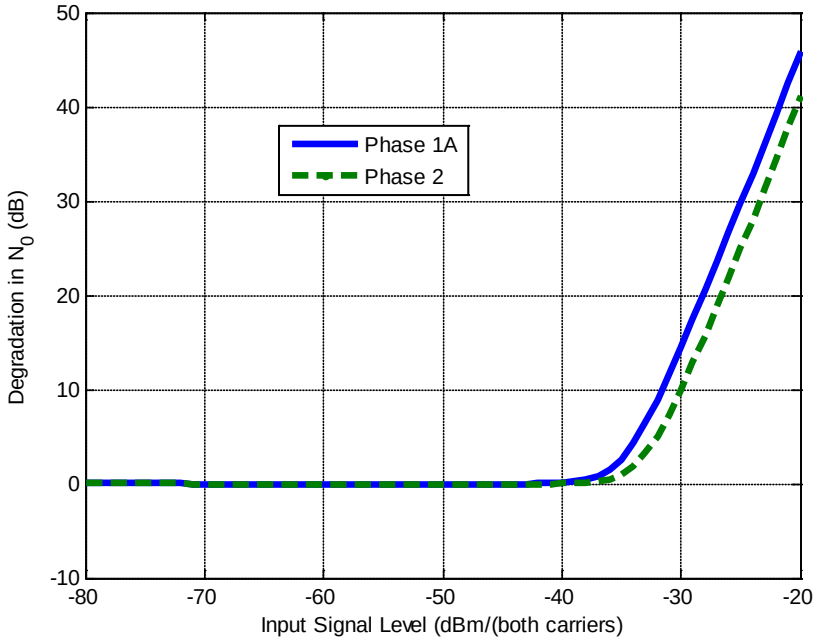

Figure C-9 Degradation to Receiver Effective Noise Floor due to the Third Order Intermodulation Product Created by Active Antenna LNA

C.3 Earlier Generation GPS Aviation Receiver Susceptibility

Only the single receiver model described above is considered within this report due to time constraints. It should be noted that, although representative, this receiver system model does not address all airborne equipment installations. For instance, some fielded equipment uses passive antennas, for which the functions found in between points A and B in Figure 2-1 would be found within the receiver-processor. Also, some aircraft are still equipped with receivers built to the first GPS MOPS published in 1991 by RTCA (DO-208). RTCA/DO-208 requires greater near-band selectivity (e.g., -40 dBm at 1555 MHz) than is required for modern installations addressed by DO-229/253/316 and the current International Civil Aviation Organization (ICAO) Standards and Recommended Practices (SARPs). The reason that the selectivity requirements from DO-208 were relaxed for the later GPS and GPS/WAAS MOPS is that DO-208 only addresses lateral guidance for enroute through non-precision approach flight phases, which can be met with narrow bandwidth C/A-code processing (e.g., a 2-MHz receiver passband) and with selective availability enabled, whereas the later MOPS enable vertically-guided precision approach operations that require wider receiver bandwidths (e.g., 20 MHz) to satisfy far more demanding performance requirements.

©2011 RTCA, Inc.

C.4 References

[C-1] SC-159, “Minimum Operational Performance Standards for Global Position System/Wide Area Augmentation System Airborne Equipment,” RTCA Document No. RTCA/DO-229D, 13 Dec. 2006

[C-2] Pozar, David M., *Microwave Engineering*, 3rd Edition, Hoboken, New Jersey: John Wiley & Sons, 2005.

[C-3] SC-159, "Minimum Operational Performance Standards for Airborne Supplemental Navigation Equipment Using Global Positioning System (GPS)," RTCA Document No. RTCA/DO-208 (with Change 1), 21 Sept. 1993

© 2011 RTCA, Inc.

This page intentionally left blank.

©2011 RTCA, Inc.

Appendix D

Experimental Test Results for Avionics GPS Receivers

© 2011 RTCA, Inc.

This page intentionally left blank.

©2011 RTCA, Inc.

D EXPERIMENTAL TEST RESULTS FOR AVIONICS GPS RECEIVERS

D.1 MOPS-based GNSS Receiver Broadband Tests

GPS receiver MOPS-based tests were conducted on four representative MOPS-compliant aviation receivers according to certain parts of Section A.1 to determine susceptibility to LightSquared signal emissions. Carrier-to-noise ratio (CNR) degradation baseline tests (Section A.1.1) were conducted to determine the 1 dB degradation and loss of tracking points for all four receivers against LightSquared Phase 0, 1 and 2 as well as 5 MHz Low and 10 MHz Low signal configurations. Additional tests comparing narrow (CW) and wide (5 MHz) bandwidth signals were done for both the Low (1528.8 MHz) and the High (1552.7 MHz) channels. SBAS message loss tests (Section A.1.3) also were conducted but due to time constraints, only two receivers were tested for the Phase 0 LightSquared configuration. The following sections document test configuration, signal generation and results.

D.1.1 Test Configuration

Figure D-1 displays a functional block diagram of the test configuration used for the MOPS-based tests. Four separate inputs were combined using a MiniCircuits ZC4PD-18-S four-way power summer. These four inputs were a simulated GPS signal, broadband white noise, a CW signal and the single- or dual-channel 5 or 10 MHz bandwidth noise representative of a LightSquared signal.

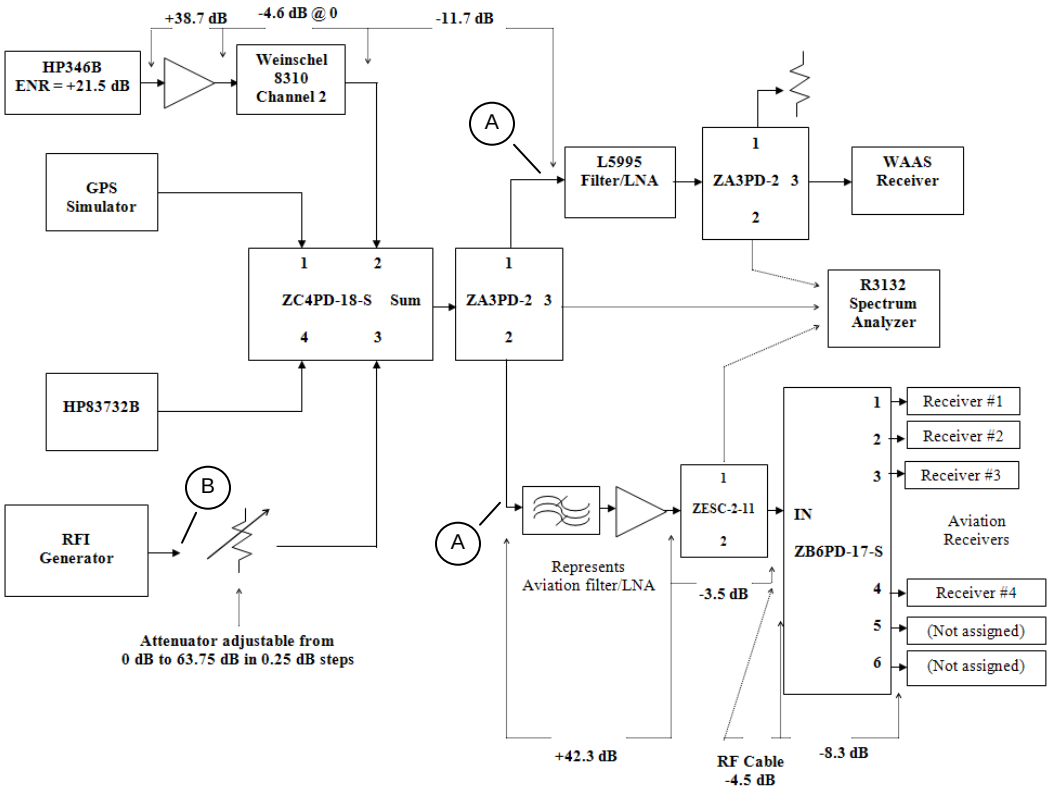

Figure D-1 Functional Test Block Diagram

Simulated GPS signals were generated using a Spirent STR2760 or SPAWAR AGNS programmed to use the specified MOPS constellation. The simulated GPS constellation

© 2011 RTCA, Inc.

consisted of 24 satellites plus one or two SBAS GEOs generating L1 C/A code, appropriate for MOPS-based tests and consistent with GPS SPS PS and RTCA/DO-229 (SBAS simulated for SBAS message loss tests only). The constellation was generated from the Yuma almanac file from April 8, 2009, with PRNs 01, 06, 18, 24, 25, 26, 32 removed and the GPS week changed to 1634. The simulated GPS scenario started 05/05/2011 01:40:00 GPS time. Regarding the power level of the simulated GPS signals, one satellite (PRN 7) was set at -120 dBm and the rest were set at -134 dBm, representing maximum and minimum levels at the input to a representative antenna filter/LNA (at locations marked "A" in Figure D-1). Note that the receivers were allowed to track for approximately 15 to 30 minutes with all satellites at -120 dBm before dropping power of all but one to -134 dBm at the start of each test. The SBAS signal(s) used the same power levels with the same timing as the GPS signals.

Broadband white noise was generated using an HP346B noise source that was amplified and then attenuated with a programmable attenuator to provide a controlled amount of additional noise. This broadband noise emulates the degradation of numerous sources that are not present for conducted tests and includes the energy of all other GNSS signals and sky noise. For the carrier-to-noise ratio (CNR) degradation test to determine a 1-dB degradation point, -173.5 dBm/Hz external noise is specified in the MOPS procedure, which required adding 4.1 dB of additional noise to the test configuration. For the SBAS message loss tests, -170.5 dBm/Hz external noise is specified, which required adding 5.6 dB of additional noise. These noise levels are intended to emulate the highly stressful RF environment in which MOPS-compliant receivers are already required to operate. Note that although some MOPS tests also require CW interference signals, which could have been provided with an HP83732B, these were not needed for the subset of tests conducted during this investigation.

The RFI generator configuration consists of a Tektronix AWG420 and HP8780 Vector Signal Generator (VSG) and various filters. The AWG420 has been programmed to generate various noise signals that occupy the bandwidth that LightSquared intends to use. The VSG also was used to generate CW signals in the upper and lower LightSquared channels for comparison tests versus certain wide bandwidth noise signals. The output of the VSG was connected to an amplifier before it was connected to a set of LightSquared Band Pass Filters (BPFs) representative of the ones that will be used by their transmitter. Two pairs of LightSquared BPFs, one pair centered at 1531 and the other pair centered at 1550 MHz, were cascaded in order to eliminate any possibility that noise generated by the HP8780 Vector Signal Generator (VSG) affected results. Figure D-2 shows a block diagram of the RFI generator. The only modification to the diagram occurred whenever only one BPF pair was needed (high or low channel only) for a given test condition; in this case the unneeded BPF pair was disconnected from the second ZAPD-2-N and the unused ports terminated.

©2011 RTCA, Inc.

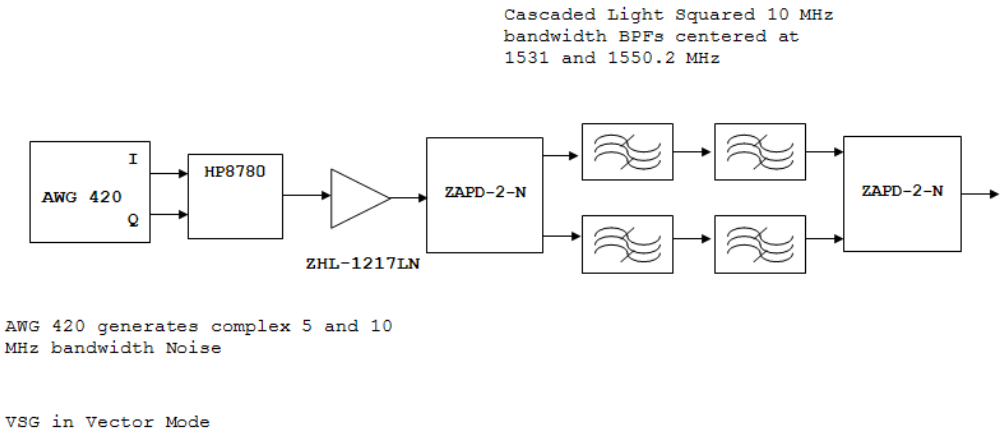

Figure D-2 RFI Generator Detail

The RFI generator output of a CW or representative LightSquared emission was provided through a controllable attenuator, combined with both the GPS signal and broadband noise, then distributed to a WAAS ground reference receiver and a number of aviation receivers. Since WAAS ground reference receivers and aviation receivers use different filter/LNA types, a power splitter was used to separately provide the combined emissions to each filter/LNA input under test. Note that the filter/LNA is considered to be located immediately after its respective antenna elements in the signal path. RFI power levels are reported as measured at the input to each filter/LNA (locations marked "A" in Figure D-1).

D.1.2 Aviation LNA

An aviation filter/LNA must meet certain performance specifications and depends on both the antenna element and the amplifier that individual manufacturers use. Since no single representative filter/LNA was available for this investigation, signal generation and amplifier components were chosen to achieve the intended functionality of the specified aviation filter/LNA. The required filter effects were achieved by shaping the white noise from the RFI generator to comply with RTCA DO-301 specifications, as described in the following section. The LNA function was implemented by cascading two separate amplifiers, shown in Figure D-3, that provide the performance characteristics DO-301 requires.

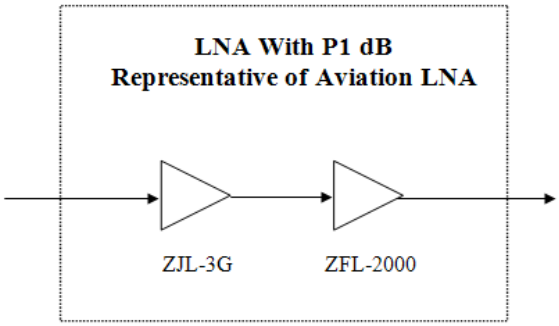

Figure D-3 LNA Representative of Aviation LNA

Table D-1 lists pertinent measured characteristics of this representative aviation LNA.

© 2011 RTCA, Inc.

Table D-1 Aviation LNA Characteristics

Gain	+42.3 dB
P1dB at input	-23.5 dBm
IP3 at input	-12.8 dBm
IP3 level at output	+29.6 dBm
Noise Figure	+3.55 dB

The measured gain of this LNA is +42.3 dB, which is higher than required. However, a number of components are between the aviation LNA output and the input of each of the aviation receivers. The net loss of these components is 16.3 dB, reducing the net gain from the input of the LNA to the input of the receivers to +26 dB. This net gain is within the expected range for GPS/SBAS aviation receivers.

D.1.3 LightSquared Signal Generation

Since no aviation filter/LNA was available for these tests, an alternate approach was used in which the LightSquared signals were shaped by the AWG in frequency to account for minimum required filtering. Figure D-4 shows the RTCA DO-301 specified frequency response of an aviation antenna filter.

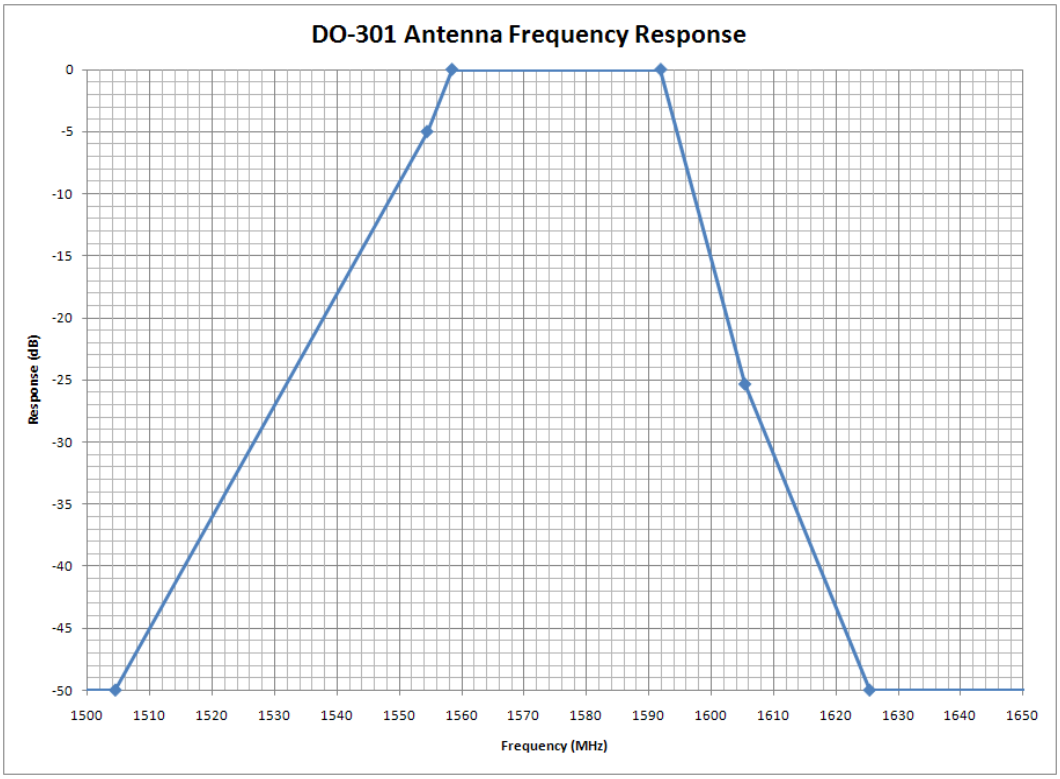

Figure D-4 Antenna Frequency Response Specified in RTCA DO-301

Shaped white noise matching RTCA DO-301 specifications allowed testing as though the signal had been filtered by a DO-301 compliant filter. However, since the actual filter is not present, any calibrated power measurement at the aviation LNA input must also take into account the insertion loss that an aviation filter would have provided. The software used to design the signals was also used to calculate the difference in total power between the filtered and unfiltered versions of each signal.

©2011 RTCA, Inc.

Table D-2 shows these differences, representing the insertion losses attributed to the various signals. These values are used to correct the power measurement made at the input to the variable attenuator (at the location marked "B" in Figure D-1) when preparing a test run, in addition to the measured losses between the input to the variable attenuator and the input to each filter/LNA (i.e. the losses between "B" and each "A" in Figure D-1).

Table D-2 Power Corrections using RTCA DO-301 Filtered Signals

Signal	DO-301 Filter Insertion Loss (dB)
Phase 0	6.3
Phase 1	9.3
Phase 2	10.9
5 MHz Low	27.9
10 MHz Low	25.3

Figure D-5 and Figure D-6 show examples of unfiltered and filtered versions of a representative LightSquared Phase 1 signal. The plots show spectra of the generated signals as they appear at the input of the programmable attenuator. Note that each signal that includes a 5 MHz component has a portion of the spectrum that is about 50 dB lower than the intended signal and immediately adjacent to the intended noise. This residual component is due to the VSG being unable to completely cancel the imaginary component of the complex representation of the signal and is typical of the performance that a VSG can achieve.

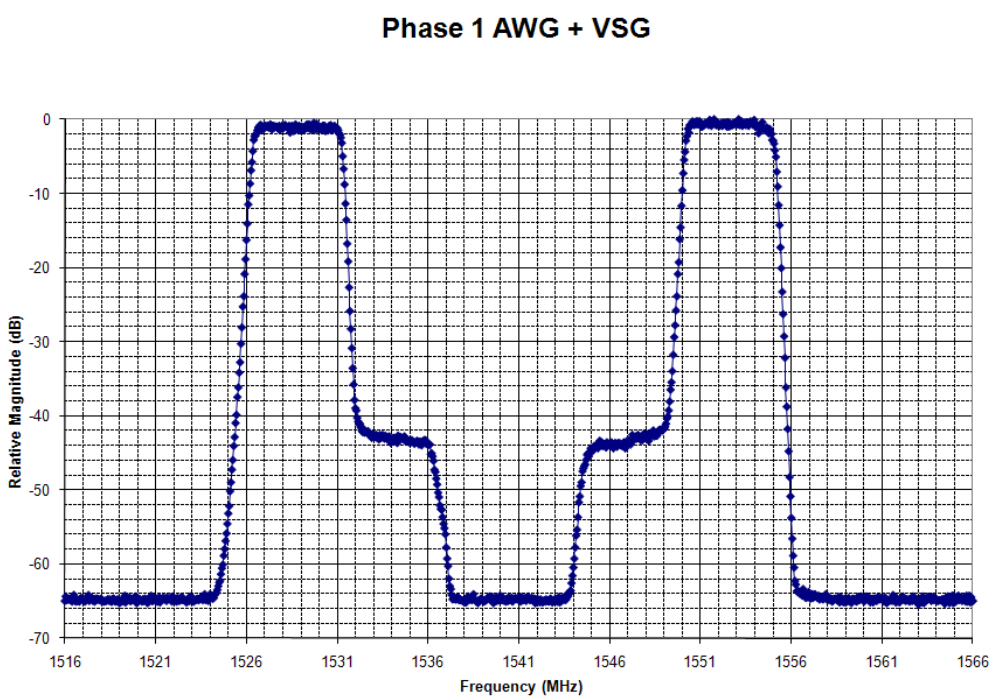

Figure D-5 Representative Unfiltered Phase 1 Signal

© 2011 RTCA, Inc.

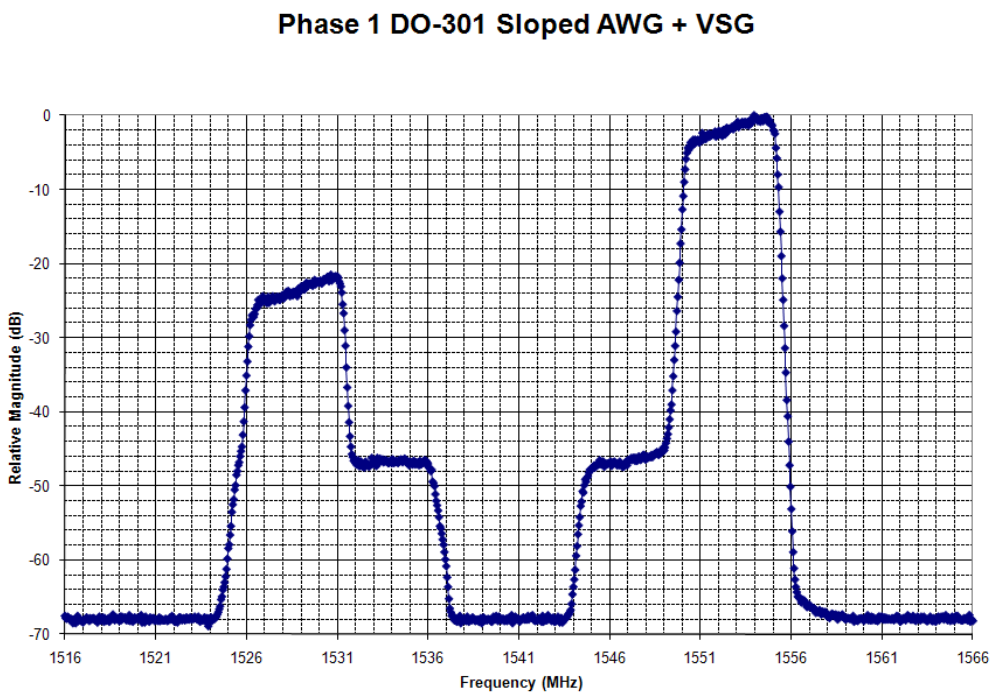

Figure D-6 Representative Filtered Phase 1 Signal with DO-301 Slope

D.1.4 Narrow- and Wide-bandwidth 1 dB CNR Degradation and Loss of Tracking Results

The 1 dB and loss of tracking results were obtained in the MOPS environment as defined in sections A.1 and A.1.1; external broadband noise was generated at an estimated level of -173.5 dBm/Hz. Table D-3 and Table D-4 provide the signal levels at which 1 dB degradation and loss of tracking occurred for the various receivers and LightSquared configurations tested.

Table D-3 Signal Power (dBm/channel) for 1 dB C/No Degradation Caused by LightSquared

Receiver	Phase 0	Phase 1	Phase 2	5 MHz Low	10 MHz Low
#1	-35.9	-35.9	-33.3	+3.4	-1.1
#2	-61.9	-62.5	-59.7	+3.7	-1.7
#3	-50.2	-50.0	-47.7	+2.9	-1.7
#4	-35.4	-38.2	-37.7	-1.0	-4.4

Table D-4 Signal Power (dBm/channel) for Loss of Satellite Tracking Caused by LightSquared

Receiver	Phase 0	Phase 1	Phase 2	5 MHz Low	10 MHz Low
#1	-28	-28	-24	+10*	+3
#2	-55	-56	-53	+9	+1
#3	-48	-48	-45	+10	+2
#4	-27	-34	-34	+7	+2

* Receiver #1 was at low C/No but maintained lock at +10 dBm

©2011 RTCA, Inc.

In conjunction with the 1 dB CNR degradation tests, tests using continuous wave interference (CWI) also were conducted to compare with results of Phase 0 (1552.7 MHz) and 5 MHz Low (1528.8 MHz) tests. Table D-5 compares the 5 MHz bandwidth noise 1 dB degradation results to the corresponding CWI results for the four aviation receivers.

Table D-5 Power Ratio for 1 dB C/No Degradation from LightSquared vs. CW RFI

Receiver	1552.7 MHz LtSq RFI / CW (dB)	1528.8 MHz LtSq RFI/ CW (dB)
#1	-7.8	+0.7
#2	-11.1	+0.8
#3	-0.5	+0.6
#4	-0.9	+0.7

The RFI power level for 1 dB C/No degradation (either CW or 5 MHz bandwidth) for all receivers exceeded the MOPS CW test limit (-86.36 dBm) at 1552.7 dB by at least 35 dB (CW) and 24 dB (5 MHz bandwidth). Total loss of tracking function occurred at approximately 7 dB higher total power than for 1 dB indicated C/No degradation.

D.1.5 SBAS Message Loss Test Results

SBAS message loss, or word error rate (WER), tests were conducted with only Receivers #3 and #4 and Phase 0 LightSquared signal configuration. Testing of additional receivers and LightSquared signal configurations could not be accomplished due to time constraints. The WER tests were conducted similar to the susceptibility tests except the receivers were allowed to acquire GPS as well as one or two SBAS satellites for at least 15 minutes prior to adjusting signal levels to be compliant with the environment required by the MOPS. Also the external wideband noise was increased to an estimated -170.5 dBm/Hz as specified in section A.1.2.1. Baseline tests without the LightSquared signal present and 1-dB degraded tests were run. For the 1-dB degraded tests, after the 30-minute warm-up period, the Phase 0 LightSquared signal was inserted at the 1 dB degradation level previously determined for the particular receiver under test. Each test was run up to approximately 3 hours with two or three SBAS channels tracking to accumulate adequate statistics for a PASS/FAIL determination on the WER rate requirement. The WER requirement is less than one error per 1000 chances.

The WER PASS/FAIL was determined statistically by modeling the word errors as a sequence of independent Bernoulli trials with (unknown) word error probability p [D-1]. The corresponding probability of obtaining exactly j errors in N independent trials is then

$$P(j) = \frac{N!}{(N-j)!\,j!} p^{j} (1-p)^{N-j},\ j = 0,1,\ldots,N \qquad \text{Equation D-1}$$

Thus, given i errors in N trials for which $i > 0.001N$ (i.e., sample mean of error rate exceeds the 0.001 WER requirement), the likelihood of WER FAIL can be expressed as 1 minus the probability of obtaining i or more errors with $p = 0.001$. That is,

© 2011 RTCA, Inc.

$$P(WER\,FAIL) = 1 - \sum_{j=i}^{N} \frac{N!}{(N-j)!\,j!}(0.001)^j\,(1-0.001)^{N-j}$$
$$= \sum_{j=0}^{i-1} \frac{N!}{(N-j)!\,j!}(0.001)^j\,(1-0.001)^{N-j}$$

Equation D-2

Also, given i errors in N trials for which $i < 0.001N$ (i.e., sample mean of error rate is less than the 0.001 WER requirement), the likelihood of WER PASS can be expressed as 1 minus the probability of obtaining i or fewer errors with $p = 0.001$. That is,

$$P(WER\,PASS) = 1 - \sum_{j=0}^{i} \frac{N!}{(N-j)!\,j!}(0.001)^j\,(1-0.001)^{N-j}$$

Equation D-3

The associated confidence levels provided below are simply the above P(WER FAIL) or P(WER PASS) probabilities expressed in percent.

The first test was a baseline run to confirm the receivers would PASS in the MOPS environment. The results show that, without the additional 1 dB degradation from LightSquared, the three tested SBAS channels in Receiver #3 had 1, 5 and 2 errors out of 9633 attempts each; these results PASS with greater than 99.9%, 91.7% and 99.6% confidence, respectively. The two tested channels in Receiver #4 had 1 and 3 errors out of 9648 attempts each; these results PASS with greater than 99.9% and 98.6% confidence, respectively.

The next tests were run with the LightSquared Phase 0 signal (1552.7 MHz) injected at the 1 dB degradation power levels determined during the CNR degradation tests (each receiver run separately at the appropriate level). The three tested channels in Receiver #3 had 22, 19 and 23 errors out of 10799 attempts each; these results FAIL with greater than 99.8%, 98.5% and 99.9% confidence, respectively. The two tested channels in Receiver #4 had 16 and 20 errors out of 11025 attempts each; these results FAIL with greater than 90.6% and 99.0% confidence, respectively.

D.2 References

[D-1] Papoulis A., *Probability, Random Variables, and Stochastic Processes*, Third Edition, 1991, p.44

©2011 RTCA, Inc.

Appendix E

Acronyms, Abbreviations and Definitions

© 2011 RTCA, Inc.

This page intentionally left blank.

©2011 RTCA, Inc.

E ACRONYMS, ABBREVIATIONS AND DEFINITIONS

E.1 Acronyms and Abbreviations

σ(sigma)	Standard deviation of a normally distributed random variable
A/D	Analog to Digital
AAD	Airborne Accuracy Designator
ABAS	Aircraft-based Augmentation System
AC	Advisory Circular or Alternating Current
ACARS	Aircraft Communications Addressing and Reporting System
A/D	Analog-to-Digital
ADS	Automatic Dependent Surveillance
ADS-B	Automatic Dependent Surveillance – Broadcast
AES	Aeronautical Electronic Systems
AFC	Automatic Frequency Control
AGC	Automatic Gain Control
AGL	Above Ground Level
AJ	anti-jam
ALI	Automatic Location Identification
AM	Amplitude Modulation
AMIDS	Airborne Interference Monitoring Detection System
AMPS	Advanced Mobile Phone System
AMSS	Aeronautical Mobile Satellite Service
AOC	Airline Operational Communications
APD	Amplitude Probability Distribution
APL	Airport Pseudolite or Applied Physics Laboratory
ARINC	Aeronautical Radio, Inc.
ARNS	Aeronautical Radionavigation Services
ARSR	Air Route Surveillance Radar
ARTCC	Air Route Traffic Control Center
ASDE	Airport Surface Detection Equipment
ASMGCS	Advanced Surface Movement and Guidance Control System
ASR	Airport Surveillance Radar
ATC	Air Traffic Control
ATCt	Ancillary Terrestrial Component
ATCRBS	Air Traffic Control Radar Beacon System
ATL	Atlanta International Airport
AWG	Arbitrary Waveform Generator
AWGN	Additive White Gaussian Noise
BER	Bit Error Rate
BO	Back Off (noise level reduction in dB during UWB testing, Appendix K)
BOC	Binary Offset Carrier
BPSK	Binary Phase Shift Keying
BRW	Barrow, Alaska
BW	Bandwidth
C/A	Coarse Acquisition Code Signal in the L1 Band
CAT I	Category I Precision Approach
CAT II	Category II Precision Approach
CAT III	Category III Precision Approach
CDF	Cumulative Distribution Function
CDMA	Code Division Multiple Access
CFR	Code of Federal Regulations

© 2011 RTCA, Inc.

CONUS	Continental United States
COSPAS	Space System for Search of Vessels in Distress (Russian acronym)
CPE	Carrier Phase Error
CRC	Cyclic Redundancy Check
CTL	Carrier Tracking Loop
CT2	Two-way digital cordless telephony technology
CW	Continuous Wave or Course Width
DA	Decision Altitude
DARS	Digital Audio Radio Services
dB	Decibel
dBc	Decibel level relative to the carrier signal level
dBi	Decibel antenna gain in a specified direction relative to an omnidirectional antenna pattern
dBic	Decibel antenna gain in a specified direction relative to the carrier signal level
dBm	Decibel level referenced to 1 milliwatt
DBS	Direct Broadcast Satellite
dBW	Decibel level referenced to 1 watt
DECT	Digital European Cordless Telecommunications
DF	Duty Factor (Burst)
DME	Distance Measuring Equipment
DGPS	Differential GPS
D/U	Desired-to-Undesired (signal ratio)
D8PSK	Differentially Encoded Eight-Phase Shift Keying
DDM	Difference in Depth of Modulation
DH	Decision Height
DME	Distance Measuring Equipment
DO	Document Designation (RTCA)
DOT	Department of Transportation
DP	Decision Point
DPSK	Differential Phase Shift Keying
DSB-AM	Double-sideband Amplitude Modulation Transmission
DSSS	Direct-Sequence Spread-Spectrum
DTV	Digital Television
ECM	Electronic Countermeasures
EGNOS	European Geostationary Navigation Overlay Service
EIRP	Effective Isotropic Radiated Power or Equivalent Isotropically Radiated Power (10.9.3.1 – second definition)
EL	Glideslope Angle
ELT	Emergency Locator Transponder
EMC	Electromagnetic Compatibility
EMI	Electromagnetic Interference
ERP	Effective Radiated Power
EUROCAE	European Organization for Civil Aviation Equipment
E-911	Enhanced 911 Emergency Calling Systems
FAA	U.S. Federal Aviation Administration
FAF	Final Approach Fix
FANS	Future Air Navigation System
FAR	Federal Aviation Regulations
FBI	Federal Bureau of Investigation
FCC	Federal Communications Commission
FDE	Fault Detection and Exclusion

©2011 RTCA, Inc.

FDD	Frequency Division Duplex
FDMA	Frequency Division Multiple Access
FEC	Forward Error Correction
FIMDS	Radio Frequency Interference Fixed Monitoring System
FM	Frequency Modulation
FM-BC	Frequency Modulation Broadcasting
FMS	Flight Management System
FOG	Fiber Optic Gyro
FRS	Family Radio Service
FSS	Flight Service Station
ft	feet
FTE	Flight Technical Error
GA	General Aviation
GAD	Ground Accuracy Designator
GALILEO	Informal Name for the European Global Navigation Satellite System
GBAS	Ground-Based Augmentation System
GBT	Ground Based Transceiver
GEO	Geo-synchronous Satellite
GFSK	Gaussian Frequency Shift Keying
GHz	Gigahertz
GLONASS	Global Orbiting Navigation Satellite System (Russian Federation)
GLS	GNSS Landing System
GMDSS	Global Maritime Distress and Safety System
GMPCS	Global Mobile Personal Communications Systems
GMRS	General Mobile Radio Service
GMSK	Gaussian Minimum Shift Keying
GPR	Ground Penetrating Radar
GRAS	Ground Based Regional Augmentation System
GSM	Global System for Mobile Communications
GSO	Geosynchronous Satellite Orbit
GTD	Geometric Theory of Diffraction
HF	High Frequency
HIL	Horizontal Integrity Limit
HIMDS	Handheld Interference Monitoring Detection System
HIRF	High Intensity Radiation Fields
HNL	Honolulu International Airport
Hpol	Horizontally Polarized (antenna)
HPL	Horizontal Protection Level
I/Q	In Phase/Quadrature Phase
I/S	Interference-to-Signal
ICAO	International Civil Aviation Organization
ICD	Interface Control Document
ICO	an MSS operator and subsidiary of Global Communications
IEEE	Institute of Electrical and Electronics Engineers
IF	Intermediate Frequency
IGEB	Interagency GPS Executive Board (replaced by the National Space-Based Positioning, Navigation, and Timing (PNT) Executive Committee
IL	Implementation Loss
ILS	Instrument Landing System
IM	Inter-modulation
IMU	Inertial Measuring Unit
INMARSAT	International Maritime Satellite Organisation

© 2011 RTCA, Inc.

INS	Inertial Navigation System
ITS	Institute for Telecommunications Sciences
ITU	International Telecommunication Union
IVDS	Interactive Video and Data Service
I3	Inmarsat-3 Satellite
JHU/APL	John Hopkins University / Applied Physics Lab
JPDO	Joint Planning and Development Office
JSC	Joint Spectrum Center
JTIDS	Joint Tactical Information Distribution System
K	Kelvin
kts	Knots (nautical miles per hour)
kW	Kilowatt
L1	GPS L-band signal 1 (1575.42 MHz)
L1C	Interoperable modernized signal in the L1 frequency band
L2	GPS L-band signal 2 (1227.6 MHz)
L5	GPS L-band civil signal (1176.45 MHz)
LAAS	Local Area Augmentation System
LAL	Lateral Alert Limit
LAX	Los Angeles International Airport
LAN	Local Area Network
LEO	Low Earth Orbit
LHCP	Left-Hand Circular Polarized
LNA	Low Noise Amplifier
LNAV	Lateral Navigation
LO	Local Oscillator
LOC	Localizer
LOL	Loss of Lock (UWB testing, Appendix K)
LOS	Line-Of-Sight
LP	Lateral Position
LPL	Lateral Protection Level
LPV	Lateral Position Velocity
LSB	Least Significant Bit
LTE	Long Term Evolution
LUT	Land User Terminal
MASPS	Minimum Aviation System Performance Standards
MB-OFDM	Multi-Band Orthogonal Frequency Division Multiplexing
M Code	A Modernized Military Signal in the L1 and L2 Bands
MDA	Minimum Decision Altitude
MEMS	Microelectromechanical System (gyro)
MES	Mobile Earth Station
MET	Mobile Earth Terminal or Mobile Earth Transmitter
METSAT	Meteorological Satellite
MHz	Megahertz
MIDS	Multifunction Information Distribution System
MLS	Microwave Landing System
MOPS	Minimum Operational Performance Standards
MOTR	Multiple Object Tracking Radar
MSAS	MTSAT Satellite-based Augmentation System - Japanese version of WAAS
MSB	Most Significant Bit
MSL	Mean Sea Level
MSK	Minimum Shift Keying
MSS	Mobile Satellite System or Mobile Satellite Services

©2011 RTCA, Inc.

MSSR	Monopulse Secondary Surveillance Radar
MSV	Mobile Satellite Ventures
MTBF	Mean Time Between Failure
MTBO	Mean Time Between Outages
MTTR	mean-time-to-respond
MW	Megawatt
NAS	National Air Space
NATS	National Air Traffic Services Ltd
NASA	National Aeronautics and Space Administration
NBFM	Narrow Band Frequency Modulation
NCO	Numerically Controlled Oscillator
NDB	Non-Directional Beacon
NE	Noise Equivalence
NEXRAD	Next Generation Weather Radar
NGS	National Geodetic Survey
nmi	Nautical Mile
NOAA	National Oceanic and Atmospheric Administration
NOCC	National Operations Control Center
NOTAM	Notice To Airmen
NPA	Non-Precision Approach
NSE	Navigation System Error
NTIA	National Telecommunications and Information Administration
OCH	Obstacle Clearance Height
OCS	Obstacle Clearance Surface
OFDM	Orthogonal Frequency Division Multiplexing
OFZ	Obstacle Free Zone
OOB	Out-of-Band
OOBE	Out-of-Band Emissions
OOK	On-Off Keying
ORD	O'Hare International Airport
OS	Open Service (Galileo)
OSM	Office of Spectrum Management
PAD	PulsON Application Developer (Time Domain UWB source)
PAN	Personal Area Network
PACS	Picture Archiving System
PCM	Pulse Code Modulation
PCS	Personal Communications Systems
PDA	Personal Digital Assistant
PDF	Probability Density Function or Probability Distribution Function
PDI	Predetection Integration
PEDs	Personal Electronic Devices
PHS	Personal Handyphone System
PIMDS	Portable Interference Monitoring and Detection Systems
PLL	Phase Lock Loop
PPM	Pulse Position Modulation
PRF	Pulse Repetition Frequency
PRN	Pseudorandom Number
PRS	Public Regulated Service (Galileo)
PSAPs	Public Safety Answering Points
PSD	Power Spectral Density
PSFD	Power Spectral Flux Density
PSK	Phase Shift Keying
P(Y)	Precise Code signal in the L1 and L2 Band

© 2011 RTCA, Inc.

QPSK	Quadrature Phase Shift Keying
QZSS	Quasi-Zenith Satellite System (Japan)
RAIM	Receiver Autonomous Integrity Monitoring
RDP	Radiation Distribution Plot
RF	Radio Frequency
RFI	Radio Frequency Interference
RFID	Radio Frequency Identification
RHCP	Right-Hand Circular Polarized
RMS	Root-Mean-Squared
RNAV	Area/Random Navigation
RNP	Required Navigation Performance
RNSS	Radionavigation Satellite Service
R & O	Report and Order
RR	Radio Regulations
RSS	Root Sum of Squares
RTCA	Requirements and Technical Concepts for Aviation
RTTY	Radioteletype
Rwy	Runway
RVR	Runway Visual Range
SAR	Specific Absorption Rate
SARPS	Standards and Recommended Practices
SARSAT	Search and Rescue Satellite
SATCOM	Satellite Communications
SBAS	Satellite-based Augmentation System
SC	Special Committee
SIS	Signal in Space
SITA	Service provider of IT business solutions and communications services to the air transport industry
SMGCS	Surface Movement Guidance and Control System
SS	Spread Spectrum
SSB	Single Sideband
SSC	Spectral Separation Coefficient
SS-MC-MA	Spread Spectrum-Multi-Carrier-Multiple Access
SSR	Secondary Surveillance Radars
STDMA	Self Organizing Time Division Multiple Access
SV	Space Vehicle
TACAN	Tactical Air Navigation
TBD	To Be Determined
TCAS	Tactical Collision Avoidance System or Traffic Alert and Collision Avoidance System
TCH	Threshold Crossing Height
TCP	Threshold Crossing Point
TCXO	Temperature Compensated Crystal Oscillator
TDD	Time Division Duplex
TDMA	Time Division Multiple Access
TDWR	Terminal Doppler Weather Radar
TERPS	Terminal Instrument Procedures
TIMDS	Transportable Interference Monitoring and Detection Systems
T-PEDs	Transmitting Personal Electronic Devices
TRS	Thales Raytheon Systems (Airport Surveillance Radar)
TSE	Total System Error
TSO	Technical Standard Order
TTFF	Time-To-First-Fix

©2011 RTCA, Inc.

TV	Television
UAT	Universal Access Transceiver
UHF	Ultra High Frequency
US	United States
USB	Universal Serial Bus
UTD	Uniform Theory of Diffraction
UWB	Ultra-Wideband
VAL	Vertical Alert Limit
VCO	Voltage Controlled Oscillator
VDB	VHF Data Broadcast
VDL-4	emerging data link technology in the VHF Aeronautical Mobile Service band; proposed to support data communications only for ADS-B (see Section 6.1)
VDLL	Vector Delay Lock Loop
VHF	Very High Frequency
VLCC	Very Large Crude Carrier
VNAV	Vertical Navigation
VOR	VHF Omnidirectional Range
VPL	Vertical Protection Level
Vpol	Vertically Polarized (antenna)
VSWR	Voltage Standing Wave Ratio
W	Watt
WAAS	Wide Area Augmentation System
WACS	Wireless Access Communication System
WER	Word Error Rate
WG-6	RTCA Working Group 6 (GPS Interference)
WIR	Wall-Imaging Radar
WLANs	Wireless Local area Networks
WP	Way Point
ZJX	Jacksonville Air Route Traffic Control Center
ZMA	Miami Air Route Traffic Control Center

E.2 Definitions

Global Navigation Satellite System (GNSS) — GNSS is a world-wide position, velocity, and time determination system, that includes one or more constellations, receivers, and system integrity monitoring, augmented as necessary to support the required navigation performance for the actual phase of operation.

Global Positioning System (GPS) — The satellite-based navigation system operated by the United States.

Height Above Threshold (HAT) — Specifically, the height above the LTP/FTP. In using this term for airborne equipment specifications, care should be taken to define the point on the aircraft (e.g., GPS antenna, wheel height, or center of mass) that applies.

Mask Angle — A fixed elevation angle referenced to the user's horizon below which satellites are ignored by the receiver software. Mask angles are used primarily in the analysis of GNSS performance, and are employed in some receiver designs. The mask angle is driven by the receiver antenna characteristics, the strength of the transmitted signal at low elevations, receiver sensitivity and acceptable low elevation errors.

© 2011 RTCA, Inc.

Misleading Information — Misleading information is defined to be any data which is output from the navigation receiver to other equipment or displayed to the pilot that has an error larger the current protection levels (HPL, LPL/VPL) for the current operation. This includes all output data, such as position and deviations.

Non-Precision Approach — A standard instrument approach procedure in which no glideslope/glide path is provided. (Source: FAA document 7110.65G.)

Precision Approach — A standard instrument approach procedure in which a glideslope/ glide path is provided. (Source: FAA document 7110.65G.)

Pseudolite — A pseudolite (pseudo-satellite) is a ground-based GNSS augmentation which provides, at GNSS ranging source signal-in-space frequencies, an additional navigation ranging signal. The augmentation may include additionally differential GNSS corrections. (Adapted from the FANS GNSS Technical Subgroup.)

Pseudorange — The distance from the user to a ranging source plus an unknown user clock offset distance. With four ranging source signals it is possible to compute position and offset distance. If the user clock offset is known, three ranging source signals would suffice to compute a position.

Satellite-Based Augmentation System (SBAS) — A differential GNSS employing satellite transponders to broadcast additional ranging signals and differential corrections usable over an extensive geographical area for the supported phases of operation.

Selective Availability (SA) — A set of techniques for denying the full accuracy and selecting the level of positioning, velocity, and time accuracy of GPS available to users of the Standard Positioning Service (L1 frequency) signal.

Standard Positioning Service (SPS) — The standard specified level of positioning, velocity and timing accuracy that is available, without qualifications or restrictions, to any user on a continuous worldwide basis.

Terminal Area — A general term used to describe airspace in which approach control service or airport traffic control service is provided.

Wide Area Augmentation System (WAAS) — The SBAS operated by the U.S. FAA.

World Geodetic Survey (WGS) — A set of parameters describing the size and shape of the earth, the positions of a network of points with respect to the center of mass of the earth, transformations from major geodetic datum, and the potential of the earth.

©2011 RTCA, Inc.